CONTRIBUTION OF SOMATOSTATIN DEFICITS AND EIF2 SIGNALING TO ANXIETY/DEPRESSIVE-LIKE BEHAVIORS

by

Li-Chun Lin

B.S. in Psychology, National Chung Cheng University, 2004

M.S. in Physiology, National Cheng Kung Univeristy, 2006

Submitted to the Graduate Faculty of

School of Medicine in partial fulfillment

of the requirements for the degree of

Doctor of Philosophy

University of Pittsburgh

2014

UNIVERSITY OF PITTSBURGH

SCHOOL OF MEDICINE

This dissertation was presented

by

Li-Chun Lin

It was defended on

May 1st, 2014

and approved by

Dr. Gregg E. Homanics, Professor, Anesthesiology, Pharmacology and Chemical Biology

Dr. Linda Rinaman, Director and Professor, Neuroscience

Dr. Colleen McClung, Associate Professor, Psychiatry

Dr. Peter Gianaros, Associate Professor, Psychology

Dr. Ronald Duman, Director and Professor, Neurobiology, Pharmacology and Psychiatry, Yale University

Dissertation Advisor: Dr. Etienne Sibille, Associate Professor, Psychiatry

CONTRIBUTION OF SOMATOSTATIN DEFICITS AND EIF2 SIGNALING TO ANXIETY/DEPRESSIVE-LIKE BEHAVIORS

Li-Chun Lin, M.S., Ph.D.

University of Pittsburgh, 2014

Somatostatin is a secretory neuropeptide and marker of gamma-aminobutyric acid (GABA) interneurons that contribute to information processing of local cortical circuits. SST deficits are frequently observed in depression and other neurological disorders with mood disturbances, but the origin of SST-related pathological changes and their role in disease processes remain elusive. We used mice lacking Sst (Sst^{KO}) to investigate the contribution of low SST to anxiety/depressive-like phenotypes (defined as emotionality) under baseline and stressed conditions. High emotionality was found in Sst^{KO} mice at baseline and after unpredictable chronic mild stress exposure. Compared to wild-type mice, unstressed Sst^{KO} mice showed high basal plasma corticosterone and reduced gene expression of *Bdnf*, *Cortistatin*, and *Gad67* in the cingulate cortex. Compared to pyramidal neurons, cell-specific transcriptome analyses indicated that SST neurons in the cingulate cortex are more vulnerable to chronic stress. Protein translation through eukaryotic initiation factor 2 (EIF2) signaling, a pathway previously implicated in neurodegenerative diseases, was most affected and suppressed in stress-exposed SST neurons. Activating EIF2 signaling with an EIF2 kinase inhibitor mitigated mouse anxiety/depressive-like behaviors that were induced by stress. Together, our results suggest a causal relationship between SST deficits and mood-related phenotypes by first showing that Sst^{KO} mice exhibit behavioral, neuroendocrine and molecular phenotypes parallel those seen in human patients with major depression. Our results further suggest a novel antidepressant function for EIF2-related

protein translational control, and may prove important in elucidating mechanisms of how chronic stress triggers and sustains selective vulnerability of SST neurons associated with mood symptoms in stress-related neuropsychiatric disorders.

TABLE OF CONTENTS

LIST OF TABLES

LIST OF FIGURES

LIST OF ABBREVIATIONS

ACC: anterior cingulate cortex

AD: Alzheimer's disease

BA: Brodmann area

BDNF: brain-derived neurotropic factor

CORT: cortistatin

CR: calretinin

CRH: corticotropin-releasing hormone

DBS: deep brain stimulation

DSM-IV: Diagnostic and Statistical Manual of Mental Disorders

ECT: electroconvulsive

EIF2: Eukaryotic initiation factor 2

ER: endoplasmic reticulum

EPM: elevated plus maze

GABA: gamma-aminobutyric acid

GAD67: glutamic acid decarboxylase, isoform 67

GC: glucocorticoids

HPA: hypothalamic-pituitary-adrenal

IPA: Ingenuity Pathway Analysis

KO: knockout

MDD: major depressive disorder

MRI: magnetic resonance imaging

mPFC: medial prefrontal cortex

NE: norepinephrine

NPY: neuropeptide Y

NSF: novelty suppressed feeding

OF: open field

PD: Parkinson's disease

PET: positron emission tomography

PERK: Protein kinase R (PKR)-like ER kinase

PTSD: post-traumatic stress disorder

PV: parvalbumin

qPCR: quantitative polymerase chain reaction

rTMS: repetitive transcranial magnetic stimulation

SNRI: selective noradrenaline reuptake inhibitor

SSRI: selective serotonin reuptake inhibitors

SST: somatostatin

Sst^{KO}: somatostatin knockout mice

SP: sucrose preference

UCMS: unpredictable chronic mild stress

UPR: unfolded protein response

YLD: years lost due to disability

PREFACE

I would first like to thank my advisor, Dr. Etienne Sibille, for providing the exceptional support and advice throughout my PhD study. His door is always open for me. He always motivates and encourages me to push forward during my dissertation research. I would also like to thank members of my Advisory Committee: Drs. Gregg Homanics, Linda Rinaman, Colleen McClung, Peter Gianaros, and Ronald Duman. They have given me prudent advice. I would like to express special gratitude to Dr. Homanics for serving as my committee chair. I would also like to thank Dr. Rinaman for giving me a solid foundation in neuroanatomy and surgical skills during my rotation, and for our numerous great conversations. I am indebted to Dr. McClung and Gianaros, their challenging questions and discussion motivated me to do better. Finally, I would like to thank my outside examiner, Dr. Ronald Duman, for taking time to participate in my defense.

I would also like to thank all the members of Sibille laboratory. I am fortunate to be a member among peers that emphasize progressive scientific concepts and utilize wide-ranging technical approaches. In particular, I would like to thank Dr. Marianne Seney, Dr. Amelie Soumier, Dr. Nicole Edgar, Beverly French, Masaki Chien-Wei Lin, Dr. Ying Ding, Dr. Jean-Phillippe Guilloux, Dr. Chris Gaiteri, Dr. Xingbin Wang, Lun-Ching Chang, Cathy Ye Chen, Honggui Jia ,Hyunjung Oh , Dr. Gaelle Guilloux Douillard, and Christin Glorioso for their

support both professionally and personally in the lab. I would also like to acknowledge Chris Walsh, Carol Moore, and Beverly French for all their great help in making tasks run smoothly in the lab. Additionally, I would like to thank members of the Lewis lab, especially Dr. Domonique Arion and Kelly Rogers, for their kind assistance. Finally, I am especially grateful to the Ph.D. program in Neurobiology for providing me with the opportunity to pursue my dreams. Dr. Linda Rinaman and Dr. Yanhua Huang have provided me with parenting advice that has been taken to heart.

Finally, I would like to dedicate my dissertation to my parents, for their continual and unwavering support. My husband, Kai, has been my rock with so much support. I thank my son, Jasper, for putting a smile on my face at the end-stage of dissertation. I thank you all for supporting me throughout this wonderful journey in Pittsburgh.

1.0 INTRODUCTION

Somatostatin (SST) is an inhibitory neuropeptide and a marker for GABAergic interneuronal subpopulations. SST-expressing interneurons preferentially target the dendrites of pyramidal neurons, contributing to information processing at the microcircuit level (Di Cristo *et al.*, 2004; Markram *et al.*, 2004; Tan *et al.*, 2008; Murayama *et al.*, 2009; Xu *et al.*, 2013). SST deficits are frequently observed in depression and other neurological disorders with mood disturbances. However, mechanistically how SST deficits contribute to the disease processes remains mostly unknown. Therefore, knowledge of how SST neurons contribute to aberrant mood regulation is important in uncovering the pathophysiology of mood dysregulation.

1.1 OVERVIEW OF MAJOR DEPRESSIVE DISORDER

1.1.1 Epidemiology of major depressive disorder

Major depressive disorder (MDD) is a common and severe psychiatric disorder with high worldwide morbidity and lifetime prevalence. In the United States, the 12-month prevalence of MDD was estimated to be 6.7% (Kessler *et al.*, 2005b). Among the surveyed patients, 30.4% of affected adults (approximately 2% of US adult population) were classified as “severe” (Kessler *et al.*, 2005a). Women are 70% more likely than men to experience depression (Kessler *et al.*,

2003). The burden on society accounts for 5 % of years lost due to disability (YLD) (Ferrari *et al.*, 2013). Hence, improving the understanding, diagnosis, and treatment of MDD is a public health priority.

1.1.2 Clinical Presentation and treatment of MDD

MDD etiology remains poorly understood. Clinical presentation of MDD can include a variety of symptoms such as negative affective states (anhedonia and anxiety), abnormal hypothalamic-pituitary-adrenal (HPA) axis, insomnia, and emergence of cognitive and physiological impairments. Moreover, MDD and anxiety disorders commonly co-occur. From both etiological and clinical perspectives, MDD is a heterogeneous disease. Therefore while many MDD biomarkers have been investigated, standalone markers seem unlikely to be applicable to a large-scale group of patients.

The first-line treatment of MDD is a combination of psychotherapy and pharmacotherapy of selective serotonin reuptake inhibitors (SSRIs) such as fluoxetine or selective noradrenaline reuptake inhibitors (SNRIs) such as venlafaxine. Upon diagnosis of MDD, 4-8 weeks of initial treatment is needed to assess its effect. To reduce the risk of relapse, patients with MDD will need to continue with antidepressant medications during the acute phase, and for another 4-9 months during the continuation phase. To reduce the risk of a recurrent depressive episode, patients with chronic MDD will also receive a maintenance phase of treatment after completing the continuation phase. A common mechanism of antidepressants is to increase the availability of monoamines in the synaptic cleft. However, side effects of antidepressants include body weight changes, insomnia, sexual dysfunction, nausea, constipation, and cardiovascular toxicity (Masand & Gupta, 2002; Cassano & Fava, 2004). Given the clinical and etiological

heterogeneity, only 50% of MDD patients achieve remission after first-line antidepressant treatments (Fava & Davidson, 1996; Trivedi *et al.*, 2006).

Although treatments that target neuropeptide receptors were well supported by basic neuroscience research, compounds that target neuropeptide receptors failed to demonstrate efficacy during clinical trials (Griebel & Holsboer, 2012). Nearly all pharmaceutical companies now continue to pursue classical monoamine-based drugs. As alternatives to pharmacological treatments, non-invasive neuromodulation procedures, for example electroconvulsive and repetitive transcranial magnetic stimulation have been shown to be effective in treating MDD (Hoffman & Cavus, 2002; Tamminga *et al.*, 2002). Nevertheless, potentially serious side effects include memory impairment and headache. Deep brain stimulation has recently been studied as an option for treatment-resistant depression (Mayberg *et al.*, 2005; Lozano *et al.*, 2008), but it is an invasive surgery procedure and still at an early experimental stage.

1.1.3 Risk factors for MDD

The HPA axis has been implicated in MDD. Although not all adults with elevated cortisol levels are MDD patients, MDD patients disproportionately show chronic HPA axis hyperactivity and an inability for this system to return to normal functioning after being exposed to a stressor (Gold & Chrousos, 2002). In addition, adults with the most severe depression also tend to have highest cortisol levels (Pruessner *et al.*, 2003). The principle regulator of the HPA axis is corticotropin-releasing hormone (CRH), which leads to the release of glucocorticoids (GC; cortisol in humans, corticosterone in rodents) from the adrenal cortex. GC maintains the basal activity of the HPA axis and influences stress-related responsiveness. In addition to altered expression of CRH and GC receptors (Webster *et al.*, 2002; Wang *et al.*, 2008; Hauger *et al.*, 2009), altered circadian

patterns of cortisol are also frequently observed in MDD patients (Bhagwagar *et al.*, 2003; Luby *et al.*, 2003; Brouwer *et al.*, 2005). Successful antidepressant treatment normalizes HPA axis hyperactivity (Heuser *et al.*, 1996; Ising *et al.*, 2007), supporting the hypothesis that a dysfunctional HPA/CRH system is involved in MDD etiology. However, whether HPA axis hyperactivity precedes a depressive episode or is a consequence of it remains unclear.

1.1.4 Animal model of depression

The association between stress and MDD onset/episodes is well-established (Kendler *et al.*, 1999; Hammen, 2005). The unpredictable chronic mild stress (UCMS) model uses environmental and social stressors (e.g., wet bedding, single housing) to increase anxiety/depressive-like behaviors, decreased consumption of palatable food, and induce physiological changes (e.g., coat state) in rodents (Santarelli et al. 2003; Pothion et al. 2004; Mineur et al. 2006). Most of the UCMS-induced behaviors can be blocked and reversed by chronic antidepressant treatment (Surget et al. 2009). Importantly, the UCMS paradigm also mimics sex differences in human MDD patients (Joeyen-Waldorf *et al.*, 2009; Guilloux *et al.*, 2011), illustrating a strong face validity for the human syndrome. Chronic corticosterone exposure is a neuroendocrine stress. Although both models lead to neuroendocrine, physical and behavioral depression-like alterations, UCMS has better construct, face and overall mechanistic validity compared to corticosterone exposure since social-environmental stress induces multi-systems disruptions that are not limited to neuroendocrine changes (Willner *et al.*, 1987; Pothion *et al.*, 2004).

1.1.5 Molecular biology of MDD

Genetic predisposition is a critical component of MDD pathogenesis. Several genetic factors have been suggested to be involved in the pathophysiology of depression and the mechanism of antidepressant actions, including serotonergic (Caspi *et al.*, 2003), GABAergic (Sanacora *et al.*, 2004; Luscher *et al.*, 2011) and BDNF signaling pathways (Duman *et al.*, 1997; Duman *et al.*, 2000; Hashimoto *et al.*, 2004). Given the complexity of MDD, single-gene effects may not fully explain the heterogeneous clinical phenotypes of MDD (Fava & Kendler, 2000; Lopez-Leon *et al.*, 2008). In addition, genetic risk factors for MDD may increase the impact after being exposed to stressors (Kendler & Karkowski-Shuman, 1997; Caspi *et al.*, 2003). Thus, this heterogeneity of accumulated gene-environment interactions reflects the unique complexities of MDD and points to the inherent difficulties in treating MDD as a homogenous entity. A challenge remains in understanding how distal effects of multiple genes converge to affect mood dysregulation.

1.1.6 Altered cingulate cortex in MDD

The medial prefrontal cortex (mPFC) is involved in top-down regulation for flexible behavior (Akana et al., 2001; Diorio et al., 1993; McKlveen et al., 2013). The mPFC is comprised of three subdivisions based on its connectivity, cytoarchitecture, and function: the anterior cingulate [human Brodmann area (BA) 24], prelimbic (human BA32), and infralimbic (human BA25) cortices (Uylings *et al.*, 2003; Vertes, 2004; Gabbott *et al.*, 2005). The anterior cingulate cortex (ACC) contains glucocorticoid receptors (GR) and plays a critical role in the inhibitory regulation of HPA axis via GR-mediated negative feedback effects of GC actions during stress (Diorio *et al.*, 1993; Devinsky *et al.*, 1995). In addition, the ACC is vulnerable to

hypercortisolism (Cerqueira *et al.*, 2005). Reduced grey matter volume and reduced metabolic activity of the ACC has been reported in positron emission tomography (PET) and magnetic resonance imaging (MRI) studies of MDD subjects (Drevets *et al.*, 1997; Coryell *et al.*, 2005). Dysregulation of GABAergic neurotransmission in the ACC has been thought to be involved in the molecular neuropathogenesis of mood dysregulation (Thompson *et al.*, 2009; Tripp *et al.*, 2011; Tripp *et al.*, 2012; Zhao *et al.*, 2012). Moreover, reduced glutamine (the molecular precursor of GABA and glutamate) is also found in the ACC (Walter *et al.*, 2009). Furthermore, functional imaging studies have documented aberrant neuronal activation of the ACC in depressed subjects (Bremner *et al.*, 2004; Alexopoulos *et al.*, 2008; Matthews *et al.*, 2008).

1.1.7 Summary of dissertation research

In order to improve medical treatment of affective spectrum disorders, it is necessary to understand the pathophysiology that underlies its core feature - mood dysregulation. The goal of this dissertation is to improve our understanding of the neural mechanisms underlying mood regulation with a focus on SST and SST-containing interneurons. We first reviewed what is known about the SST system in the central nervous system and SST deficits in the context of neurological disorders (Chapter 2). Based on known functions of SST and SST neurons in the brain and pathology of SST in neurological disorders, we tested our overarching hypothesis that SST deficits play a causal role in mood dysregulation (Chapters 4-6). We first collected behavioral, molecular, and neuroendocrine data from mice with low SST (Chapter 3), and found that compared to wild-type mice, mice lacking SST showed increased emotionality and altered BDNF-GABA signaling in the cingulate cortex. A known physiological function of SST is neuroendocrine modulation. Accordingly, hyperactivity of the HPA axis is observed in some

depressed patients, and elevated stress hormones can lead to depression, although these are not consistent observations (Wolkowitz *et al.*, 2009). We found elevated basal corticosterone in SST heterozygous mice that exhibited normal emotionality, suggesting that corticosterone is not sufficient to induce high emotionality associated with SST deficits (Chapter 4). Furthermore, we found altered protein translation control in SST neurons of the cingulate cortex from mice that were exposed to chronic stress; suggesting that protein homeostasis could influence selective vulnerability to stress. Finally, we found that enhancing protein translation during stress mitigated stress-related emotionality, further suggesting that protein translation control is involved in mood regulation (Chapter 5). The studies collectively explored the functional roles of SST and possible pathogenetic mechanisms of selective vulnerability of SST neurons to stress in mice, and provided new insights for the pathophysiological mechanisms underlying MDD in humans.

2.0 PAPER 1: REDUCED SOMATOSTATIN IN MOOD DISORDERS: A COMMON PATHOPHYSIOLOGICAL SUBSTRATE AND DRUG TARGET?

Li-Chun Lin, M.S. and Etienne Sibille, Ph.D.

Note on my contributions to this paper: I contributed to writing and submission the manuscript.

*This work has been accepted and published in *Frontiers in Pharmacology. 2013; 110 (4)1-12.*

2.1 ABSTRACT

Our knowledge of the pathophysiology of affect dysregulation has progressively increased, but the pharmacological treatments remain inadequate. Here, we summarize the current literature on deficits in somatostatin, an inhibitory modulatory neuropeptide, in major depression and other neurological disorders that also include mood disturbances. We focus on direct evidence in the human postmortem brain, and review rodent genetic and pharmacological studies probing the role of the somatostatin system in relation to mood. We also briefly go over pharmacological developments targeting the somatostatin system in peripheral organs and discuss the challenges of targeting the brain somatostatin system. Finally, the fact that somatostatin deficits are frequently observed across neurological disorders suggests a selective cellular vulnerability of somatostatin-expressing neurons. Potential cell intrinsic factors mediating those changes are discussed, including nitric oxide induced oxidative stress, mitochondrial dysfunction, high inflammatory response, high demand for neurotrophic environment, and overall aging processes. Together, based on the co-localization of somatostatin with GABA, its presence in dendritic-targeting GABA neuron subtypes, and its temporal-specific function, we discuss the possibility that deficits in somatostatin play a central role in cortical local inhibitory circuit deficits leading to abnormal corticolimbic network activity and clinical mood symptoms across neurological disorders.

2.2 INTRODUCTION

Mood disturbances are commonly observed in many neurological disorders. The chronic, recurrent and long duration of mood disturbances not only place an enormous emotional and financial burden on patients, but also on their families and society. Nearly 10% of all primary care office visits are depression-related (Stafford *et al.*, 2000), but only 30% of patients with mood disturbances achieve remission with initial treatment (Trivedi *et al.*, 2006). Somatostatin is a peptide expressed in multiple organs. In the brain, somatostatin (also known as somatotrophin release inhibiting factor and often abbreviated as SST, SRIF, or SOM) acts as a modulatory and inhibitory neuropeptide that is co-localized with gamma-aminobutyric acid (GABA), and that is involved in regulating multiple aspects of physiological and behavioral stress responses, including inhibition of hypothalamic hormone release, amygdala central nucleus output, and cortical local circuit integration of sensory input. Research advances over the past three decades suggests a critical role for somatostatin in the pathophysiology of mood disorders, and potential new therapeutic strategies. Several recent reviews have summarized the role of the somatostatin system, including in receptor subtypes (Patel, 1999; Csaba & Dournaud, 2001), pharmacological developments (Neggers & van der Lely, 2009), and during normal and pathological aging (Patel, 1999; Viollet *et al.*, 2008; Martel *et al.*, 2012). This article highlights current findings on the functional roles of somatostatin in local neuronal circuits, and reviews somatostatin deficits across neurological disorders, including neuropsychiatric disorders [e.g., MDD, bipolar disorder, schizophrenia], and neurodegenerative disorders [e.g., Parkinson's, Alzheimer's disease, Huntington's diseases] (Table 1). This raises interesting questions, including first; whether the somatostatin deficits observed in neurological disorders represent common, distinct, or partly overlapping mechanisms of symptoms across disorders and, second, what may be the causes and

biological mechanisms underlying the selective neuronal vulnerability of somatostatin-expressing neurons. In addition, we review somatostatin findings associated with affect regulation at the genetic, cellular, and pharmacological levels in animal studies. So far, these findings suggest that somatostatin deficits across different brain systems and diseases may play a central role in the affective symptom dimension rather than non-specific signals in neurological disorders (Figure 1). As somatostatin itself is not an ideal drug target, including for antidepressant effect, we suggest that further studies characterizing the intrinsic properties and biological vulnerabilities of somatostatin-expressing neurons, may identify novel targets with implications for understanding the function of local cell circuits and brain regions underlying affective symptoms across several neurological disorders.

2.3 LOW SOMATOSTATIN IN NEUROPSYCHIATRIC AND NEURODEGENERATIVE DISORDERS

2.3.1 Major depressive disorder

MDD patients show decreased somatostatin levels in the cerebrospinal fluid (CSF) (Agren & Lundqvist, 1984; Molchan *et al.*, 1991; Kling *et al.*, 1993), and transiently decreased CSF somatostatin which normalize with recovery in MDD (Rubinow *et al.*, 1985; Post *et al.*, 1988). Evidence for low levels of CSF somatostatin was found to correlate significantly with elevated urinary cortisol in MDD patients (Molchan *et al.*, 1993). This is consistent with the altered HPA axis function described in some depressed patients (Holsboer, 2000). The route and characterization, however, from CSF somatostatin to MDD pathophysiology is not direct,

potentially due to a paucity of information on factors regulating CSF somatostatin, and to inconclusive somatostatin/HPA axis studies in MDD patients. Hence, despite these early findings, interest in somatostatin in mood disorders declined over time.

Human post-mortem studies from our group have described region-specific somatostatin deficits in MDD patients, including a down-regulation of *somatostatin* gene expression in the dorsolateral prefrontal cortex (dlPFC), subgenual anterior cingulate cortex (sgACC), and amygdala (Sibille *et al.*, 2011; Tripp *et al.*, 2011; Guilloux *et al.*, 2012; Tripp *et al.*, 2012). In addition, two peptides co-localized with somatostatin, neuropeptide Y and cortistatin, are both significantly down-regulated in MDD patients (Tripp *et al.*, 2011; Tripp *et al.*, 2012).These three neuropeptides (somatostatin, neuropeptide Y, and cortistatin) are markers of GABAergic neurons that specifically target the dendritic compartment of pyramidal cells (de Lecea *et al.*, 1997; Viollet *et al.*, 2008), and that are essential in gating incoming sensory information. Other types of GABAergic cell markers, such as parvalbumin and cholecystokinin, are mostly not affected by MDD [although see (Tripp *et al.*, 2012)]. Interestingly, these somatostatin deficits were systematically more robust in female subjects across cohorts and regions (Sibille *et al.*, 2011; Tripp *et al.*, 2011; Guilloux *et al.*, 2012; Tripp *et al.*, 2012), consistent with the female heightened vulnerability to develop MDD, and suggesting that low somatostatin may represent a molecular correlate of sexual dimorphism in vulnerability to affect dysregulation. Notably, these findings are also consistent with earlier postmortem studies showing reduced calbindin-positive cell numbers in MDD (Rajkowska *et al.*, 2007; Maciag *et al.*, 2010), as somatostatin is mostly expressed in a subgroup of calbindin-positive cells [reviewed in (Viollet *et al.*, 2008)]. Converging evidence from down-regulation of *somatostatin* co-localized GABA markers in MDD across multiple human post-mortem studies suggests that this particular GABA

subpopulation in the forebrain is selectively vulnerable, among other subtypes of GABA neurons. Furthermore, these local cell circuit-based findings introduce a new role for somatostatin in depression, which is distinct from its previously investigated role in the regulation of the HPA axis (Rubinow *et al.*, 1983; Molchan *et al.*, 1993; Weckbecker *et al.*, 2003).

2.3.2 Other neuropsychiatric disorders

Schizophrenia is a neuropsychiatric disorder characterized by positive (e.g., hallucination), negative (e.g., emotional blunting, apathy) and cognitive symptoms. Somatostatin deficits in schizophrenia are demonstrated by a reduction of CSF somatostatin (Bissette *et al.*, 1986; Reinikainen *et al.*, 1990), decreased *somatostatin* gene expression in the dlPFC (Morris *et al.*, 2008; Guillozet-Bongaarts *et al.*, 2013), and decreased number and density of somatostatin-expressing neurons in the hippocampus (Konradi *et al.*, 2011a), caudal entorhinal cortex and parasubiculum (Wang *et al.*, 2011).

Changes in somatostatin are also identified in bipolar disorder, which is clinically characterized by fluctuating mood. Studies in subjects with bipolar disorder indicate decreases in somatostatin cellular density in the caudal entorhinal cortex and parasubiculum (Wang *et al.*, 2011), number of somatostatin-expressing neurons in the hippocampus (Konradi *et al.*, 2011b), *somatostatin* gene expression in the dlPFC [trend level; (Sibille *et al.*, 2011)] and hippocampus (Konradi *et al.*, 2011b). In addition, patients with bipolar disorder show elevated CSF somatostatin during manic states (Sharma *et al.*, 1995).

2.3.3 Neurodegenerative disorders

Alzheimer's disease is a neurodegenerative disease with neuropsychiatric symptoms (Bungener *et al.*, 1996). Decreased CSF somatostatin (Bissette *et al.*, 1986; Tamminga *et al.*, 1987) and decreased somatostatin immune-reactivity across cortical and subcortical regions is reported in subjects with Alzheimer's disease, including temporal cortex, frontal cortex, and hippocampus (Davies *et al.*, 1980; Rossor *et al.*, 1980; Davies & Terry, 1981; Candy *et al.*, 1985; Dournaud *et al.*, 1994).

Depression is a common comorbid symptom in Parkinson's disease and predicts greater disability at any assessment point (Aarsland *et al.*, 1999). Decreased CSF somatostatin, decreased somatostatin immune-reactivity, and binding sites are also observed in the temporal cortex and frontal cortex of patients with Parkinson's disease (Beal *et al.*, 1986; Epelbaum *et al.*, 1988). Notably, reduced CSF somatostatin in Parkinson's disease appears to be irreversibly present at the onset of symptoms (Dupont *et al.*, 1982).

2.4 REDUCED SOMATOSTATIN AND LOW MOOD?

2.4.1 Introduction

The evidence outlined in this review provides only a glimpse of the potential full range of somatostatin deficits across neurological disorders, as multiple other brain regions and disease categories await further characterization (Table 1). Taken together, the cumulative evidence demonstrates that somatostatin deficits are common neurochemical and molecular features in

individuals with neurological disorders, regardless of their categorical diagnosis. While somatostatin studies of cell number and gene expression in human postmortem brains suggest a specific alteration of somatostatin-positive neurons across neurological disorders, it is possible that changes and dys-synchronization of additional components of local neuronal circuits contributes to a common symptom dimension, which we speculate includes low affect and mood dysregulation. Hence, this review is not comprehensive, but rather, highlights the recent findings in brain somatostatin signaling and the potential role of somatostatin deficits in affect dysregulation for integrating categorical models of mood symptoms into a dimensional model across neurological disorders.

Table 1. Low somatostatin in human neurological disorders

Neurological disorders	Brain region	Pathological findings	References
Major depressive disorder	CSF	decreased	(Agren & Lundqvist 1984; Kling et al 1993; Molchan et al 1993)
	dorsolateral prefrontal cortex	decreased (RNA expression)	(Sibille et al 2011)
	anterior cingulate cortex	decreased (RNA expression)	(Tripp et al 2011; Tripp et al 2012)
	amygdala	decreased (RNA and protein expression)	(Guilloux et al 2012)
Schizophrenia	CSF	decreased	(Bissette et al 1986; Reinikainen et al 1990)
	dorsolateral prefrontal cortex	decreased (RNA expression)	(Guillozet-Bongaarts et al 2013; Morris et al 2008)
	hippocampus	decreased (neuron number and density)	(Konradi et al 2011a)
	caudal entorhinal cortex	decreased (neuron number and density)	(Wang et al 2011)
	parasubiculum	decreased (neuron number and density)	(Wang et al 2011)
Bipolar disorder	caudal entorhinal cortex	decreased (neuron density)	(Wang et al 2011)
	parasubiculum	decreased (neuron density)	(Wang et al 2011)
	hippocampus	decreased (neuron number and RNA expression)	(Konradi et al 2011b)
	dorsolateral prefrontal cortex	decreased (RNA expression; trend level)	(Sibille et al 2011)
Alzheimer's disease	CSF	decreased	(Bissette et al 1986; Tamminga et al 1987)
	temporal cortex	decreased (immune-reactivity)	(Candy et al 1985; Rossor et al 1980)
	frontal cortex	decreased (immune-reactivity)	(Candy et al 1985; Davies & Terry 1981)
	hippocampus	decreased (gene expression per cell)	(Dournaud et al 1994)
	Parahippocampal cortex	decreased (neuronal density)	(Dournaud et al 1994)
Parkinson's disease	CSF	decreased	(Dupont et al 1982)
	frontal cortex	decreased (radioimmune-reactivity)	(Epelbaum et al 1988)
	temporal cortex	decreased (immune-reactivity)	(Beal et al 1986)

2.5 SOMATOSTATIN: GENES, NEURONS AND PHARMACOLOGY

2.5.1 Somatostatin signaling

Somatostatin is a modulatory neuropeptide that synergizes with GABA-mediated inhibition, and that specifically targets the distal dendritic compartment of pyramidal neurons in cortical microcircuits (Kawaguchi & Kubota, 1997; Gentet *et al.*, 2012). Somatostatin inhibits release of numerous hormones from the hypothalamus, including CRH (Wang *et al.*, 1987; Patel, 1999). The somatostatin gene product is composed of 14 or 28 amino-acid residues. Both forms of somatostatin, somatostatin-14 and somatostatin-28, are generated by tissue-specific post-translational processing of 116 amino-acid pre-pro-somatostatin peptide (Warren & Shields, 1984; Tostivint *et al.*, 2008). Somatostatin-14 is predominantly produced in the central nervous system (CNS) but also in many peripheral organs (Epelbaum, 1986). Somatostatin-28 is mainly synthesized along the gastrointestinal tract (Fitz-Patrick & Patel, 1981). The 5'-upstream sequence of the *somatostatin* gene contains cyclic-AMP response element (CRE) (Montminy *et al.*, 1986), making its expression activity-dependent. Thus, *somatostatin* expression is preferentially altered by various stressors, such as seizures (Vezzani & Hoyer, 1999; Tallent & Qiu, 2008) and electrical foot shock (Ponomarev *et al.*, 2010). Moreover, mice with conditional homozygous and constitutive heterozygous brain-derived neurotrophic factor (*Bdnf*) knockout or disruption of exon IV-expressing *Bdnf* transcripts show decreased *somatostatin* gene expression (Glorioso *et al.*, 2006; Martinowich *et al.*, 2011; Guilloux *et al.*, 2012), demonstrating that the levels of *somatostatin* expression depend on *Bdnf* function. However, the molecular mechanisms by which this neurotrophic factor controls somatostatin and somatostatin-expressing neurons are still unknown.

Somatostatin, cortistatin and their receptors are closely intertwined systems [(de Lecea *et al.*, 1996; de Lecea *et al.*, 1997), reviewed in (Spier & de Lecea, 2000; de Lecea, 2008)]. Sharing high structural homology with somatostatin, cortistatin binds to all somatostatin receptor subtypes and is known to be regulated by exon IV-expressing *Bdnf* transcripts (Martinowich *et al.*, 2011). However, distinct from somatostatin, cortistatin binds to additional receptors (e.g., growth hormone secretagogue receptor 1a and Mas-related gene X2 receptor) (Robas *et al.*, 2003; Siehler *et al.*, 2008) and has different physiological properties (e.g., activation of cation selective currents not responsive to somatostatin) (Spier & de Lecea, 2000), suggesting that somatostatin and cortistatin may both contribute to affect regulation in an integrated, yet differential mode. The intracellular pathway of somatostatin signaling coupled to all five somatostatin receptors subtypes (Sst_{1-5}) is through the activation of inhibitory G protein (Gi) and the following inhibition of adenylyl cyclase, leading to reduction of cAMP levels, activation of phosphotyrosine phosphatases, and modulation of mitogen-activated protein kinases and phospholipase C (Koch & Schonbrunn, 1984; Koch *et al.*, 1988). Sst_{1-5} present different patterns of coexpression in the brain (Kluxen *et al.*, 1992; Moller *et al.*, 2003) [reviewed in (Martel *et al.*, 2012)].

Sst1 is found in retina, basal ganglia and hypothalamus, Sst2 is highly abundant in several telencephalic structures (neocortex, hippocampus, and amygdala), Sst3 immunoreactivity has only been described in neuronal cilia (Schulz *et al.*, 2000), Sst4 is expressed in olfactory bulb, cerebral cortex and CA1 region of the hippocampus (Schreff *et al.*, 2000), and expression of Sst5 has been detected in cerebral cortex, hippocampus, amygdala, preoptic area, and hypothalamus (Stroh *et al.*, 1999; Strowski *et al.*, 2003; Olias *et al.*, 2004). Interestingly, when co-expressed in the same cells, Sst5 influences Sst2 internalization

and trafficking and modulates cellular desensitization to the effects of somatostatin-14 (Sharif *et al.*, 2007), suggesting that the precise actions of somatostatin depend on the specific interaction of the Sst_{1-5} receptors expressed locally in each brain region.

2.5.2 Genetic polymorphisms in the somatostatin system

The relatively high degree of amino acid conservation across species indicates that somatostatin-related genes have been highly constrained during evolution (Patel, 1999; Olias *et al.*, 2004). Accordingly, there are currently very few reports linking *somatostatin* gene polymorphisms with neurological disorders. A primate-specific single nucleotide polymorphism (SNP) in the human *somatostatin* gene [C/T polymorphism (rs4988514)] is associated with increased risk in Alzheimer's disease progression and additive effect with the APOE epsilon4 allele(Vepsalainen *et al.*, 2007; Xue *et al.*, 2009), although this was not confirmed in larger GWAS studies (Hollingworth *et al.*, 2011; Guerreiro *et al.*, 2013). Leu48Met and Pro335Leu SNPs in the *SST5* gene are of potential significance to patients with bipolar disorder (Nyegaard *et al.*, 2002), but no associations of SST5 SNPs are found in patients with autism (Lauritsen *et al.*, 2003). The paucity of associations with somatostatin gene variants is surprising and may reflect either strong negative selection against genetic variations in this gene, or alternatively, dilution of signal due to heterogeneity of Diagnostic and Statistical Manual of Mental Disorders (DSM)-IV-based cohorts in genetic association studies. So, dimensional phenotypes, as defined by clusters of mood symptoms, which are closer to gene functions may have implications for future genetic studies of somatostatin and other genes.

2.5.3 Somatostatin-expressing neurons: diversity and roles

GABA neurons are a diverse group of inhibitory cells which co-release neuropeptides in order to support a fine-tuning of neuronal signaling and architecture. The local inhibitory circuits provide spatiotemporal control of information processing through at least 20 subtypes of cortical GABA neurons, which are based on their expression of different calcium binding proteins and neuropeptides, localization, targeting, and differential electrophysiological properties. Recent detailed reviews on GABA neuron subpopulations have been published (Csaba & Dournaud, 2001; Di Cristo *et al.*, 2004; Markram *et al.*, 2004; Tan *et al.*, 2008; Fishell & Rudy, 2011; Gentet *et al.*, 2012; DeFelipe *et al.*, 2013; Le Magueresse & Monyer, 2013). Approximately 20-30 % of GABA neurons in the mouse somatosensory cortex express somatostatin (Lee *et al.*, 2010; Rudy *et al.*, 2011), and 40-50 % of GABA neurons contain parvalbumin without overlapping with somatostatin in the frontal cortex, primary somatosensory cortex and visual cortex of mouse (Gonchar *et al.*, 2007; Xu *et al.*, 2010) and the visual cortex of rat (Gonchar & Burkhalter, 1997).

Recent reports focusing on patterns of cortical neuronal connectivity show that somatostatin-expressing interneurons mediate the firing of pyramidal neurons with a fine level of specificity among cortical layers. Integrating optogenetic and electrophysiology approaches, mouse somatostatin-expressing interneurons in layer 2/3 of the somatosensory cortex provide a tonic inhibition to the distal dendrites of excitatory pyramidal neurons by sharpening selectivity during periods of quiet wakefulness, which may contribute to synchronized firing in cortical networks and sensorimotor integration (Gentet *et al.*, 2012). Interestingly, in mouse somatosensory cortex, somatostatin-expressing interneurons show a spatially precise connectivity with pyramidal neurons through direct targeting in layers 2/3 or indirectly through

inhibition of local parvalbumin interneurons in layer 4 (Xu *et al.*, 2013). Moreover, in layers 2/3 of the mouse prefrontal cortex, somatostatin-expressing interneurons compartmentalizes inhibitions of calcium signaling to spine heads, not shafts, suggesting that dendrite-targeting inhibition though somatostatin-expressing interneurons may contribute to downstream cellular processes such as synaptic plasticity (Chiu *et al.*, 2013). In mouse visual cortex, somatostatin-expressing interneurons are found to mediate response levels of specific subsets of pyramidal neurons whereas parvalbumin-expressing neurons alter response gain (Wilson *et al.*, 2012). Parvalbumin-expressing neurons receive excitatory input from the thalamus and make strong synapses on the soma and axons of their target cells (Kawaguchi & Kubota, 1997) to control spike timing of the output neurons. In contrast, somatostatin-expressing neurons mostly do not receive input from thalamus (Beierlein *et al.*, 2003; Cruikshank *et al.*, 2010) and are instead activated through feed-forward mechanisms by activated pyramidal cells. Somatostatin-expressing interneurons preferentially target distal dendrites of pyramidal neurons in layer 2/3 to modulate the processing of incoming sensory information before it is integrated at the soma (Di Cristo *et al.*, 2004; Markram *et al.*, 2004; Tan *et al.*, 2008; Murayama *et al.*, 2009; Xu *et al.*, 2013). Hence, the distinct GABAergic and prototypical inhibitory populations, expressing either parvalbumin or somatostatin, shape the spatiotemporal control of multiple post-synaptic potentials in cortical local circuits, and provide a framework to investigate the role of inhibitory circuits in physiology and pathology.

2.5.4 Genetic approaches to investigate the somatostatin system

Mice mutant for somatostatin were created by deleting the coding region of the pre-pro-somatostatin (the last ten codons of the first exon) (Zeyda *et al.*, 2001). Somatostatin knockout

(KO; Sst^{KO}) mice show intact motor coordination and motor learning, but have a significant impairment in motor learning as demands of motor coordination are increased. Overall, a detailed analysis demonstrated that Sst^{KO} mice are healthy, fertile, and show no overt behavioral phenotypes, including anxiety-like behavior in the open-field and fear conditioning tests. Notably, Sst^{KO} mice display high basal plasma levels of corticosterone and growth hormone (Zeyda *et al.*, 2001), confirming somatostatin-mediated inhibition of HPA axis function. Similarly, mice lacking individual $Sst_{1\text{-}5}$ receptors have been tested in numerous biological functions. Of these, Sst_2 emerged as the primary receptor of interest (Zeyda & Hochgeschwender, 2008), and Sst_2^{KO} mice display increased anxiety-like behavior in the elevated plus maze and open field, increased immobility in the forced swim test, decreased locomotion coupled with an increase of pituitary adrenocorticotropic hormone release instead of growth hormone (Viollet *et al.*, 2000). In line with the observed changes in Sst_2^{KO} mice, acute predator stress in rats led to up-regulated *Sst*$_2$ gene expression in the amygdala and ACC, shown correlated with Fos expression in the amygdala (Nanda *et al.*, 2008). As the product of a different gene, cortistatin shares a high structural and functional similarity with somatostatin-14 (de Lecea *et al.*, 1996; de Lecea *et al.*, 1997). Notably, compared with the weak inhibitory effects of somatostatin on the basal release of CRH from rat hypothalamus and hippocampus, cortistatin exhibits strong inhibition of the expression and release of basal CRH (Tringali *et al.*, 2012). These findings suggest that Sst2 may regulate affective phenotypes and HPA axis responses both through somatostatin and cortistatin. Given the limitations of human studies, Sst^{KO} mice provide an opportunity to explore the causal role of somatostatin in affect dysregulation and the underlying neural mechanisms. Such insights, however, will require systematic behavioral characterization with fine spatial and temporal resolution by including female cohorts and

region-specific manipulation at different developmental stages. Based on the published studies to date, it is still unclear whether these mutants recapitulate behavioral features of mood disorders. Knowing the effects of somatostatin signaling on neuroendocrine regulation, future studies need to assess the molecular and cellular systems that somatostatin mutations converge upon, and where the exact neural circuits are affected. Moreover, combining genetic and environmental factors in animal models is critical to enhance the accuracy of disease modeling and translational efforts. For example, acute or chronic exposure to stress or to stress hormones may capture how such etiological factors determine the vulnerability to develop high behavioral emotionality, in contrast to baseline behavioral testing. In addition, mood disorder-related sex differences are observed in community-based epidemiological studies, where the factor of seeking treatment is removed (Kornstein *et al.*, 2000; Leach *et al.*, 2008) and findings of low somatostatin in the amygdala appear more robust in postmortem studies of female MDD subjects (Tripp *et al.*, 2012), suggesting that gender/sex may represent a biological predisposing factor, or at least a moderating factor, in the intrinsic vulnerability of the somatostatin system.

Although many mood disorders emerge during adolescence (Paus *et al.*, 2008), behavioral abnormalities including affect dysregulation are often heritable and apparent before diagnostic criteria are met (McGuffin *et al.*, 2003; Geller *et al.*, 2006). It is unclear when somatostatin deficits occur and potentially begin to contribute to the formation of affective symptoms. Tracking somatostatin system using new anatomic techniques with refined cellular definition, from Brainbow (Livet *et al.*, 2007) to CLARITY(Chung *et al.*, 2013) and SeeDB (Ke *et al.*, 2013), across different developmental stages may help identify age-dependent neural architecture and disease mechanisms related to somatostatin function.

2.5.5 Somatostatin analog development and pharmacological studies

As native somatostatin peptides have a very short half-life time (approximate 1-3 minutes) (Sheppard *et al.*, 1979), long-acting and highly potent somatostatin analogues are currently available for the treatment of acromegaly and neuroendocrine tumors, including octreotide (long-acting; LAR-OCT) (Bauer *et al.*, 1982) and Lanreotide (slow release or autogel) (Bevan, 2005; Molitch, 2008). Compared to somatostatin, pharmacological tools of the five somatostatin receptor subtypes have lagged behind, partly due to the lack of high-affinity antagonists.

In addition, several novel somatostatin therapy models are available: 1) Universal somatostatin (Schmid & Schoeffter, 2004): a somatostatin molecular analog with high binding affinity to all or most human somatostatin receptors. An example is SOM230, which interacts with $Sst_{1,2,3,5}$ and particularly potent at Sst_5 compared with LAR-OCT; 2) Chimeric somatostatin/dopamine molecule (Saveanu *et al.*, 2002; Pivonello *et al.*, 2005): a somatostatin and dopamine hybrid agonist, based on reports that dopamine and somatostatin receptors can hetero-oligomerize to enhance functional responses (Rocheville *et al.*, 2000). An example is BIM-23A760, which accelerates the suppression of growth hormone and adrenocorticotropic hormone by the interaction with Sst_2 and Drd2 simultaneously; 3) Chimeric-somatostatin vaccinations (Haffer, 2012): a fusion protein expressing chloramphenicol acetyl transferase protein and somatostatin. Two somatostatin vaccinations, JH17 and JH18, can effectively reduce weight gain and reduce final body weight percentage of normal, non-obese mice and mice with diet-induced obesity via the intra-peritoneal route; 4) Non-peptide antagonists, such as SRA880 (Sst_1 selective), ACQ090 (Sst_3 selective) and Sst_4 selective β peptide agonists (Rivier *et al.*, 2003; Hoyer *et al.*, 2004). Despite this extensive list, the practical use of somatostatin in the brain is hampered by the multiple effects of the peptide, by the need for small molecules targeting

specific, high affinity receptors on the target cells in specific brain regions, and by the need for feasible routes of administration that lead to fast delivery into the brain.

The potential for using somatostatin analogues as treatment in the CNS is emerging for treatment of epilepsy (Vezzani & Hoyer, 1999; Tallent & Qiu, 2008), pain (Mollenholt *et al.*, 1994; Taura *et al.*, 1994), headaches (Sicuteri *et al.*, 1984; Kapicioglu *et al.*, 1997); potential use for treatment of mood disorders is suggested by reversal of emotion-like behaviors in rodent models. Several pharmacological studies support a role of somatostatin in affect regulation. Intra-ventricular administration of somatostatin in rats produces anxiolytic- and antidepressant-like behaviors in the elevated plus-maze and forced swim tests, and a neurophysiological signature of anxiolytic drugs (e.g., reduction of theta frequency and theta frequency curve slope) (Engin *et al.*, 2008). Mice with intra-amygdalar and intra-septal microinfusions of somatostatin-14 and somatostatin-28 display reduced anxiety-like behavior in the elevated plus-maze and shock-probe tests (Yeung *et al.*, 2011). Moreover, anxiolytic effects in the elevated plus-maze test are described after intra-cerebroventricular infusions of a selective Sst_2 receptor agonist, but not after infusions of the other four receptor agonists; antidepressant-like effects in the forced swim test are observed following infusions of either Sst_2 or Sst_3 agonists (Engin & Treit, 2009). Another agent to enhance somatostatin functioning, SRA880 (an antagonist of auto-receptor Sst_1), synergizes with imipramine in causing antidepressant-like effects in the tail suspension test and increases *Bdnf* mRNA expression in the mouse cerebral cortex (Nilsson *et al.*, 2012).

2.5.6 Effects of antidepressants on somatostatin in the CNS

Significant efforts have been directed toward the characterization of the downstream targets of antidepressant treatment, with a focus on somatostatin. A recent study demonstrates that chronic

imipramine treatment increases somatostatin expression in mouse hypothalamus (Nilsson *et al.*, 2012). However, there is inconsistency regarding the effect of chronic citalopram treatment on somatostatin levels in rats (Kakigi *et al.*, 1992; Prosperini *et al.*, 1997; Pallis *et al.*, 2006; Pallis *et al.*, 2009). Repeated administration of imipramine, maprotiline, mianserin, carbamazepine or zotepine has no effect on somatostatin levels in various brain regions of rats (Weiss *et al.*, 1987; Kakigi *et al.*, 1992).

While some somatostatin receptors seem to exert anxiolytic or antidepressant-like effects, there is no direct evidence supporting somatostatin receptors as downstream targets of current antidepressants. Together, these findings suggest that somatostatin levels are mostly unchanged by antidepressants. It is unclear whether somatostatin, GABA, or GABA functioning in somatostatin-expressing interneurons may be the real mediators or antidepressant targets. Future studies are needed to determine the involvement of somatostatin receptors and associated intracellular signaling pathways in the therapeutic effects of antidepressants, or whether somatostatin effects are independent of current antidepressant modalities.

2.6 POTENTIAL MECHANISMS OF SELECTIVE VULNERABILITY OF SOMATOSTATIN-EXPRESSING INTERNEURONS

It is possible that low somatostatin in diseases acts as a biomarker for deregulated function of somatostatin-expressing neurons. As such, it is essential to identify upstream factors responsible for the dysfunction of somatostatin-expressing interneurons in neurological diseases. We speculate that intrinsic cellular properties in somatostatin-expressing neurons may determine their selective vulnerability to various insults. Pathways underlying this high vulnerability may

include high intrinsic oxidative stress related to mitochondria, high sensitivity to inflammation, high dependence on neurotrophic environment, and cellular developmental and aging processes. These canonical pathways might provide novel cell-based perspectives in the treatment of affected somatostatin-expressing cells across neurological disorders.

2.6.1 Oxidative stress and mitochondrial dysfunctions

Oxidative stress produced by mitochondria during respiration is a common pathogenic mechanism implicated in neurological disorders (Sorce & Krause, 2009; Stefanescu & Ciobica, 2012). Depressed states in mood disorders are associated with decreased brain energy generation (Baxter *et al.*, 1985; Baxter *et al.*, 1989). Dysfunctional mitochondria together with the oxidative stress accumulation has been proposed to synergistically contribute to the neuro-endangerment processes underlying depression (Gardner *et al.*, 2003; Burnett *et al.*, 2005) and neurodegenerative diseases (Lin & Beal, 2006; Mancuso *et al.*, 2007; Petrozzi *et al.*, 2007). Similarly, high baseline oxidative stress could be an intrinsic characteristic of vulnerable neuronal populations. Notably, neuronal nitric oxide synthase (nNOS) and NADPH diaphorase (NADPHd), two enzymes that produce reactive oxidative species, are extensively and almost exclusively co-localized with somatostatin and neuropeptide Y (Dun *et al.*, 1994; Figueredo-Cardenas *et al.*, 1996; Jaglin *et al.*, 2012), hence providing a neurochemical basis for high susceptibility of somatostatin-expressing neurons to generate oxidative stress in response to pathophysiological insults.

2.6.2 High dependence on neurotrophic environment

BDNF and its receptor neurotrophic tyrosine kinase receptor type 2 (TrkB) have been implicated in mood disorders (Guilloux *et al.*, 2012; Tripp *et al.*, 2012). BDNF-TrkB signaling is one of the key mediators for maintaining normal *somatostatin* gene expression (Glorioso *et al.*, 2006; Martinowich *et al.*, 2011).Progressively decreasing BDNF-TrkB signaling in patients with mood disturbances may directly impact the biology of somatostatin-expressing neurons, resulting in somatostatin deficits. In addition, Bdnf-TrkB signaling itself is vulnerable to increased inflammation (Goshen *et al.*, 2008; Koo & Duman, 2008; Song & Wang, 2011) and high glucocorticoid insults (Hodes *et al.*, 2012). Mild oxidative stress inhibits tyrosine phosphatases activity (Barrett *et al.*, 2005), potentially leading to impaired TrkB downstream signaling. Cortistatin and neuropeptide Y expression partly overlaps with the somatostatin neuron population in rodents (Figueredo-Cardenas *et al.*, 1996; de Lecea *et al.*, 1997; Xu *et al.*, 2010). Comparing the profile of gene changes between subjects with MDD and mice with genetically-altered Bdnf signaling suggest that the reduced *somatostatin*, *neuropeptide Y* and *cortistatin* are partly downstream from a combination of reduced constitutive and activity-dependent Bdnf signaling (Guilloux *et al.*, 2012). In contrast, markers for other GABA neuron subtypes targeting the perisomatic area region cell body and axon initial segment of pyramidal neurons (i.e., cholecystokinin and calretinin), appear to be independent of BDNF signaling and unaffected in MDD patients (Guilloux *et al.*, 2012; Tripp *et al.*, 2012). Hence, it is possible that the somatostatin-specific cellular function and vulnerability are partly mediated by BDNF-TrkB signaling during both physiological and pathological processes of affect regulation.

2.6.3 Inflammation and cellular aging

Inflammation has been implicated as a contributing factor in the onset and progression of many neurological disorders (Di Filippo *et al.*, 2008). Mood disturbances are associated with an activated inflammatory response system (Padmos *et al.*, 2008; Miller *et al.*, 2009), including increased levels of peripheral interleukins and tumor necrosis factor-alpha in MDD patients (Kaestner *et al.*, 2005; Howren *et al.*, 2009; Dowlati *et al.*, 2010; Maes, 2011). Inflammatory illnesses are associated with more depressive episodes (Celik *et al.*, 2010; Maes *et al.*, 2012), suggesting that prior depression may sensitize inflammatory responses. Patients treated with inflammatory cytokines, such as interferon-α, are at greater risk of developing depressive episodes (Castera *et al.*, 2006; Lotrich *et al.*, 2007). Somatostatin released from sensory nerves and somatostatin receptors on peripheral blood mononuclear cells play a crucial role in anti-inflammation through inhibition of pro-inflammatory peptide release (Szolcsanyi *et al.*, 1998; Kurnatowska & Pawlikowski, 2000; Helyes *et al.*, 2004). Rats with chronic inflammation induced by lipopolysaccharide show decreased hippocampal *somatostatin* expression (Gavilan *et al.*, 2007). It is possible that there is crosstalk among peripheral inflammation, somatostatin function, and central effects of somatostatin-expressing neurons. Hence, decreasing somatostatin expression due to cellular impairment in the progress of neurological diseases may further enhance inflammation in a vicious cycle, leading to exacerbated cellular vulnerability of somatostatin-expressing neurons.

Aging is associated with a considerable increase in an activated, pro-inflammatory state (Wei *et al.*, 1992; Bruunsgaard & Pedersen, 2003), a decline in circulating levels of Bdnf (Erickson *et al.*, 2010), and increased oxidative damage (Sohal & Weindruch, 1996). *Somatostatin* expression is significantly decreased with age in human cortical regions, but

parvalbumin expression is not altered by age (Erraji-Benchekroun *et al.*, 2005; Glorioso *et al.*, 2011). Similarly, the number of hippocampal somatostatin-expressing interneurons decreases in aged rats, but the number of parvalbumin-expressing neurons remains the same (Vela *et al.*, 2003). Somatostatin and IL-1β mRNA expression are negatively correlated in aged hippocampus of rats (Gavilan *et al.*, 2007). Comparing the effects of aging on *somatostatin* expression in the sgACC, an accelerated reduction is found in patients with major depression compared to normal aging subjects (Tripp *et al.*, 2012), suggesting a pattern resulting in an early aging phenomenon which we have speculated may be synergistically induced by normal age-related changes and depression-related pathological change (Douillard-Guilloux *et al.*, 2013).

2.7 CONCLUSION

Here we have focused on somatostatin, a GABA marker, down-regulated in MDD, schizophrenia, bipolar disorder, and neurodegenerative diseases. Exploring cross-disease molecular (somatostatin) and cellular units (somatostatin-expressing interneurons) pathological findings suggests a dimensional pathological phenotype that is specific to the somatostatin gene/cell biological entity rather than to categorical brain disorders. Based on these results we speculate that a common mechanism affecting somatostatin and somatostatin-expressing neurons may impact information processing by the local inhibitory cell circuit in cortical regions (Figure 1). Clarifying the role of somatostatin and its regulation of GABA inhibition in affect regulation would provide new strategies for predicting, delaying, and treating neurological diseases with mood disturbances. A number of questions remain. For example, are the prevalent somatostatin deficits seen in multiple diseases reflected in a common symptom dimension, such as low mood,

across neurological diseases? What are the critical events that determine the vulnerability of somatostatin-expressing neurons? And what are the pathogenic mechanisms that mediate the observed disease-related molecular and cellular phenotypes? One possibility is that inflammation, oxidative stress, aging, and reduced neurotrophic support may all converge to affect somatostatin-expressing neurons. Targeting these pathways may exert neuro-protective effects on somatostatin-expressing neurons, as a potential therapeutic approach with implications for several neuropsychiatric disorders and neurodegenerative diseases.

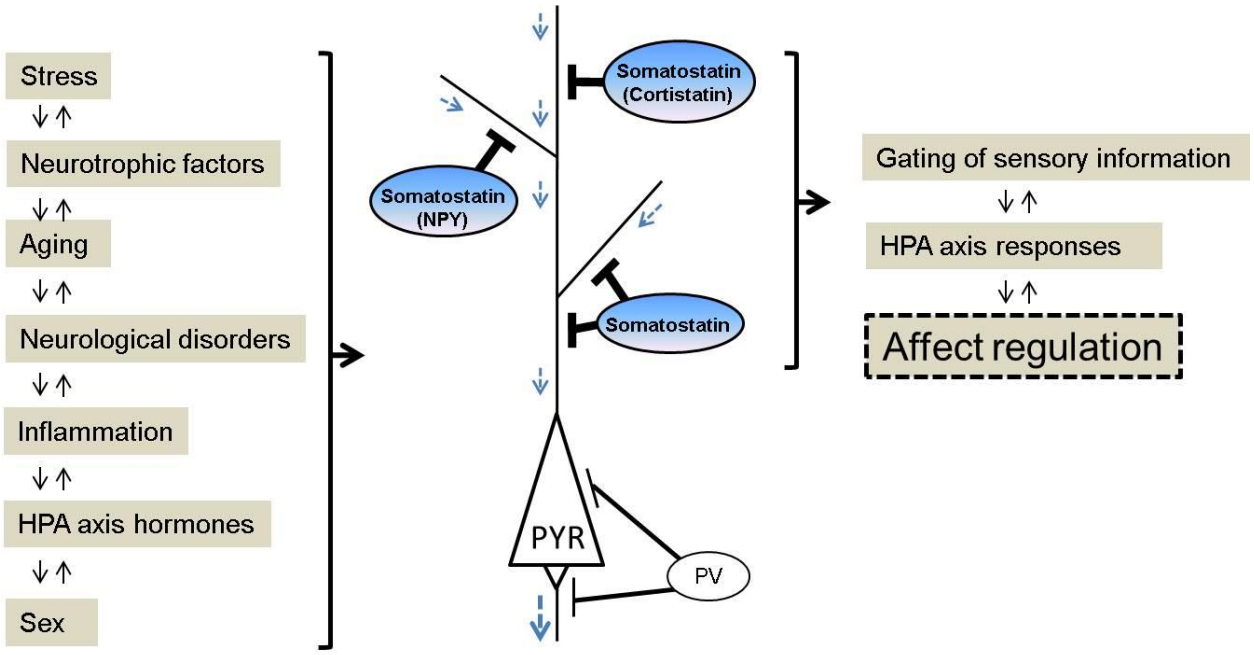

Figure 1. Schematic of somatostatin signaling, pathological regulators and biological functions relevant to affect regulation.

Somatostatin pathway activity is responsive to (left panel), and regulates (right panel), several biological events, and molecular and cellular properties that have been linked to mood disturbances. Somatostatin and somatostatin-expressing interneurons are key conduits for somatostatin signaling regulation and output. *NPY*, neuropeptide Y; *PYR*, pyramidal neuron; *PV*, parvalbumin.

3.0 CAUSAL ROLE OF SOMATOSTATIN IN MOOD REGULATION

3.1 ABSTRACT

SST deficits appear to be a common feature of depression and other neurological disorders with mood dysregulation. However, whether SST deficits play a causal role in mood dysregulation is not clear. Consequently, in this study we used a battery of behavioral tests to characterize anxiety/depressive-like behaviors in SST knockout (Sst^{KO}) mice at baseline and after exposure to 6 weeks of unpredictable chronic mild stress (UCMS). In addition, we explored the molecular phenotypes associated with mood dysregulation in mice with low SST. Under baseline unstressed conditions, compared to Sst^{WT} mice Sst^{KO} mice showed increased latency to begin eating in the novel suppressed feeding (NSF) test and elevated overall behavioral emotionality. After UCMS treatment, increased latency to feed in the NSF test and higher emotionality were found in stressed Sst^{KO} mice compared to stressed Sst^{WT} mice. In addition, when compared to non-stressed Sst^{WT} mice, non-stressed Sst^{KO} mice exhibited molecular changes in the cingulate cortex, including low expression of *Cort*, *Bdnf*, and *Gad67*. On the other hand, non-stressed Sst^{HZ} mice showed elevated *Cort* and reduced *Bdnf* expression. The compensatory upregulation of *Cort* may account for generally better preserved SST functions in Sst^{HZ} mice. Together, these findings support the hypothesis that SST deficits play a causal role in mood dysregulation.

3.2 INTRODUCTION

Converging evidence from susceptibility genes is beginning to slowly uncover the polygenetic mechanisms underlying the pathophysiology of mood dysregulation. For instance, somatostatin (SST; also called SOM or SRIF) deficits are frequently observed in neurological disorders with mood disturbances, such as schizophrenia, bipolar disorder and Alzheimer's disease (Martel *et al.*, 2012; Lin & Sibille, 2013). In depression, *Sst* gene expression is robustly affected in the prefrontal cortex, cingulate cortex, and amygdala, three brain regions involved in mood regulation (Sibille *et al.*, 2011; Tripp *et al.*, 2011; Guilloux *et al.*, 2012).

SST is an inhibitory modulatory neuropeptide that is co-expressed with gamma-aminobutyric acid (GABA). SST-expressing interneurons preferentially target the dendrites of pyramidal neurons (Hendry *et al.*, 1984; Melchitzky & Lewis, 2008; Xu *et al.*, 2010). Thus, it has been hypothesized that SST neurons regulate information input by providing spatiotemporal integration of postsynaptic potential in local cortical circuits (Gentet *et al.*, 2012; DeFelipe *et al.*, 2013; Le Magueresse & Monyer, 2013). Biological stressors, such as seizure or electrical foot shock, can selectively affect SST interneurons or *Sst* expression (Vezzani & Hoyer, 1999; Ponomarev *et al.*, 2010). Moreover, brain-derived neurotrophic factor (BDNF) signaling, a key pathway for the maintenance of normal *Sst*- and other GABA- related gene expression is reduced in depression (Grosse *et al.*, 2005; Glorioso *et al.*, 2006; Martinowich *et al.*, 2011). MDD-related phenotypes may represent distal effects of these multiple genes.

Here, we utilized elevated plus maze (EPM), open field (OF), novelty-suppressed feeding (NSF), and sucrose preference (SP) test in mice lacking Sst (Sst^{KO}) mice to characterize trait (baseline) and state (after UCMS) anxiety/depressive-like behavioral phenotypes. Z-score normalization was applied to summarize quantitative phenotypes in behavioral tests. In addition,

we utilized real-time qPCR to investigate the molecular phenotypes associated with mood dysregulation, including expression of *Sst, Npy, Cortistatin, Gad67, Bdnf* in the cingulate cortex in mice with low SST.

3.3 MATERIALS AND METHODS

3.3.1 Animals

By crossing with Sst^{HZ} mice, littermates *of* Sst^{KO}, Sst^{HZ} and Sst^{WT} were used in these studies. Sst^{KO} mouse line was previously generated and purchased from the Jackson Laboratory (stock no. 008117) (Zeyda *et al.*, 2001). Genotypes were identified by Polymerase Chain Reaction (PCR) analysis of DNA isolated from tail cuts. Cohort 1 consisted of 27 mice [18 Sst^{WT} (9 males, 6 females), Sst^{KO} (6 males, 6 females)] and was used exclusively for the behavioral assessments. Accordingly, cohort 1 was tested for behavioral phenotypes in the EPM, OF, NSF, and SP at 3 months of age, before and after stress treatment. Cohort 2 consisted of 36 mice [16 Sst^{WT} (8 males, 11 females), 20 Sst^{KO} (8 males, 9 females)] and was used to validate behavioral phenotypes using the same battery of tests. Cohort 3 consisted of 48 mice (n =16 per genotype, 8/sex), and was used to examine molecular phenotypes. The use of animals, including all treatments, was conducted in compliance with the NIH laboratory animal care guidelines and with protocols approved by the Institutional Animal Care and Use Committee of University of Pittsburgh. All experiments were performed with 3- to 5 month-old male and female littermates. All mice were cared under standard conditions (12/12-hour light/dark cycle, lights on at 07:00 h), 22 ± 1°C, with food and water *ad libitum*).

3.3.2 Unpredictable chronic mild stress

To receive UCMS treatment, mice were subjected to six weeks of a random schedule consisting of 1-3 environmental stressors per day, seven days per week (Surget *et al.*, 2009). Stressors included repeated bedding change, no bedding, reduced housing space, forced bath (~2 cm of water in cage), wet bedding, aversive smell (exposure to fox or bobcat urine), social stress (rotate mice into previously occupied cages or single-housing), 45° tilted cage, and mild restraint (stay in 50-ml falcon tube with air hole). Weekly assessment of weight and fur was performed to monitor physiological progression of the UCMS syndrome. The social isolation treatment began from the fifth week of UCMS until the day of euthanasia.

3.3.3 Behavior

Anxiety/depressive-like behaviors were tested in the elevated plus maze (EPM), open field (OF), novelty suppressed feeding (NSF), and sucrose preference test (SP) in the following order for each mouse: EPM, OF, NSF, SP, separated by a minimum of 1 day. All tests were performed during the light phase of the circadian cycle, between 9 am and 3 pm.

Elevated plus maze (EPM)

Anxiety-like behaviors and locomotion were measured in a cross maze with two open and two closed arms (30 cm x 5 cm) as previously described (Sibille *et al.*, 2000). Entries and time spent in the open arms were recorded for 10 min to assess anxiety-like behaviors. Total number of entries was assessed as an index of locomotion.

Open field (OF)

Anxiety-like behaviors and locomotion were measured in a 76 x 76 cm chamber divided in 16 even-size squares and monitored for 10 min using the Any-maze video-tracking software (Stoelting, Wood Dale, IL). Percentage of walking distance and time spent in the four center squares were assessed to evaluate anxiety-like behaviors. Total walking distance in the chamber was used as an index of locomotion.

Novelty suppressed feeding (NSF)

Anxiety/depressive-like behaviors were measured for 11 min in a 76 x 76 cm chamber, with a food pellet in the bright-lit center. The drive to overcome the aversive center was increased by 16 hours of food deprivation before testing. The latency to start eating the food pellet was measured as an index of anxiety/depressive-like behaviors. Food consumption in the home cage for six minutes after the test was used as a measure for appetite after NSF testing and food deprivation.

Sucrose preference test (SP)

The sucrose test was performed using a two-bottle test: a bottle filled with a 2% sucrose solution and a bottle filled with water. Mice had free access to both water and a 2% sucrose solution 48 hours before the test in their home cage to reduce neophobia. For the next two days, a sucrose preference/consumption test began in a new single-house cage for 16 h from 18:00 pm-10:00 am. Position of bottles was counterbalanced across the left and the right sides from test to test. Sucrose preference (percent) was calculated as follows: preference = [sucrose solution intake

(ml)/total fluid intake (ml)] × 100. Sucrose consumption was calculated as: consumption = [sucrose solution intake (ml)/ body weight (g)].

Z-scoring

To investigate the consistency of behavioral performance across related tests, emotionality- or locomotion- related data were normalized using a Z-score methodology (Guilloux *et al.*, 2011). Z-scores calculate how standard deviation (σ) and observation (X) is above or below the mean of the control group (μ). Raw measures for EPM (time in open arm; % crosses into open arm), OF (time in center; % distance in the center), NSF (latency to feed), and SP (sucrose consumption and sucrose preference) were converted to standard deviations relative to respective means of the control group (Sst^{WT} mice). The directionality of scores was adjusted so that decreased score values indicated reduced anxiety/depressive-like behaviors (termed emotionality). Finally, values across tests were averaged for each mouse to produce individual emotionality Z-scores. Locomotion Z-scores were similarly applied and obtained from EPM (total crosses) and OF (Total distance traveled) data.

3.3.4 Physiological Evaluation

The body weight and coat state of all the animals were assessed and scored (0-2 points) weekly by a double-blinded experimenter until the end of the UCMS treatment. The total score of the coat state resulted from the sum of the score of five different body parts: head, neck, dorsal and ventral fur, tails and paws. A score of 0 was given for a well-groomed fur and increased to 2 for an unkempt fur.

3.3.5 Estrous phase

Female mice were assessed for estrous phase on the day of behavioral testing (EPM, OF, NSF, SP) to control for potential effects of hormonal fluctuations on behavior. Estrus, metestrus, diestrus, and proestrus were determined via vaginal cytology.

3.3.6 Real-time quantitative polymerase chain reaction

Brains were flash frozen on dry ice after sacrifice. Bilateral cingulate cortex (between bregma + 1.42 to -0.5 mm; **Figure 2**) was obtained using a cryostat and a 1-mm-bore tissue punch.

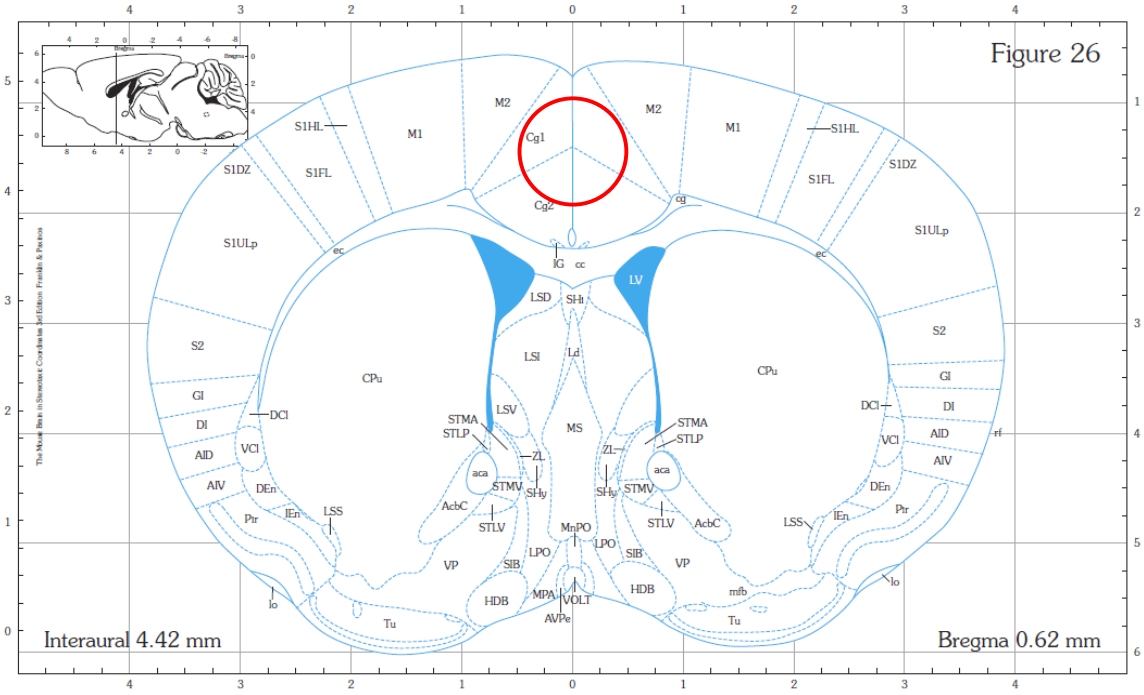

Figure 2. Coronal section of mouse brain.

Aadapted from "The mouse brain" G. Paxinos, (2008). For sampling of mouse cingulate cortex, the tissue punch was placed in the circled area. *Cg1*: cingulate cortex, area 1. *Cg2*: cingulate cortex, area 2.

Total RNA from mouse cingulate cortex was extracted using the RNeasy Micro Kit (Qiagen) according to the manufacturer's instructions. Reverse transcription reaction was performed using the qScript cDNA Supermix (Quanta Biosciences, Gaithersburg, MD). As previously described (Sibille *et al.*, 2009b), all validated primer sets were listed in Table 2 (Tripp *et al.*, 2012). The comparative threshold cycle (Ct) measurement was performed for quantification with SYBR green fluorescence signal (Invitrogen, Carlsbad, CA) using a Mastercycler® ep Realplex2 real-time PCR machine (Eppendorf, Westbury, NY). PCR thermal cycling was 65°C to 59°C touch-down followed by 40 cycles (95 ˚C for 10 sec, at 59 ˚C for 10 sec, and 72 ˚C for 10 sec). Samples were run in triplicate and the difference in cycle threshold (ΔCt) values for each GABA/BDNF-related transcript was determined by comparison to the geometric mean of three control genes (actin, GAPDH, cyclophilin). The relative expression level of each targeted transcript was determined as 2^{-dCt}.

Table 2. Primer pairs.

Gene	Accession	Size	Forward primer	Reverse primer
Neuropeptide Y (Npy)	NM_023456.2	146	CAGCCCTGAGACACTGATT	AGATGAGATGAGGGTGGAAA
Cortistatin (Cort)	NM_007745.3	72	CCTTCTCCTCGTGCAAGTA	AGGTCTCGTTGGCATCTC
Brain-derived neurotrophic factor (Bdnf)	NM_001048139.1	159	CATTGAGCTCGCTGAAGTTG	ACCTGGTGGAACTTCTTTGC
Glutamic acid decarboxylase 67 (GAD67)	NM_008077.4	76	AGACCTCCGATACACTGACC	TGCACACCCTAAATGCAC

3.3.7 Statistical analysis

Statistical analyses were carried out using GraphPrism Version 6.0 (Graph Pad. Software Inc., San Diego, CA, USA). Student's *t* test was used to compare means between two groups. Correlations between food consumption and emotionality/latency to feed were assessed by Pearson correlation. All data are expressed as means ± standard error of the mean. Statistical significance was set at $p < 0.05$. Sst^{KO} mice display high baseline/trait emotionality.

3.4 RESULTS

3.4.1 *Sst*^{KO} mice display high baseline/trait emotionality

To investigate the role of SST in mood regulation, we characterized baseline/trait anxiety/depressive-like behaviors in *Sst*^{KO} mice under baseline unstressed conditions. We employed emotionality z-scores to summarize the results from different behavioral tests. For the first analysis, results from independent tests were as follows: in the EPM, *Sst*^{KO} mice spent comparable time in and had a comparable number of entries into the open arms; in the OF, *Sst*^{KO} mice spent significantly less time ($p < 0.05$) and entered proportionately less often ($p < 0.05$) into the center compared to controls); in the NSF, *Sst*^{KO} mice had significantly increased latencies to eat the pellet ($p < 0.01$); in the SP, *Sst*^{KO} mice had normal sucrose consumption and preference (**Figure 3**).

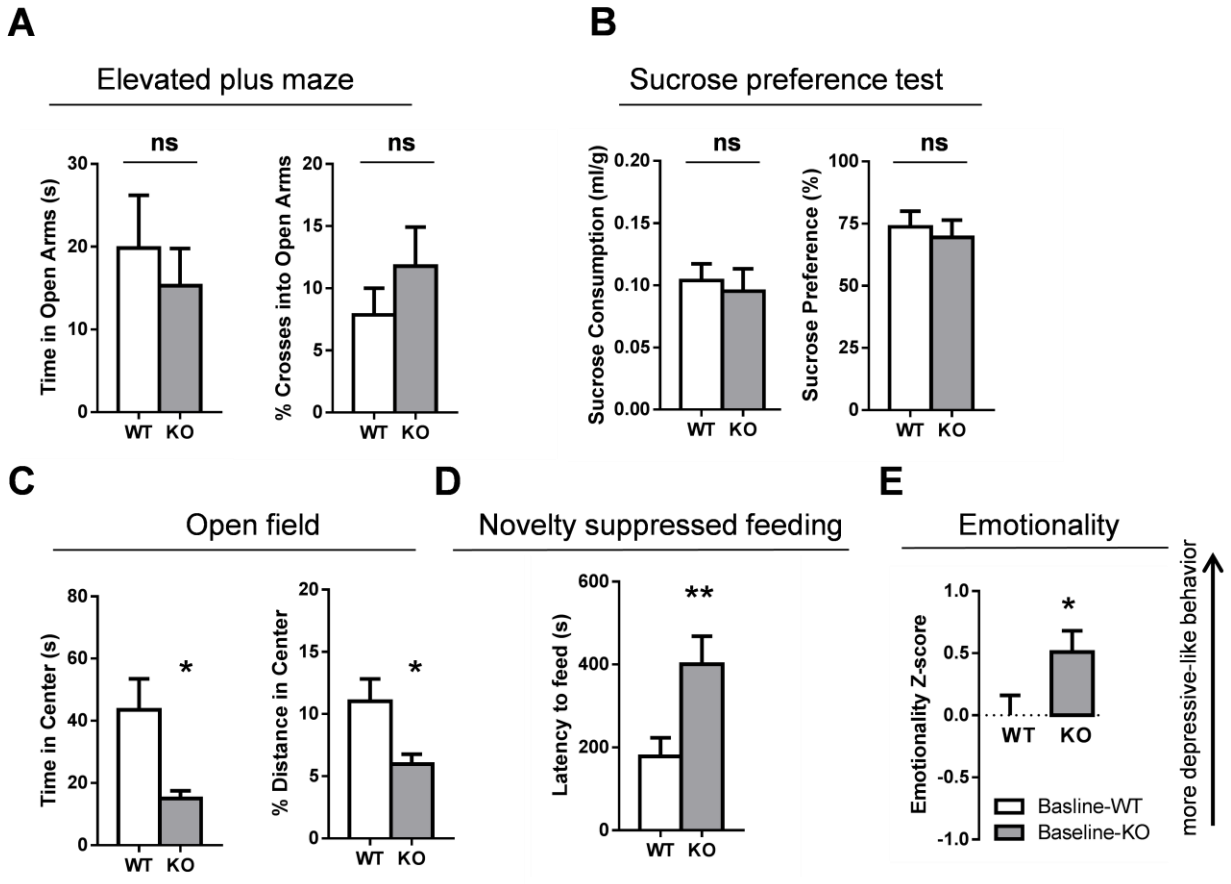

Figure 3. Assessment of anxious/depressive-like behaviors in non-stressed *Sst*^{KO} mice.

Behavioral phenotypes, including anxious/depressive-like behaviors, overall emotionality scores in the elevated plus maze (EPM; A), sucrose preference test (SP; B), open field (OF; C), and novelty suppressed feeding test (NSF; D) were examined in *Sst*^{KO} and wild-type mice at baseline. Overall emotionality Z scores were summarized (E). * p <0.05, ** p <0.01. Error bars represent the standard error of the mean (N=12-15/genotype, 6-9 mice/sex).

3.4.2 *Sst*^{KO} mice display normal locomotion

While EPM and OF emotionality measures were controlled for locomotion, we found that *Sst*^{KO} mice displayed normal total entries in the EPM and total traveled distance in the OF. Consistent with a prior report (Zeyda *et al.*, 2001), non-stressed *Sst*^{KO} mice showed normal locomotion. We used a locomotion z-score to summarize results in the EPM and OF tests for locomotion (**Figure**

4). As there were no differences in locomotion, baseline/trait emotionality in *Sst*^{KO} mice was unlikely to reflect deficits of locomotion.

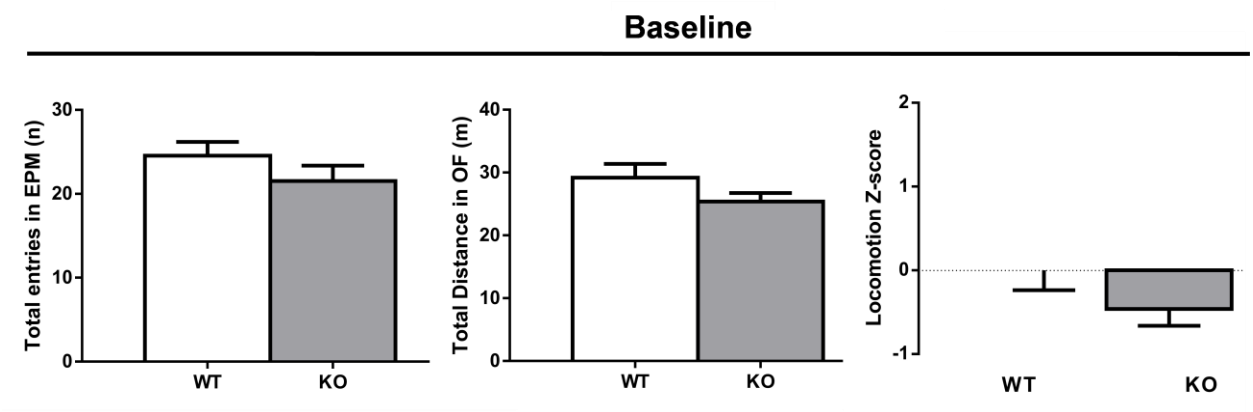

Figure 4. Assessment of locomotion in non-stressed *Sst*^{KO} mice.

Locomotion, including total entries in the elevated plus maze (EPM; left) and total distance in the open field (OF; middle), and overall locomotion scores (right), was examined in *Sst*^{KO} and *Sst*^{WT} mice. Error bars represent the standard error of the mean (N=12-15/group, 6-9 mice/sex).

3.4.3 *Sst*^{KO} mice display normal physiological responses to chronic stress

Chronic stress exposure is an exogenous, risk factor associated with mood symptoms (Keller *et al.*, 2007), and its interaction with endogenous, genetic risk factors is shown to increase susceptibility to mood dysregulation (Caspi *et al.*, 2003). UCMS is a well-validated paradigm that increases anxiety/depressive-like behaviors in mice and that induces neuroendocrine and molecular changes associated with major depression (Surget *et al.*, 2009). To investigate the effects of *Sst* ablation on behavioral emotionality in response to stress, we exposed the same cohort of mice to UCMS.

The progressive degradation of the fur coat quality clearly indicated that both groups significantly responded to UCMS (**Figure 5A**). Moreover, UCMS-induced coat changes and weight (**Figure 5B**) did not differ across groups, together demonstrating that the elevated

behavioral emotionality phenotype of *Sst*^{KO} mice did not correlate with any overall physical changes.

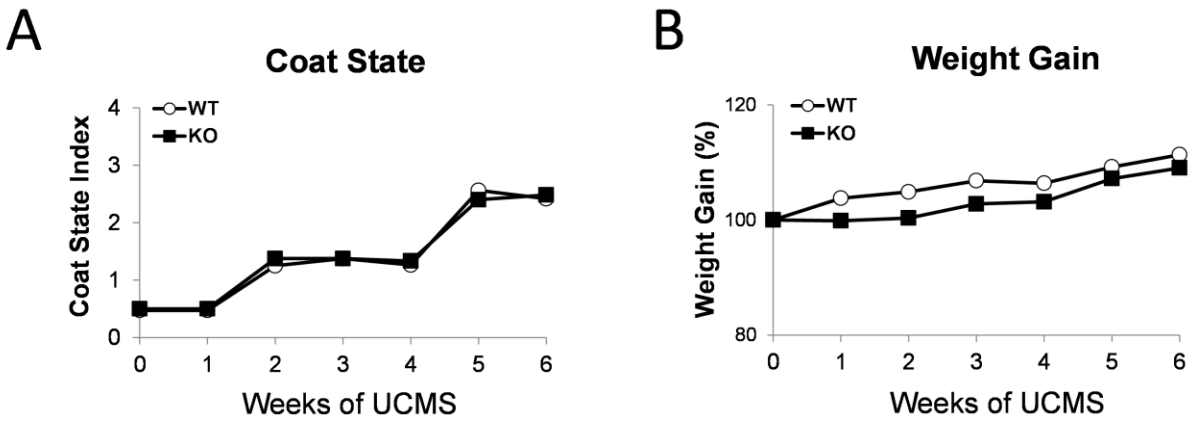

Figure 5. Assessment of changes in coat state and body weight during unpredictable chronic mild stress.

(A) The increased fur coat degradation clearly indicated that both groups significantly responded to unpredictable chronic mild stress (UCMS), and no differences between *Sst*^{KO} and wild-type (WT) mice. (B) No differences in weight gain between *Sst*^{KO} and *Sst*^{WT} mice. (N=12-15/group, 6-9 mice/sex).

3.4.4 Sst^{KO} mice display high state emotionality after chronic stress

Behavioral testing in the last two weeks of the 8-week UCMS protocol found increased latency to feed in the NSF test (**Figure 6D)** and higher emotionality z-scores ((**Figure 6E**) in stressed *Sst*^{KO} mice, compared to stressed *Sst*^{WT} mice. Although normal variability in behavioral testing precluded comparison of absolute values across time in a longitudinal study design (baseline followed by post-UCMS behavioral testing), we did not find any genotype by stress interaction, instead *Sst*^{KO} mice maintained a similarly higher behavioral emotionality over *Sst*^{WT} littermates under baseline unstressed [1.51 ± 0.17 fold (s.e.m.) relative to control] and stressed conditions [1.69 ± 0.11 fold (s.e.m.) relative to control].

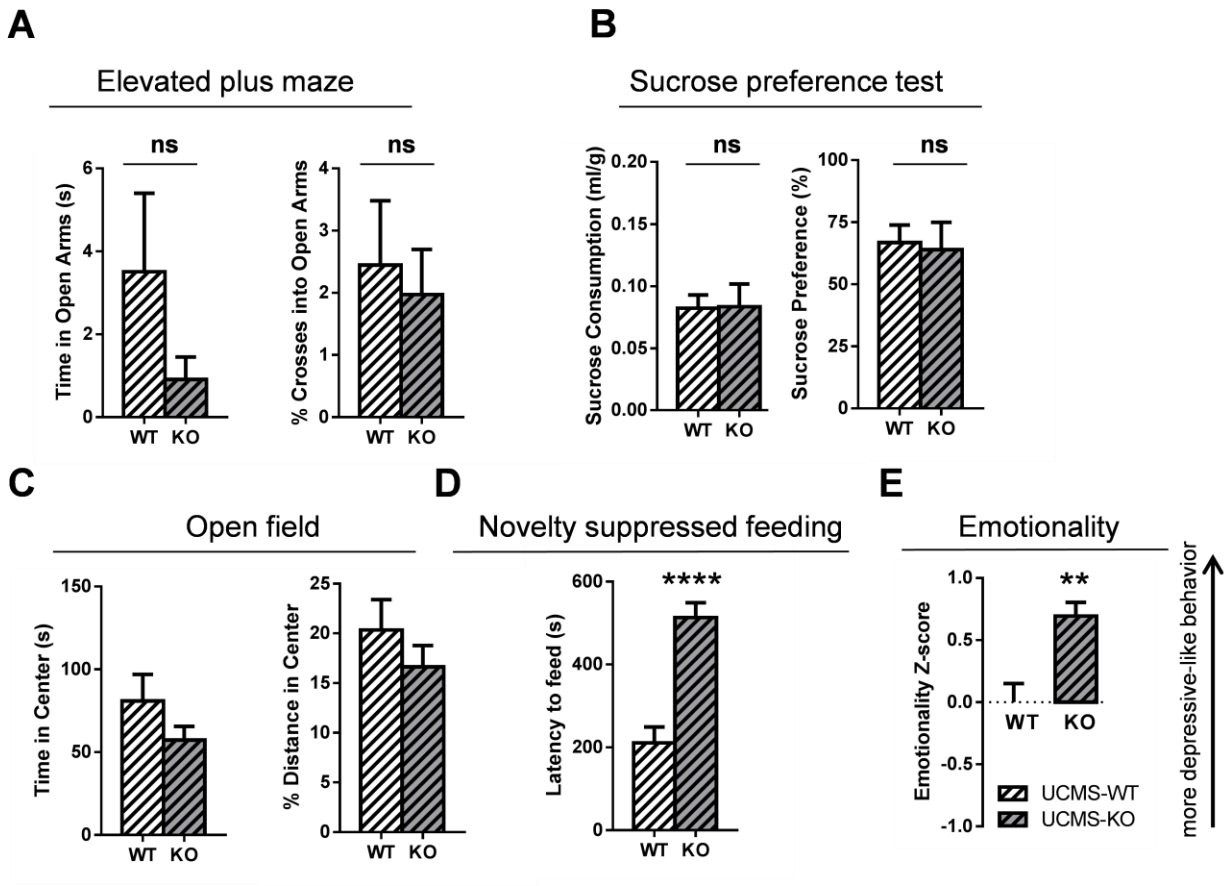

Figure 6. Assessment of anxious/depressive-like behaviors in *Sst*^{KO} mice after UCMS.

Behavioral phenotypes, including anxious/depressive-like behaviors and overall emotionality scores in the elevated plus maze (EPM; A), sucrose preference test (SP; B), open field (OF; C), and novelty suppressed feeding test (NSF; D) were examined in *Sst*^{KO} and *Sst*^{WT} mice after UCMS. Overall emotionality Z scores were summarized (E). ** p <0.01, **** $p < 0.001$. Error bars represent the standard error of the mean (N=12-15/group, 6-9 mice/sex).

3.4.5 *Sst*^{KO} mice display normal locomotion after chronic stress

Following UCMS treatment, locomotion was reduced in stressed *Sst*^{KO} mice in the open field but not in the EPM or overall locomotion Z-score (**Figure 7**) compared to stressed *Sst*^{WT} mice.

Figure 7. Assessment of locomotion in *Sst*^{KO} mice after UCMS.

Locomotion, including total entries in the elevated plus maze (EPM; left) and total distance in the open field (OF; middle), and overall locomotion scores (right), was examined in *Sst*^{KO} and *Sst*^{WT} mice after UCMS. * p <0.05. Error bars represent the standard error of the mean (N=12-15/group, 6-9 mice/sex).

3.4.6 Validation of emotionality in *Sst*^{KO} mice using an independent cohort

To replicate previous findings on behavioral emotionality, we used a second independent cohort of mice to examine the robustness of the SST^{KO} mouse phenotypes. Consistent with previous results, we confirmed that increased latency to feed in the NSF test and higher emotionality z-scores in *Sst*^{KO} mice compared to normal *Sst*^{WT} mice (**Figure 8**).

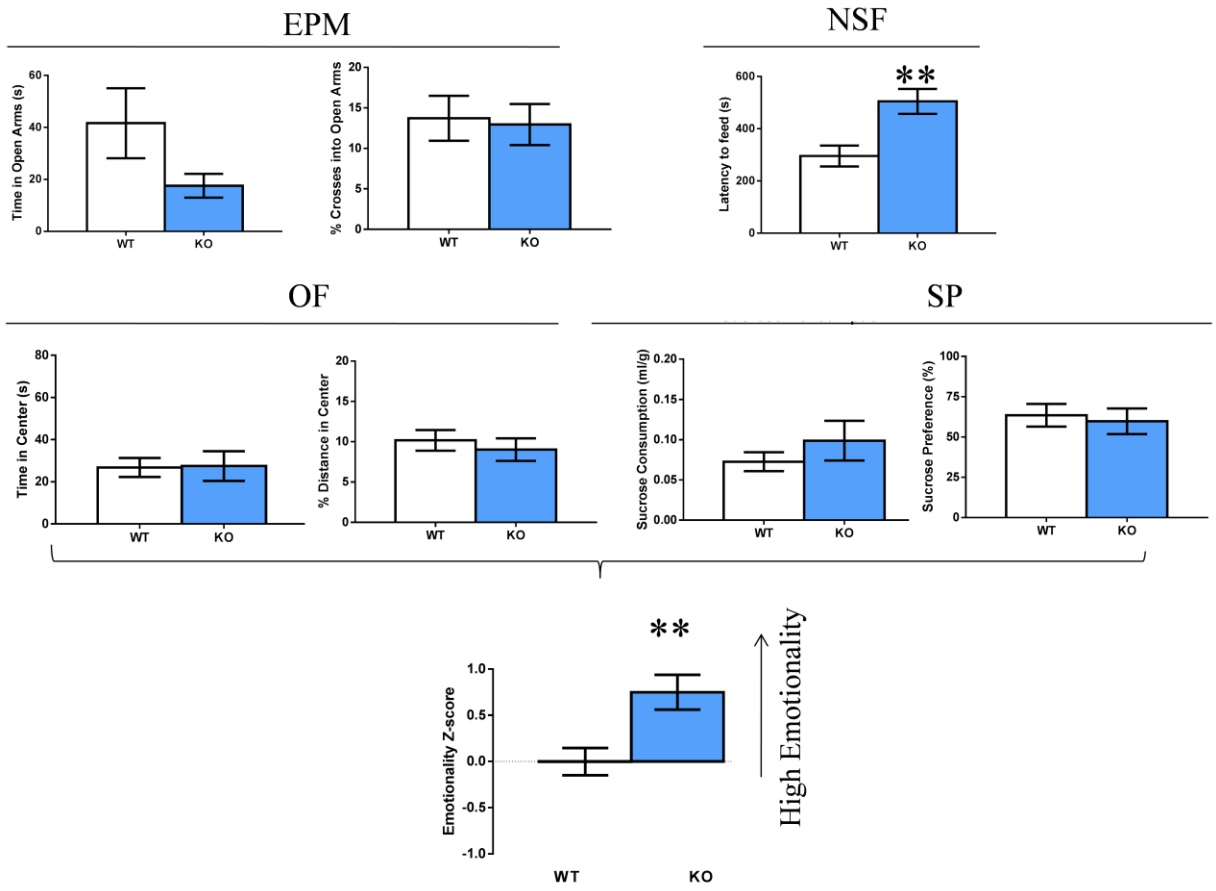

Figure 8. Validation of anxiety/depressive-like behaviors in unstressed *Sst*^{KO} mice.

Behavioral phenotypes, including anxious/depressive-like behaviors and overall emotionality scores in the elevated plus maze (EPM), sucrose preference test (SP), open field (OF), and novelty suppressed feeding test (NSF) were examined in Sst^{KO} and Sst^{WT} mice at baseline. Overall emotionality Z scores were summarized at the bottom. ** p <0.01. Error bars represent the standard error of the mean (N=17-19/genotype, 8-11 mice/sex).

Following UCMS exposure, stressed Sst^{KO} mice maintained a higher behavioral emotionality compared to stressed Sst^{WT} littermates (**Figure 9**). Thus, the behavioral phenotypes of Sst^{KO} mice were reproduced independently.

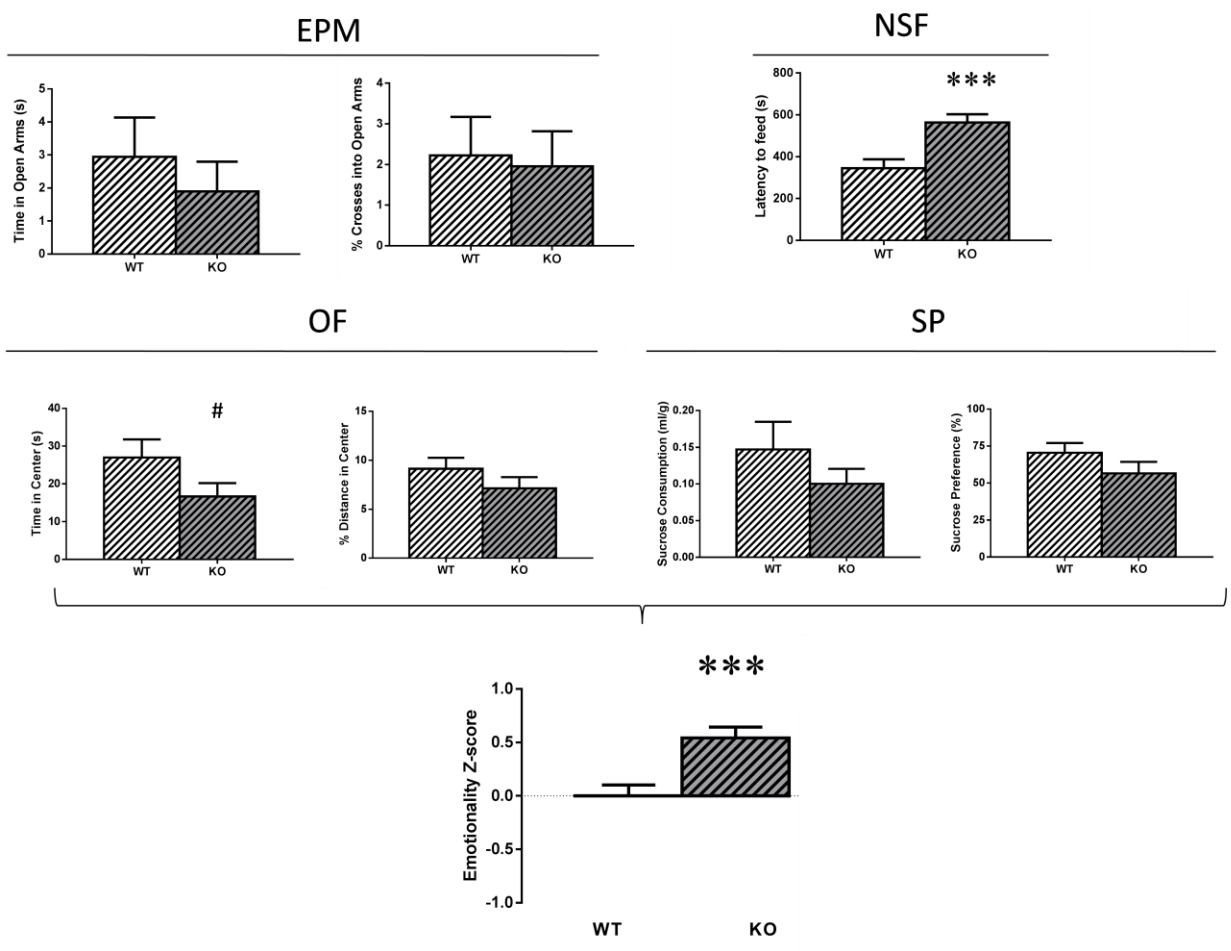

Figure 9. Assessment of anxiety/depressive-like behaviors in Sst^{KO} mice after UCMS in a second, independent cohort.

Behavioral phenotypes, including anxious/depressive-like behaviors, overall emotionality scores in the elevated plus maze (EPM), sucrose preference test (SP), open field (OF), and novelty suppressed feeding test (NSF) were examined in Sst^{KO} and wild-type mice at baseline and after UCMS. Overall emotionality Z scores were summarized at the bottom. $^{\#}p$ <0.1, *** p< 0.005. Error bars represent the standard error of the mean (N=17-19/group, 8-11 mice/sex).

3.4.7 Home-cage food consumption in *Sst^{KO}* mice following food deprivation and NSF test

Notably, in the NSF paradigm, we measured appetitive drive by measuring the amount of food consumed in the home cage for 6 min, upon reaching the food pellets in an open-field arena. In the first cohort, we found a small but significant reduction in food consumption in *Sst^{KO}* mice immediately following the NSF test under baseline unstressed conditions, but not after UCMS exposure (**Figure 10**). In the second cohort, there was a trend for *Sst^{KO}* mice to eat less food under unstressed and post-UCMS conditions (**Figure 10**).

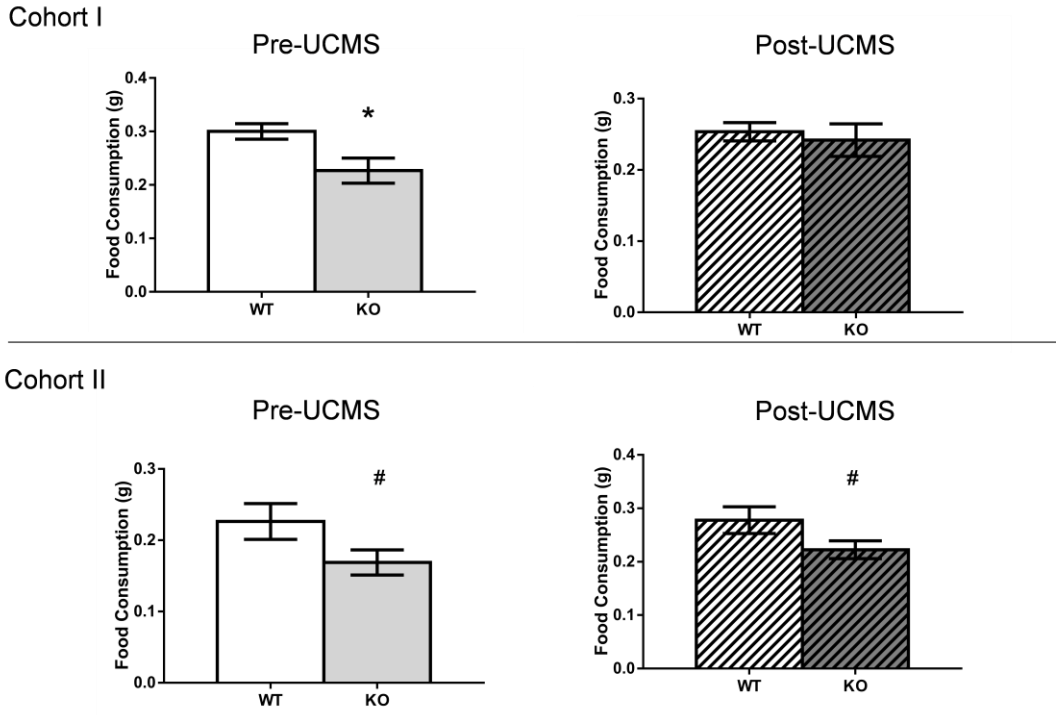

Figure 10. Assessment of food consumption after 16 hours of food deprivation and NSF test in *Sst*^{KO} mice.

In the first cohort, unstressed *Sst*^{KO} mice ate less food when they returned to their home cage after NSF testing. Stressed *Sst*^{KO} mice had normal food consumption when they returned to their home cage. In the first cohort, a trend of reduced food consumption under unstressed and stressed conditions. *p <0.05, $^{\#}$ p <0.1. Error bars represent the standard error of the mean (N=12-19/group, 6-11 mice/sex).

To explore the relationship between post-NSF food consumption and anxiety/depressive-like behaviors (i.e. latency to feed) during the NSF, we examined the correlation between food consumption and latency to feed in two cohorts of *Sst*^{KO} mice under baseline and after CUMS conditions. We found no significant correlation under baseline (p = 0.77, r = -0.05) or after UCMS (p = 0.24, r = -0.23) conditions (**Figure 11A**). In addition, no significant correlation between home-cage food consumption and baseline/trait emotionality (p = 0.95, r = 0.01) or post-UCMS state emotionality (p = 0.81, r = 0.047) was found in *Sst*^{KO} mice (**Figure 11B**).

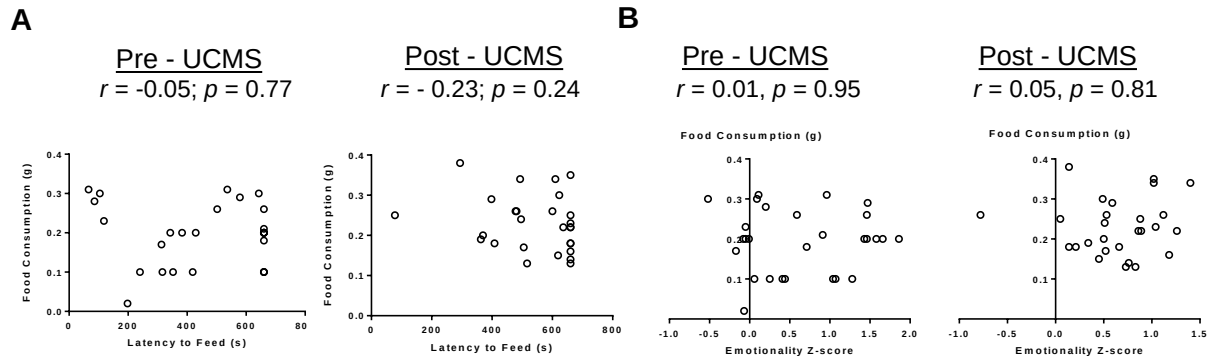

Figure 11. Assessment of food consumption after 16 hours of food deprivation and NSF test in *Sst*^{KO} mice.

In the first cohort, unstressed *Sst*^{KO} mice ate less food when they returned to their home cage after NSF testing. Stressed *Sst*^{KO} mice had normal food consumption when they returned to their home cage. In the first cohort, a trend of reduced food consumption under unstressed and stressed conditions. *p <0.05, $^{\#}$ p <0.1. Error bars represent the standard error of the mean (N=12-19/group, 6-11 mice/sex).

Moreover, compared to wild-type littermates, the body weight of *Sst*^{KO} mice was consistently normal, even after 16 hours of food deprivation for NSF. Collectively, this aberrant feeding behavior immediately after NSF testing could be interpreted as post-NSF residual anxiety-like behavior that suppresses food consumption at home cage for a short period of time. Again, the results indicated that the elevated behavioral emotionality phenotype of *Sst*^{KO} mice did not correlate with any overall physical changes.

3.4.8 Female *Sst*^{KO} mice display more robust emotionality phenotypes

To explore potential sex differences in *Sst*^{KO} mouse phenotypes, we separated the above-described data by sex groups (male and female cohorts) in the NSF analyses. We observed that the increased anxiety/depressive-like behaviors in the NSF were more robust in female *Sst*^{KO} mice under baseline and chronic stress conditions (**Figure 12**). Note that there was no statistical interaction between sex and treatment, indicating that the results in female *Sst*^{KO} were more robust rather than different from male *Sst*^{KO}.

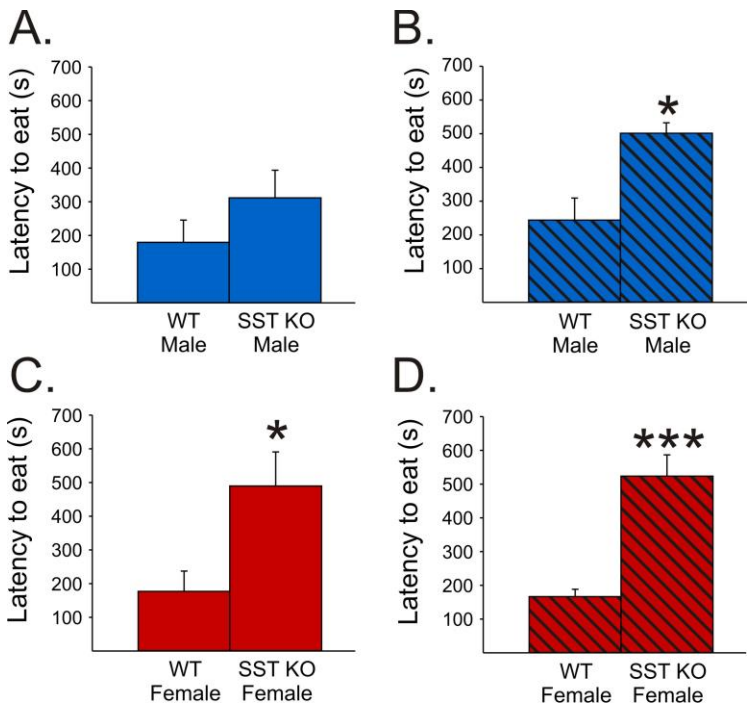

Figure 12. Increased *Sst*^{KO} female vulnerability to high anxiety/depressive-like behaviors in the NSF test.

Female *Sst*^{KO} mice showed more robust phenotypes in NSF under baseline unstressed (trait-like; A, C) and chronic stress (B, D) conditions. Males are in blue, females in red. Hashed bars indicate chronic stress groups. * p <0.05, *** p < 0.005. Error bars represent the standard error of the mean (N=6-9 mice/sex).

At baseline, there was a trend for female *Sst*^{KO} mice to display higher emotionality that integrated four behavioral tests (p < 0.1; **Figure 13B**) compared to female *Sst*^{WT} mice. After UCMS exposure, stressed female *Sst*^{KO} mice showed significantly higher emotionality (p < 0.005; **Figure 13D**) compared to stressed female *Sst*^{WT} mice. Overall, high emotionality of *Sst*^{KO} mice appeared driven by female mice, revealing an interesting parallel with the heightened human female vulnerability to mood disorders (Perugi *et al.*, 1990; Kornstein *et al.*, 2000).

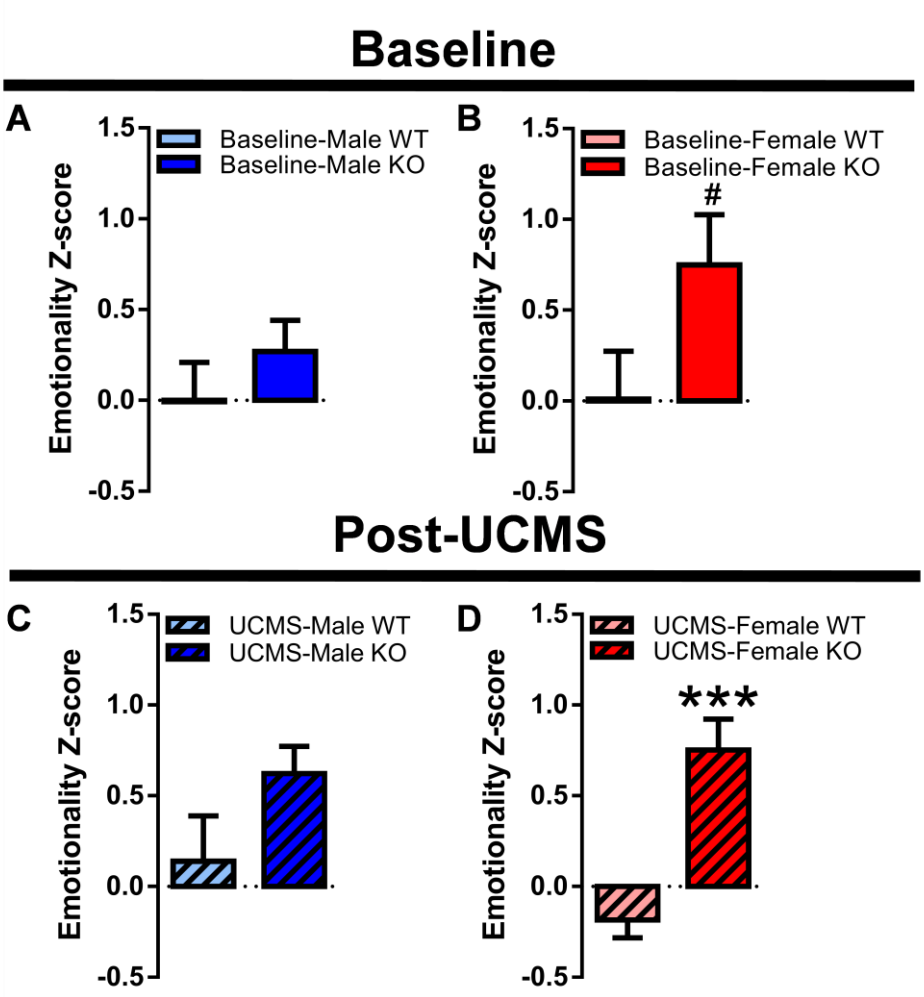

Figure 13. Assessment of sexually dimorphic role of SST in behavioral emotionality.

In contrast to male mice (A, C), female Sst^{KO} mice showed more robust phenotypes at baseline (B) and after chronic stress (D). $^{\#}p < 0.1$, *** $p < 0.005$. Error bars represent the standard error of the mean (N=6-9 mice/sex).

3.4.9 Molecular phenotypes and functional compensation of BDNF-GABA signaling in mice with low SST

SST is a cellular marker overlapping with NPY, CORT, and the 67 kDa isoform of GABA-synthesizing enzyme glutamic acid decarboxylase (GAD67), together contributing the majority of inhibitory input onto pyramidal dendrites (de Lecea *et al.*, 1997; Viollet *et al.*, 2008). Expression of these GABA markers is down-regulated in the anterior cingulate cortex and amygdala of depressed patients, and in mice with reduced BDNF (Tripp *et al.*, 2011; Guilloux *et al.*, 2012; Tripp *et al.*, 2012), suggesting a vulnerable BDNF/GABA-enriched gene module in SST neurons associated with mood regulation. To examine whether loss of SST affected this particular gene module, we performed qPCR to measure *Cort*, *Npy*, *Gad67*, and *Bdnf* expression in the cingulate cortex of mice with low SST. Results show that SST ablation induced further changes, including low expression of *Cort*, *Bdnf*, and *Gad67* (**Table 3**), when compared to Sst^{WT} mice. Notably, the gene profile observed in Sst^{KO} mice was similar to key gene changes observed in mice with altered BDNF function and in depressed patients. On the other hand, Sst^{HZ} mice showed elevated *Cort* and reduced *Bdnf* expression (**Table 3**).

Table 3. Altered expression of Bdnf and GABA-related genes in Sst^{KO} and Sst^{HZ} mice, and comparison to mice with low BDNF, and to human subjects with MDD.

Gene	Mouse				Mouse (Tripp et al., 2012)	Human (Guilloux et al., 2011; Tripp et al., 2012)
	SST $^{HZ\ vs.\ WT}$ qPCR		SST $^{KO\ vs.\ WT}$ qPCR		Bdnf $^{KIV\ or\ +/-}$	MDD
	Change (%)	P-value	Change (%)	P-value		
Cort	**50.5 ± 19.8**	**0.02**	**- 57.7 ± 8.3**	**6.06E-03**	↓	↓
Npy	-16.4 ± 12.9	0.24	- 7.8 ± 9.4	0.35	↓	↓
Gad67	- 10.4 ± 15.7	0.31	**- 48.9 ± 19.5**	**0.02**	↔	↓
Bdnf	**- 31.5 ± 7.4**	**0.01**	**- 22.3 ± 8.9**	**0.04**	↓	↓#

(Left) Altered expression of *Bdnf* and GABA-related genes in Sst^{KO} and Sst^{HZ} mice. (Right) *Bdnf*-dependency of *Cort* and *Npy* expression is shown in $Bdnf^{HZ}$ and *Bdnf* $^{exon\text{-}IV}$ *knockout* mice (From Tripp et al., 2012) and core depression-related gene profile in human subjects (From Guilloux et al., 2011; Tripp et al., 2012; $^{\#}$ represents decreased BDNF-TrkB signaling in postmortem corticolimbic regions of depressed subjects). Error bars represent the standard error of the mean (n = 8-16/ per genotype).

3.5 CONCLUSION AND DISCUSSION

A conserved molecular feature in neurological disorders is consistently reduced SST; hence, we previously hypothesized that SST deficits play a causal role in mood dysregulation across diseases (Lin & Sibille, 2013). Moreover, expression of co-localized markers (i.e., GAD67, NPY, CORT) in depressed patients is consistently reduced, indicating a robust cell-based pathology in depression (Tripp *et al.*, 2011; Guilloux *et al.*, 2012). Our findings indicate that Sst^{KO} mice recapitulate behavioral (high emotionality) and molecular (down-regulated BDNF/GABA profile) phenotypes that are observed in depressed patients and thought to be involved in mood dysregulation. Hence, our results suggest that SST deficits may work as an up-stream factor, contributing to dysfunctional inhibitory neurotransmission and mood dysregulation.

The present study shows that unstressed Sst^{KO} mice exhibit anxiety/depressive-like behaviors in the open field and novelty-suppressed tests. In previous pharmacological studies, microinjections of SST isoforms (SST-14 and SST-28) into amygdala or ventricle exert anxiolytic effects on anxiety-like behaviors in the elevated plus maze (Yeung *et al.*, 2011; Yeung & Treit, 2012). Zeyda et al., (2001) indicated that unstressed Sst^{KO} mice displayed non-significant trend ($p > 0.08$) toward increased anxiety-like behaviors in the light/dark-avoidance

test but not in the open field test ($p > 0.3$) (Zeyda *et al.*, 2001). Albrecht et al., (2013) further investigated Sst^{KO} mice in two days of the dark cycle (during rodent active phase) and found that non-stressed Sst^{KO} mice showed increased anxiety-like behaviors during the second, but not the first day of the active phase (Albrecht *et al.*, 2013). Zeyda et al., (2001) maintained the Sst^{KO} mice on a 129/Sv-background and used the F2 generation (two generations after the founder line). In the present study, animals originated from breeding Sst^{HZ} mice that were backcrossed into the C57BL/6J inbred mouse strain for one generation during importation. We speculate that the discrepancies of the observed behavioral phenotypes might be due to different genetic backgrounds and time points of testing.

No significant correlation between home-cage food consumption and baseline/trait emotionality ($r = 0.01$, $p = 0.95$) or post-UCMS state emotionality ($r = 0.05$, $p = 0.81$) was found in Sst^{KO} mice. In addition, Sst^{KO} mice displayed normal body weight compared to wild-type littermates, under all conditions. Together these control studies did not identify any consistent pattern of differences and thus suggest that the increased latency to feed in the NSF and the overall elevated behavioral emotionality of Sst^{KO} mice were not confounded by physiological or activity changes.

Cortistatin (Cort) binds to all SST receptors and shares similar structural, functional, pharmacological properties with SST (de Lecea, 2008). In contrast to previous Sst^{KO} studies that did not find changes or compensatory up-regulation of *Cort* (Zeyda et al., 2001; Ramirez et al., 2002; Cammalleri et al., 2006), we found that *Cort* mRNA levels in the cingulate cortex were significantly down-regulated in Sst^{KO} mice, but upregulated in Sst^{HZ} mice. One previous study has found that SST expression is normal in *Cort* knockout mice (Zeyda & Hochgeschwender, 2008); however, little is known about SST expression in *Cort* null mutant animals. The

inconsistent molecular effects in SST and *Cort* expression suggest that the effects of SST on *Cort* expression are possibly regulated in a dose- and regionally specific manner. In addition, we speculate that compensatory upregulation in *Cort* may account for generally better preserved SST functions in Sst^{HZ} and thus prevents high behavioral emotionality. The observation of down-regulated *Bdnf* expression further implicates homeostatic changes in *Bdnf* as an upstream regulator of SST expression (Tripp *et al.*, 2012). Finally, our data also demonstrate that additional factors might be at play in SST-associated mood regulation since low *Gad67* was observed in Sst^{KO} but not in Sst^{HZ} mice.

Overall, mice with low SST provide a valuable genetic model for investigating mood dysregulation and antidepressant efficiency. In addition, it remains to be seen whether loss of *Sst* in specific regions and developmental stages is critical for affect dysregulation.

4.0 ROLE OF CORTICOSTERONE IN SOMATOSTATIN-RELATED EMOTIONALITY

4.1 ABSTRACT

Hyperactivity of the HPA axis is observed in some depressed patients, and elevated stress hormones can lead to depression, although these are not consistent observations. A known physiological function of SST is neuroendocrine modulation, as confirmed by Sst^{KO} mice displaying elevated circulating corticosterone. Thus, we were interested in whether the observed differences of emotionality between Sst^{KO} and Sst^{WT} mice were mediated by HPA dysregulation. We also characterized the behavioral emotionality in Sst^{HZ} mice, and assessed the responsiveness of the HPA axis in mice with low SST by measuring plasma corticosterone during the basal, acute restraint stress, and recovery periods. Consistent with previous observations, we found high basal plasma levels of corticosterone in Sst^{KO} mice. We further found that Sst^{HZ} mice displayed similar elevated corticosterone levels, but surprisingly normal behavioral emotionality under baseline unstressed and chronic stress conditions. The HPA axis responses to restraint stress and following 1-h recovery were normal in both Sst^{KO} and Sst^{HZ} mice. Hence, these

observations indicate that high basal levels of the corticosterone in mice with low SST may not sufficiently increase emotionality.

4.2 INTRODUCTION

The HPA axis is a major neuroendocrine system that regulates stress responses. Neurons within the medial parvocellular subdivision of the paraventricular nucleus (mpPVN) in the hypothalamus synthesize corticotropin-releasing hormone (CRH). The released CRH binds to CRHR1/CRHR2 receptors on the cell membrane of corticotrophs, which then synthesize and release adrenocorticotropic hormone/corticotrophin (ACTH). The HPA axis is activated by a brief secretion of ACTH, followed by the negative feedback of glucocorticoids on ACTH and CRH release (Tasker & Herman, 2011; Myers *et al.*, 2014). Corticosterone, the major murine glucocorticoid (cortisol in humans, non-human primates; stress hormones) and final effector of the HPA axis, is synthesized by the cortex of adrenal glands in response to ACTH. Glucocorticoids can in turn affect the overall balance of limbic neurons to control behavioral stress responsiveness. Hyperactivity of the HPA axis is observed in some depressed patients (Gold & Chrousos, 1999; Wong *et al.*, 2000), and elevated glucocorticoids can lead to depression (Starkman *et al.*, 1981; Kathol, 1985; Murphy, 1991). Because a known physiological function of SST is neuroendocrine modulation, past research in SST has mostly focused on its neuroendocrine-related function (Patel, 1999). SST knockout mice display elevated circulating corticosterone (Zeyda *et al.*, 2001; Luque *et al.*, 2006). However, how glucocorticoids contribute to SST-related behavioral phenotypes remains unclear. Hence, the current study provided an

extended characterization of corticosterone profile in mice with low SST (heterogeneous and homogeneous), and explored the correlation of high corticosterone with behavioral emotionality.

4.3 MATERIALS AND METHODS

4.3.1 Animals

Sst^{KO}, Sst^{HZ}, Sst^{WT} littermates were generated by crossing Sst^{HZ} mice. The Sst^{KO} mouse line was purchased from the Jackson Laboratory (stock no. 008117) (Zeyda *et al.*, 2001). Genotypes were identified by PCR analysis of DNA isolated from tail cuts. Cohort 4 consisted of 71 mice [Control group: n = 21 Sst^{WT} (11 males, 10 females), 14 Sst^{HZ} (6 males, 8 females); UCMS group: n = 20 Sst^{WT} (10 males, 10 females), 16 Sst^{HZ} (7 males, 9 females)] and was used exclusively for behavioral assessments. Accordingly, cohort 4 was tested in EPM, OF, NSF, and SP at 5 months of age. Cohort 5 consisted of 40 mice [n =13 Sst^{WT} (6 males, 7 females), 14 Sst^{HZ} (7 males, 7 females), 13 Sst^{KO} (7 males, 6 females)] and was used to examine HPA axis function. The use of animals, including all treatments, was conducted in compliance with the NIH laboratory animal care guidelines and with protocols approved by the Institutional Animal Care and Use Committee of the University of Pittsburgh. All experiments were performed with 3- to 5 month-old male and female mice littermates, between 9 am and 3 pm. All mice were group housed and maintained under standard conditions (12/12-hour light/dark cycle, lights on at 07:00 h), 22 ± 1°C, with food and water *ad libitum*).

4.3.2 Corticosterone Measurements

The stress reactivity test consisted of a 30-min restraint period, corresponding to an acute, moderate stressor. The blood samplings were drawn at three time points: immediately before, during a 30-min exposure to restraint stress, as well as 60 min after ending the stress session (recovery period). The animals were restrained in a 50-ml Falcon tube with a ventilation hole and a hold in the lid for the tail. Tail blood (30 µl) from mice was collected into a *Microtainer*® tube with Lithium Heparin (BD Vacutainer Systems, Franklin Lakes, NJ) at 10:00-14:00. Bleeding was induced by cutting the tip of the tail, and plasma was separated by centrifugation at 1200 g, 4 °C for 10 min, and then stored at -80°C until use. All samples were ran in duplicate and measured by Corticosterone *ELISA* Kit (EnzoLife Sciences, Farmingdale, NY) according to the instructions of the manufacturer.

4.3.3 Unpredictable chronic mild stress

Mice were subjected to six weeks of a random schedule consisting of 1-3 environmental stressors per day, seven days per week (Surget *et al.*, 2009). Stressors included repeated bedding change, no bedding, reduced housing space, forced bath (~2 cm of water in cage), wet bedding, aversive smell (exposure to fox or bobcat urine), social stress (rotate mice into previously occupied cages or single-housing), 45° tilted cage, and mild restraint (stay in 50-ml falcon tube with air hole). Weekly assessment of weight and fur was performed to monitor physiological progression of the UCMS syndrome. The social isolation treatment began from the fifth week of UCMS until the day of euthanasia.

4.3.4 Behavior

Anxiety/depressive-like behaviors were tested in the elevated plus maze (EPM), open field (OF), novelty-suppressed feeding (NSF), and sucrose preference test (SP) in the following order for each mice: EPM, OF, NSF, SP, separated by a minimum of 1 day. All tests were performed during the light phase of the circadian cycle, between 9 am and 3 pm.

Elevated plus maze (EPM)

Anxiety-like behaviors and locomotion were measured in a cross maze with two open and two closed arms (30 cm x 5 cm) as previously described (Sibille *et al.*, 2000). Entries and time spent in the open arms were recorded for 10 min to assess anxiety-like behaviors. Total number of entries was assessed as an index of locomotion.

Open field (OF)

Anxiety-like behaviors and locomotion were measured in a 76 x 76 cm chamber divided in 16 even-size squares and monitored for 10 min using the Any-maze video-tracking software. Percentage of walking distance and time spent in the four center squares were assessed to evaluate anxiety-like behaviors. Total walking distance in the chamber was used as an index of locomotion.

Novelty-suppressed feeding (NSF)

Anxiety/depressive-like behaviors were measured for 11 min in a 76 x 76 cm chamber, with a food pellet in the bright-lit center. The drive to overcome the aversive center was increased by 16 hours of food deprivation before testing. The latency to start eating food pellet was measured as

an index of anxiety/depressive-like behaviors. Six minutes of food consumption in the home cage after the test was used as a measure for appetite after NSF testing and food deprivation.

Sucrose preference test (SP)

The sucrose test was performed using a two-bottle test: a bottle filled with a 2% sucrose solution and a bottle filled with water. Mice had free access to both water and a 2% sucrose solution 48 hours before the test in their home cage to reduce neophobia. For the next two days, a sucrose preference/consumption test began in a new single-house cage for 16 h from 18:00 pm-10:00 am. Position of bottles was counterbalanced across the left and the right sides from test to test. Sucrose preference (percent) was calculated as follows: preference = [sucrose solution intake (ml)/total fluid intake (ml)] × 100. Sucrose consumption was calculated as: consumption = [sucrose solution intake (ml)/ body weight (g)].

Z-scoring

To investigate the consistency of behavioral performance across related tests, emotionality- or locomotion- related data were normalized using a Z-score methodology, as previously described (Guilloux *et al.*, 2011). Z-scores calculate how standard deviation (σ) and observation (X) is above or below the mean of the control group (μ). Raw measures for EPM (time in open arm; % crosses into open arm), OF (time in center; % distance in the center), NSF (latency to feed), SP (sucrose consumption and sucrose preference) were converted to standard deviations relative to respective means of the control group (*Sst* ^{WT} mice). The directionality of scores was adjusted so that decreased score values indicated reduced anxiety/depressive-like behaviors (termed emotionality). Finally, values across tests were averaged for each mouse to produce individual

emotionality Z-scores. Locomotion Z-scores were similarly applied and obtained from EPM (total crosses) and OF (Total distance traveled) data.

4.3.5 Physiological Evaluation

The body weight and coat state of all the animals were assessed and scored (0-2 points) weekly by a double-blinded experimenter until the end of the UCMS treatment. The total score of the coat state resulted from the sum of the score of five different body parts: head, neck, dorsal and ventral fur, tails and paws. A score of 0 was given for a well-groomed fur and increased to 2 for an unkempt fur.

4.3.6 Statistical Analysis

Statistical analyses were carried out using GraphPrism Version 6.0 (Graph Pad. Software Inc., San Diego, CA, USA). Student's *t* test was used to compare means between two groups, and one-way or two-way analysis of variance followed by Tukey's post hoc among means were used to determine significant differences among multiple groups. All data are expressed as means ± standard error of the mean. For brevity, uninformative non-significant results were omitted from the text.

4.4 RESULTS

4.4.1 Mice with low SST display high basal corticosterone

It was previously reported that *Sst*^{KO} mice showed high basal levels of plasma corticosterone (Zeyda *et al.*, 2001). Our findings are consistent with this observation, and found high basal plasma levels of corticosterone in both *Sst*^{KO} and *Sst*^{HZ} mice (**Figure 13A**). In addition, stress-induced and recovery levels of corticosterone were normal in *Sst*^{KO} and *Sst*^{HZ} mice (ANOVA $p > 0.05$; **Figures 13B-C**).

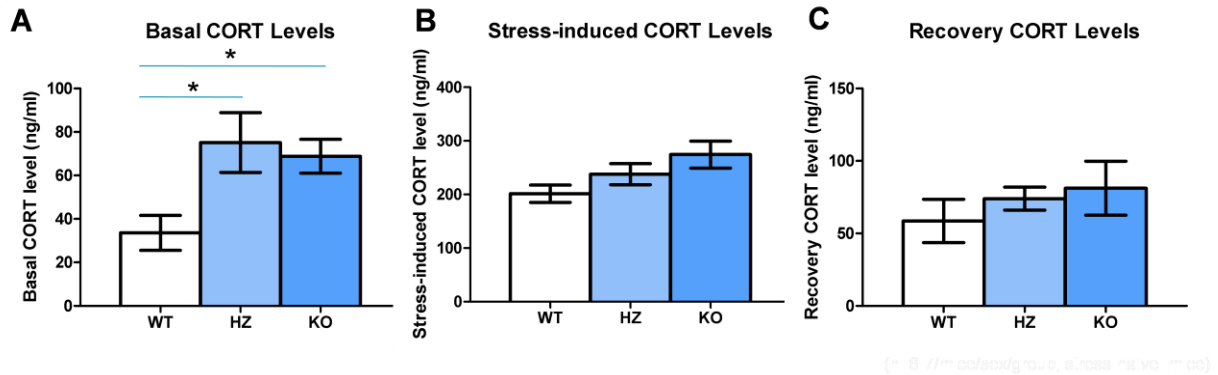

Figure 14. Altered basal levels of corticosterone in *Sst*^{KO} and *Sst*^{HZ} mice.

(A) Altered basal levels of corticosterone (CORT) in *Sst*^{KO} and *Sst*^{HZ} mice. (B) Acute stress-induced corticosterone levels were normal in mice with low SST. (C) No abnormal corticosterone levels were detected in mice with low SST during the recovery period.* $p < 0.05$. Error bars represent the standard error of the mean (N=13-14/genotype).

4.4.2 *Sst*^{HZ} mice display normal baseline/trait and state emotionality

To gain insight into the role of SST and corticosterone in mood regulation, we examined *Sst*^{HZ} and *Sst*^{WT} mice treated with UCMS or remained unstressed. Based on previous findings in MDD and *Sst*^{KO} mice, we predicted that *SST*^{HZ} mice would display high emotionality under basal

unstressed and chronic stress conditions. Surprisingly, when compared to Sst^{WT} mice, Sst^{HZ} mice exhibited normal behavioral phenotypes. In addition, Z-score analyses revealed that UCMS treatment increased emotionality in Sst^{HZ} and Sst^{WT} mice, but to a similar extent in Sst^{HZ} and Sst^{WT} mice (**Figure 14;** details in **Appendix B**).

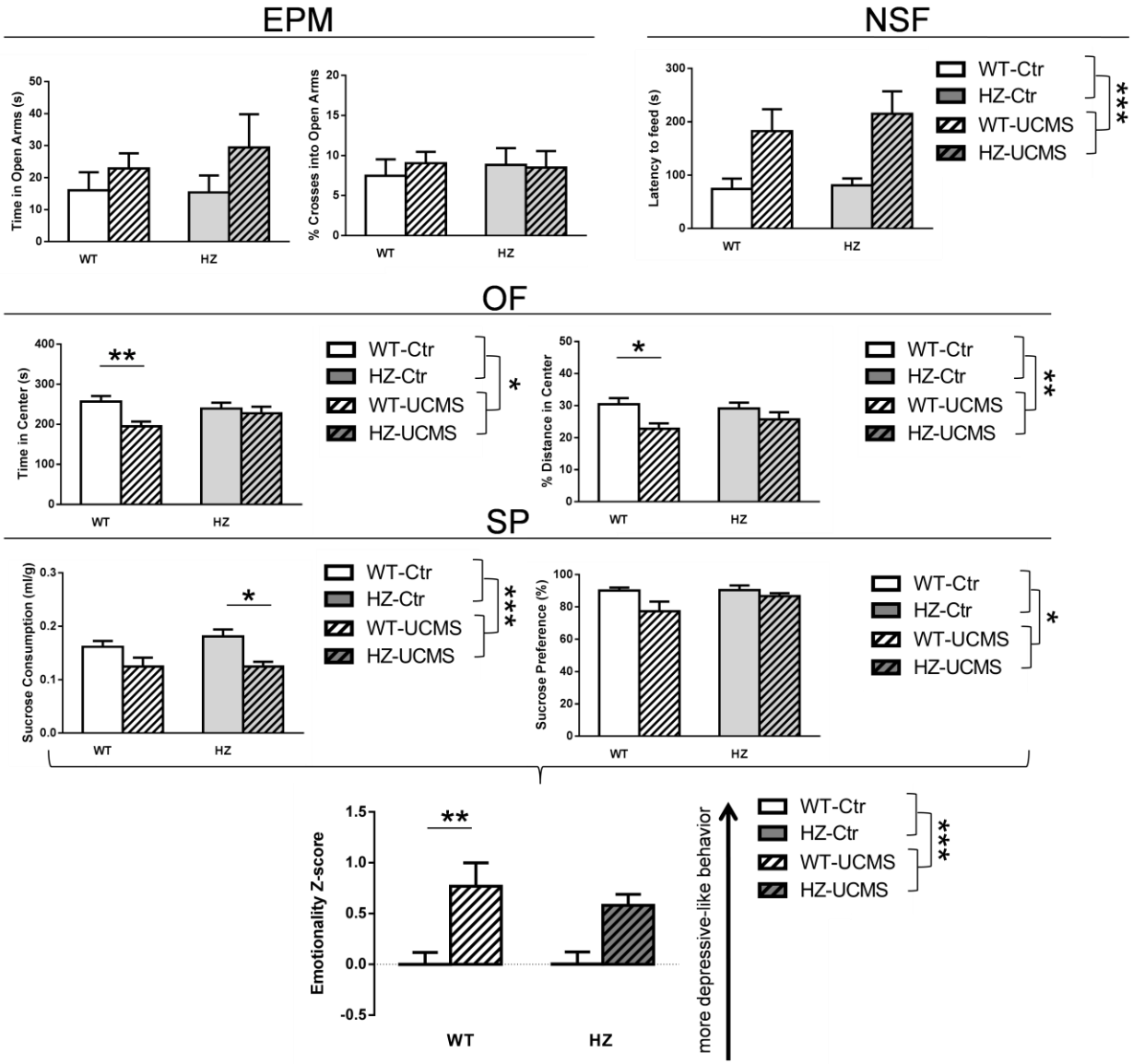

Figure 15. Assessment of anxiety/depressive-like behaviors in Sst^{HZ} mice under baseline unstressed and chronic stress conditions.

Overall emotionality Z scores indicated that UCMS increased emotionality in *Sst*^{HZ} and *Sst*^{WT} mice, and S*st*^{HZ} mice exhibited normal emotionality compared to *Sst*^{WT} mice under baseline unstressed or chronic stress conditions. * p <0.05, ** p <0.01, *** p < 0.005. Error bars represent the standard error of the mean (N=14-21/group, 6-11 mice/sex).

4.4.3 *Sst*^{HZ} mice display normal locomotion

Consistent with prior results in *Sst*^{KO} mice, we measured locomotion and found that *Sst*^{HZ} exhibited normal locomotion in the EPM and OF tests (**Figure 15**). Compared to non-stressed controls, UCMS-treated *Sst*^{HZ} and *Sst*^{WT} mice were significantly more hyperactive in the EPM and OF test, and displayed higher overall locomotion Z-scores. No genotype effects nor interactions were found.

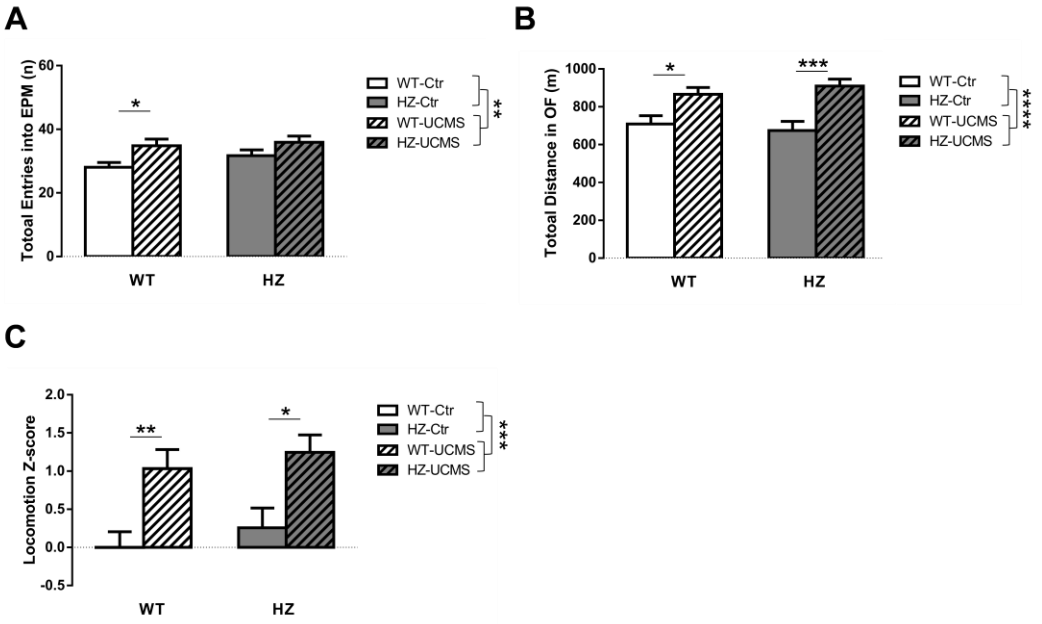

Figure 16. Assessment of locomotion in *Sst*^{HZ} mice.

Locomotion, including total entries in the elevated plus maze (EPM; A), total distance in the open field (OF; B), and overall locomotion scores (C), was examined in *Sst*^{HZ} and *Sst*^{WT} mice under baseline unstressed or chronic stress

(UCMS) conditions. * p <0.05, ** p <0.01, *** p < 0.005, **** p < 0.001. Error bars represent the standard error of the mean (N=14 -21/genotype/group).

4.4.4 Home-cage food consumption in *Sst*^{HZ} mice following food deprivation and NSF test

Consistent with prior NSF results from *Sst*^{KO} mice, *Sst*^{HZ} mice displayed less 6-min food consumption in their home cage (**Figure 16A**). However, *Sst*^{HZ} mice exhibited normal body weight and normal behavioral emotionality under baseline unstressed and chronic stress conditions. In addition, there was no significant correlation between emotionality z-scores and food consumption (**Figure 16B**; $p > 0.05$; $r = -0.05$), together further indicating that home-cage food consumption immediately after NSF test is not sufficient to explain the behavioral emotionality.

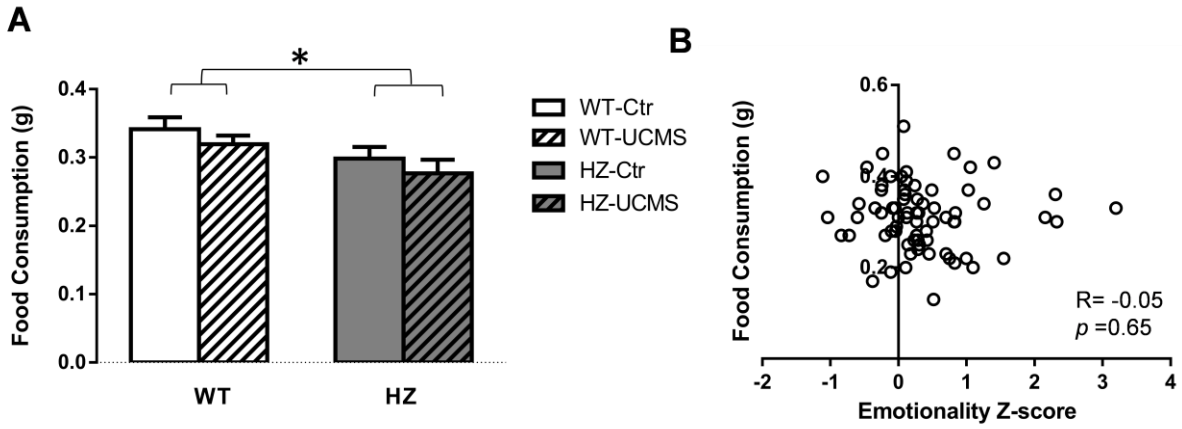

Figure 17. Assessment of feeding differences in *Sst*^{HZ} mice under baseline unstressed or chronic stress conditions.

(A) After NSF testing, *Sst*^{HZ} mice ate less food when returned to their home cage. (B) Food consumption did not correlate with emotionality z-scores in *Sst*^{HZ} mice. * p < 0.05. Error bars represent the standard error of the mean (N=14-21/genotype/group, 6-9 mice/sex).

4.5 CONCLUSION AND DISCUSSION

HPA axis dysfunction is frequently observed in depressed patients (Gold & Chrousos, 1999; Wong *et al.*, 2000). A high incidence of depression is found in Cushing's syndrome, a hormonal disorder caused by high levels of cortisol. Hence, we aimed to investigate whether high corticosterone in Sst^{KO} mice could explain the high emotionality we observed in Sst^{KO} mice. Our results showed that Sst^{KO} mice had high basal levels of corticosterone in the plasma. In addition, we found that loss of SST did not significantly impact the stress-induced fast and negative feedback mechanisms of the HPA axis. Interestingly, similar to Sst^{KO} mice, Sst^{HZ} mice showed high basal levels of corticosterone but exhibited normal behavioral emotionality, suggesting that while high corticosterone may be a biomarker of SST deficits, it does not directly contribute to mood dysregulation. In support of this notion, a previous study found no correlations among basal concentrations of SST, ACTH, or cortisol and the responses of these hormones following the treatment of synthetic corticotropin-releasing hormone in depressed subjects (Lesch *et al.*, 1989). Conversely, infusion of SST in healthy adult humans, at a dose that inhibited basal GH secretion, was linked to an activation of HPA axis by elevating plasma levels of cortisol and ACTH (Ambrosio *et al.*, 1998). Under baseline unstressed conditions, basal levels of corticosterone release follows a circadian rhythm, with a peak at the initiation of the awaking cycle (Butte *et al.*, 1976; Allen-Rowlands *et al.*, 1980). The steady-state level of basal corticosterone is involved in the organization of sleep- , body growth-, and daily-related events (Malisch *et al.*, 2007; de Kloet & Sarabdjitsingh, 2008). It will be of interest to examine circadian patterns of corticosterone in mice with low SST. Here we did not directly address the impact of corticosterone on SST-associated high emotionality because the administration of exogenous corticosterone did not normalize corticosterone after removal of adrenal glands

(adrenalectomy) in my own work (not shown). In addition, side effects of adrenalectomy include alterations in body weight, food intake, and locomotion. Addressing these confounding factors is essential for future experiments. As discussed above, corticosterone release is regulated by circadian oscillators. It remains to be determined whether SST ablation alters characteristics of the pulsatile pattern of corticosterone release, possibly with frequent automated blood sampling. If so, rhythmic patterns of corticosterone secretion are also an important component of SST-associated emotionality that needs to be further investigated. Taken together, the data demonstrate that (i) basal plasma levels of corticosterone were higher in mice with low SST, when compared to Sst^{WT} mice, (ii) Sst^{KO} and Sst^{HZ} mice have normal stress-induced fast response and negative feedback regulation of HPA axis, and (iii) Sst^{HZ} mice exhibit high corticosterone normal mood regulation. Thus, we conclude that corticosterone is not sufficient to induce high anxiety/depressive-like behaviors in Sst^{KO} mice. Its potential as a biomarker indicating SST deficits should be further investigated.

5.0 MOLECULAR ADAPTATIONS OF SST NEURONS IN THE CINGULATE CORTEX OF STRESSED MICE

5.1 ABSTRACT

SST is a secretory neuropeptide and a marker of GABAergic interneuron subpopulations that contribute the majority of inhibitory input onto pyramidal dendrites. In the corticolimbic regions of depressed patients and elder people, reduced expression of SST and other co-localized cellular markers are observed, suggesting a selective vulnerability of SST neurons. Using cell-type specific transcriptome analysis, we found that mouse SST neurons in the cingulate cortex are more vulnerable to UCMS compared to pyramidal neurons. Markers of SST neurons (*Sst* and *Gad67* expression) were down-regulated in SST neurons of stressed mice. Protein translation through eukaryotic initiation factor 2 (EIF2) signaling, a pathway previously implicated in neurodegenerative diseases, was most affected and suppressed in SST neurons of stressed mice. Activating EIF2 signaling with an EIF2 kinase inhibitor mitigated mouse anxiety/depressive-like behaviors induced by UCMS. Thus, our findings suggest that chronic stress induces imbalance of protein homeostasis via compromised EIF2 pathway, leading to SST deficits and mood dysregulation.

5.2 INTRODUCTION

The GABAergic inhibitory system includes a diverse class of neurons that regulate excitatory glutamatergic transmission in the brain. SST is an inhibitory modulatory neuropeptide and a marker for approximately 30% of GABA interneurons that do not contain parvalbumin (PV) or calretinin (CR) (Gonchar *et al.*, 2007; Kubota *et al.*, 2011). Among the inhibitory neurons, SST-expressing interneurons preferentially target their synapses to the dendrites of cortical pyramidal neurons (Hendry *et al.*, 1984; Melchitzky & Lewis, 2008; Xu *et al.*, 2010). As a gate keeper to regulate information input, SST neurons are positioned to provide spatiotemporal integration of postsynaptic potential in local cortical circuits (Gentet *et al.*, 2012; DeFelipe *et al.*, 2013; Le Magueresse & Monyer, 2013). SST deficits in corticolimbic regions are a common feature observed across several neurological diseases and during aging. Studies have identified a selective neuronal vulnerability of SST-containing interneurons, as lower levels of *GAD67*, *SST*, *NPY* have been identified in the corticolimbic regions in depressed or older humans (Glorioso *et al.*, 2011; Sibille *et al.*, 2011; Tripp *et al.*, 2011; Guilloux *et al.*, 2012). Moreover, biological stressors, such as seizure and electrical foot shock, have been found to affect SST interneurons or *Sst* expression (Vezzani & Hoyer, 1999; Ponomarev *et al.*, 2010). Exposure to chronic stress is a main exogenous risk factor associated with mood symptoms (Keller *et al.*, 2007), and the interaction of stress with endogenous, genetic risk factors is shown to increase susceptibility to mood dysregulation (Caspi *et al.*, 2003). Unpredictable chronic mild stress (UCMS) is a well-validated behavioral paradigm that increases anxiety/depressive-like behaviors in mice and that induces neuroendocrine and molecular changes associated with major depression (Surget *et al.*, 2009).

Unlike the candidate-based approach in Chapter 4, here we applied the unbiased microarray analysis to identify molecular changes in SST neurons from cingulate cortex of stressed mice that were exposed to UCMS. By looking at the differentially expressed target genes and pathways deduced from these genes, using the Ingenuity Pathway Analysis (IPA), we identified here the most significantly altered pathways associated with protein homeostasis, oxidative stress, and mitochondrial dysfunction. Eukaryotic initiation factor 2 (EIF2) signaling is one of the most enriched pathways in stressed SST neurons. The interest in this pathway was further enhanced by the recent discoveries showing that genetic or pharmacological manipulations of EIF2 signaling can reverse cellular and/or behavioral deficits in several neurodegenerative diseases (Moreno *et al.*, 2012; Ma *et al.*, 2013; Kim *et al.*, 2014). In this chapter, we also investigated the pathological and functional significance of EIF2 signaling underlying mood regulation.

5.3 MATERIALS AND METHODS

5.3.1 Animals

To generate SST-GFP mice, the mouse line carrying a somatostatin promoter-driven Cre recombinase expression (SST-ires-cre knock-in homozygous mice; Jackson Laboratory; stock no. 013044) was crossed with a $Rosa^{GFP\text{-}floxed}$ reporter mouse line carrying a loxP-flanked STOP cassette (Ai6 $Rosa26^{\text{-}loxP\text{-}STOP\text{-}loxP\text{-}ZsGreen}$; Jackson Laboratory; stock no. 008242), as described previously (Taniguchi *et al.*, 2011). Cohort 6 consisted of 30 mice (Control group: 14;

Unpredictable chronic mild stress group: 16) and was used exclusively for the molecular assessments.

5.3.2 Unpredictable chronic mild stress

Mice (3 months of age) were subjected to six weeks of random schedule consisting of 1-3 mild stressors per day, seven days per week (Surget *et al.*, 2009). Stressors included repeated bedding change, no bedding, reduced housing space, forced bath (~2 cm of water in cage), wet bedding, aversive smell (exposure to fox or cat urine), social stress (rotate mice into previously occupied cages or single-housing), 45° tilted cage, and restraint stress (stay in 50-ml falcon tube with air hole). The social isolation began from the fifth week of UCMS until the day of euthanasia.

5.3.3 Visualization of individual neurons in mice

For single-cell analyses, mice were rapidly transcardially perfused with 1 ml of 1X *Tris-buffered saline* and 1 ml of 4% paraformaldehyde in phosphate buffer (pH 7.4) to lightly fix tissue while preserving GFP signal and RNA integrity. Cryostat sections (20 μm) were cut from coronal blocking containing cingulate cortex, thaw-mounted onto on polyethylene napthalate membrane coated slides (Leica Microsystems; #11505158; Bannockburn, IL, USA) that had been treated with UV at 254 nm for 30 min. Before microdissection, slides for SST neurons were dehydrated through 100% ethanol for 10 seconds. For pyramidal neurons, cryostat sections from mice with GFP-tagged SST neurons were dried briefly and stored at -80˚C. Immediately before microdissection, slides were immersed in an ethanol-acetic fixation solution, stained with thionin, dehydrated with 100% ethanol, as described previously (Lin *et al.*, 2011). Pyramidal

neurons were visually identified based on their location and characteristic somal morphology including pyramidal shape, large size, and thick apical dendrite (**Figure 17;** method used in **Appendix A**).

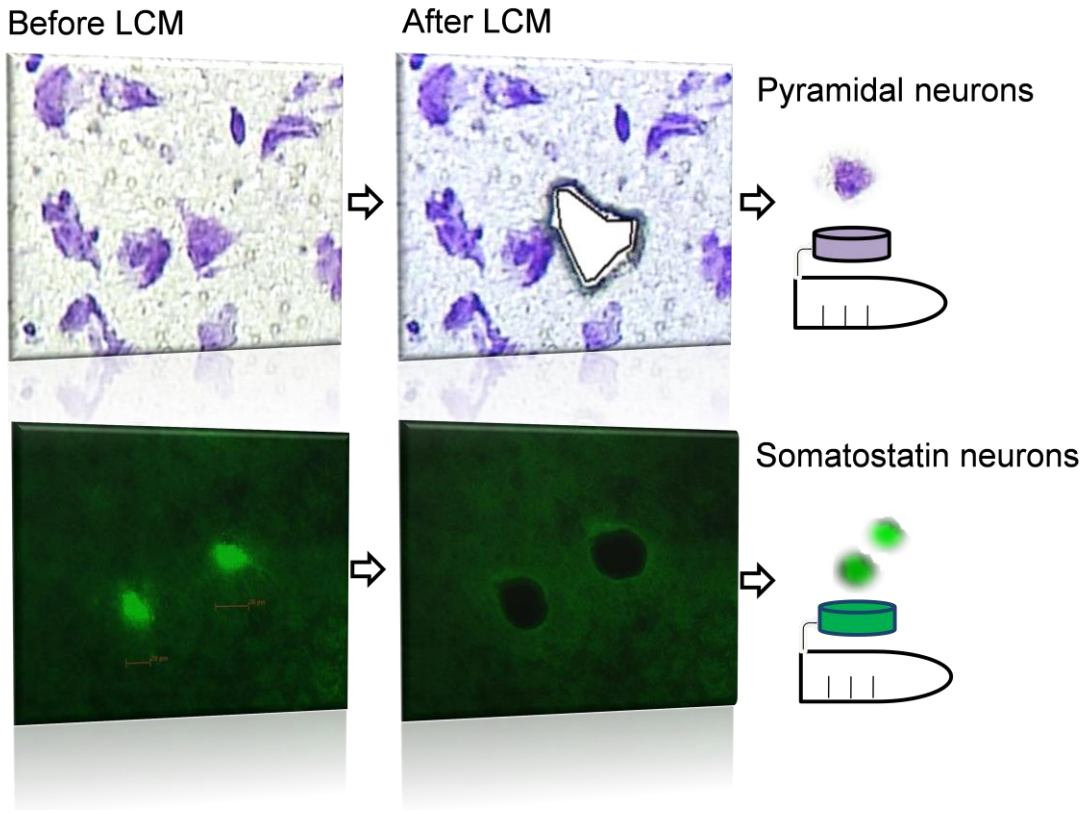

Figure 18. Scheme depicting the use of laser capture microdissection (LCM) to capture cells.

Sections stained with thionin for pyramidal neurons or two somatostatin neurons that can be observed with GFP signal; before LCM and after LCM.

5.3.4 Laser microdissection and gene expression profiling

Laser microdissection was performed using a Leica LMD6500 system under a 40×Objective in the fluorescence mode (for Sst cells) or bright-field mode (for Pyramidal cells). Cutting and collection steps were subsequently examined in fluorescent or bright-field mode. 100 cells in the mouse cingulate cortex (between bregma + 1.42 to -0.5 mm; as shown in 4.3.6) from a given

section were collected in RNA lysis buffer (Qiagen, Valencia, CA) within a 3-hour time span, and stored at −80 °C until further processing. Total RNA was then extracted using the RNeasyPlus Micro Kit (Qiagen) according to the manufacturer's instructions. RNA samples were amplified with NuGEN® Ovation Pico WTA System V2 (NuGen, San Carlos, CA). The fragmented labeled cDNA samples were processed and hybridized to Affymetrix® Mouse Gene 1.1 ST Array Plates (Affymetrix).

5.3.5 Data mining

Gene expression information was obtained with the Affymetrix console software. Genes (dataset targets) showing significant differences (Student t-test p <0.005, >1.2 fold cutoff) in expression between stressed and unstressed SST neurons were analyzed using the IPA software (Ingenuity Systems, Redwood, CA).

a. Canonical pathway analysis. The Ingenuity Knowledge Database includes 642 well-characterized, canonical pathways that were derived from journal articles, textbooks, and the KEGG database, all manually curated by PhD-level scientists. Canonical pathways that differed most significantly were determined by Fisher's exact test. As a result, a p-value was obtained for determining the probability that the association between our dataset targets and the canonical pathway can be explained by chance. In addition, a ratio was determined by the number of dataset targets that map to the pathway divided by the total number of molecules that exist in the canonical pathway.

***b. Upstream regulator analysis*.** Based on previous knowledge of expected causal effects between upstream regulators/drugs and their target genes stored in the Ingenuity® Knowledge Database, this analysis predicted which upstream regulators can explain the observed alterations

of our dataset targets by Fisher's exact test. As a result, a *p*-value was obtained for determining the significance of enrichment of network-regulated genes (the dataset targets downstream of an upstream regulator).

5.3.6 Real-time quantitative polymerase chain reaction

Brains were flash frozen on dry ice after sacrifice. Bilateral cingulate cortex (between bregma + 2.34 to + 0.5 mm) was obtained using a cryostat and a 1-mm-bore tissue punch. Total RNA from mouse cells were amplified with NuGEN® Ovation Pico WTA System V2 (NuGen, San Carlos, CA). All primer sets were listed in Table 3. The comparative threshold cycle (Ct) measurement was performed for quantification with SYBR green fluorescence signal (Invitrogen, Carlsbad, CA) using a Mastercycler® ep Realplex2 real-time PCR machine (Eppendorf, Westbury, NY). PCR thermal cycling was 65°C to 59°C touch-down followed by 50 cycles (95 ˚C for 10 sec, at 59 ˚C for 10 sec, and 72 ˚C for 10 sec). Samples were run in triplicates and the difference in cycle threshold (ΔCt) values for each transcript was determined by comparison to a non-biased control gene, neurofilament (NEFM). The relative expression level of each targeted transcript was determined as 2^{-dCt}.

Table 4. Primer pairs.

Gene	Accession	Size	Forward primer	Reverse primer
Somatostatin (Sst)	NM_009215.1	109	CAACTCGAACCCAGCAAT	GGTCTGGCTAGGACAACAA
eukaryotic translation initiation factor 2A (Eif2a)	NM_001005509.2	97	TGGGACGCCTAACCTACAAC	TGACCAGGAAGGACACCAAT

NADH dehydrogenase (ubiquinone) 1 beta subcomplex 4 (Ndufb4)	NM_026610.1	51	TCCTAATTTCAGGCCCACTC	CCTGCCACAGCTCCTAAAAG
Glutamic acid decarboxylase 67 (GAD67)	NM_008077.4	76	AGACCTCCGATACACTGACC	TGCACACCCTAAATGCAC
neurofilament, medium polypeptide (Nefm)	NM_008691.2	73	GACTTCAGCCAGTCCTCGTC	TCTCGTTAGAGCGGGACAGT

5.3.7 RNAscope Assay for *in situ* RNA Detection

Probe sequences of mouse somatostatin conjugated to Alexa Fluor 488, and eIF2A conjugated to 546 were custom-made and proprietary (Advanced Cell Diagnostics, Hayward, CA). Fresh-frozen cryostat sections (10 µm) were placed on slides and fixed in cold 4% paraformaldehyde for 1 hour, followed by dehydration in an ethanol series. Tissue sections were then dried at room temperature for 30 min, followed by protease digestion at room temperature for 10 min. Using RNAscope Fluorescent Multiplex Reagent Kit (Advanced Cell Diagnostics; # 32085), tissue sections were then rinsed in deionized water, and immediately treated with target probes, preamplifier, amplifier, and label probe in a HybEZ hybridization oven (Advanced Cell Diagnostics, Hayward, CA) according to the instructions of the manufacturer.

5.3.8 Microscopic Imaging

Images were acquired using an Olympus IX71 fluorescent microscope (Olympus, Tokyo, Japan) and a *Fast 1394* CCD *Camera* (QImaging, BC, *Canada*). Overlapping signals from different fluorophores were separated and visualized under a 20x objective lens with MetaMorph Advanced software *(Molecular Devices*, CA, USA). The ratio of overlapping fluorescent signal areas from EIF2A and SST mRNA transcripts was determined in the cingulate cortex (between bregma + 1.42 to -0.5 mm; as shown in 4.3.6), based on 5 microscopic images from 3 tissue sections of each animal (Control group: 14; Unpredictable chronic mild stress group: 14).

5.3.9 Drug Administration

The selective EIF2A phosphatase inhibitor complexes, Salubrinal (Millipore, Billerica, MA, USA) and the EIF2AK3/PERK inhibitor, GSK2606414 (Millipore, Billerica, MA, USA) were dissolved in 100% dimethyl sulfoxide (DMSO) and later diluted in saline (0.9% NaCl). Based on previous studies (Moreno *et al.*, 2012; Ma *et al.*, 2013; Moreno *et al.*, 2013; Kim *et al.*, 2014), vehicle (10% DMSO/saline), Salubrinal (1.5 mg/kg), and GSK2606414 (30 mg/kg) were administered by oral gavage once daily for 7 days to mice treated with 3 weeks of UCMS before behavioral testing. Concentrations were adjusted to administer 10 ml/kg. After 7 days of drug treatments, anxiety/depressive-like behaviors and locomotion were tested in the elevated plus maze (EPM), open field (OF), and novelty suppressed feeding (NSF) with the following order: EPM, NSF, OF, separated by one day of booster administration. All tests were performed during the light phase of the circadian cycle, between 9 am and 3 pm.

Elevated plus maze (EPM)

Anxiety-like behaviors and locomotion were measured in a cross maze with two open and two closed arms (30 cm x 5 cm) as previously described (Sibille *et al.*, 2000). Entries and time spent in the open arms were recorded for 10 min to assess anxiety-like behaviors. Total number of entries was assessed as an index of locomotion.

Open field (OF)

Anxiety-like behaviors and locomotion were measured in a 76 x 76 cm chamber divided in 16 even-size squares and monitored for 10 min using the Any-maze video-tracking software. Percentage of walking distance and time spent in the four center squares were assessed to evaluate anxiety-like behaviors. Total walking distance in the chamber was used as an index of locomotion.

Novelty suppressed feeding (NSF)

Anxiety/depressive-like behaviors were measured for 11 min in a 76 x 76 cm chamber, with a food pellet in the bright-lit center. The drive to overcome the aversive center was increased by 16 hours of food deprivation before testing. The latency to start eating food pellet was measured as an index of anxiety/depressive-like behaviors. Six minutes of food consumption in the home cage after the test was used as a measure for appetite after NSF testing and food deprivation.

Z-scoring

To investigate the consistency of behavioral performance across related tests, emotionality- or locomotion- related data were normalized using a Z-score methodology, as previously described (Guilloux *et al.*, 2011). Z-scores calculate how standard deviation (σ) and observation (X) is above or below the mean of the control group (μ). Raw measures for EPM (time in open arm; % crosses into open arm), OF (time in center; % distance in the center), and NSF (latency to feed) were converted to standard deviations relative to respective means of the control group (Sst^{WT} mice). The directionality of scores was adjusted so that decreased score values indicated reduced anxiety/depressive-like behaviors (termed emotionality). Finally, values across tests were averaged for each mouse to produce individual emotionality Z-scores. Locomotion Z-scores were similarly applied and obtained from EPM (total crosses) and OF (Total distance traveled) data.

5.3.10 Statistical Analysis

Statistical analyses were carried out using GraphPrism Version 6.0 (Graph Pad. Software Inc., San Diego, CA, USA). Student's *t* test was used to compare means between two groups, and one-way or two-way analysis of variance followed by Tukey's post hoc among means were used to determine significant differences among multiple groups. All data are expressed as means ± standard error of the mean. For brevity, uninformative non-significant results were omitted.

5.4 RESULTS

5.4.1 Unpredictable chronic mild stress affects the transcriptome of SST neurons but not pyramidal cells

To investigate whether the above-described changes in BDNF/GABA/SST gene module correspond to broader molecular changes in SST neurons, we applied UCMS to mice expressing green fluorescent protein (GFP) in SST neurons, captured GFP-positive SST neurons and thionin-stained pyramidal neurons from cingulate cortex using laser capture microdissection (LCM), and analyzed RNA profiles of neurons from non-stressed and UCMS-exposed mice, using Affymetrix Gene 1.1 ST microarrays. First, we constructed probability density histograms for the alterations of all gene probesets in SST neurons (**Figures 18A-B**, red bins) and pyramidal neurons (**Figures 18A-B**, black bins), including effect sizes and statistical significance values. Patterns of expression alterations were strikingly different between SST neurons and pyramidal neurons (Kolmogorov-Smirnov test, $p < 0.001$). We found that UCMS affected a large portion of the entire transcriptome of SST neurons, as the frequency distributions of effect size beyond ± 0.3 (changes > 20%; **Figure 18A**) and significance beyond 1.3 ($p < 0.05$; **Figure 18B**) were relatively large in SST neurons from mice exposed to UCMS. In addition, the robust shift to the left in effect size combined with the peak in low p-values distribution in SST neurons indicated profound transcriptome alterations in SST neurons, and mostly characterized by down-regulated expression. In contrast, we observed mostly small and non-significant changes of gene expression in stressed pyramidal neurons.

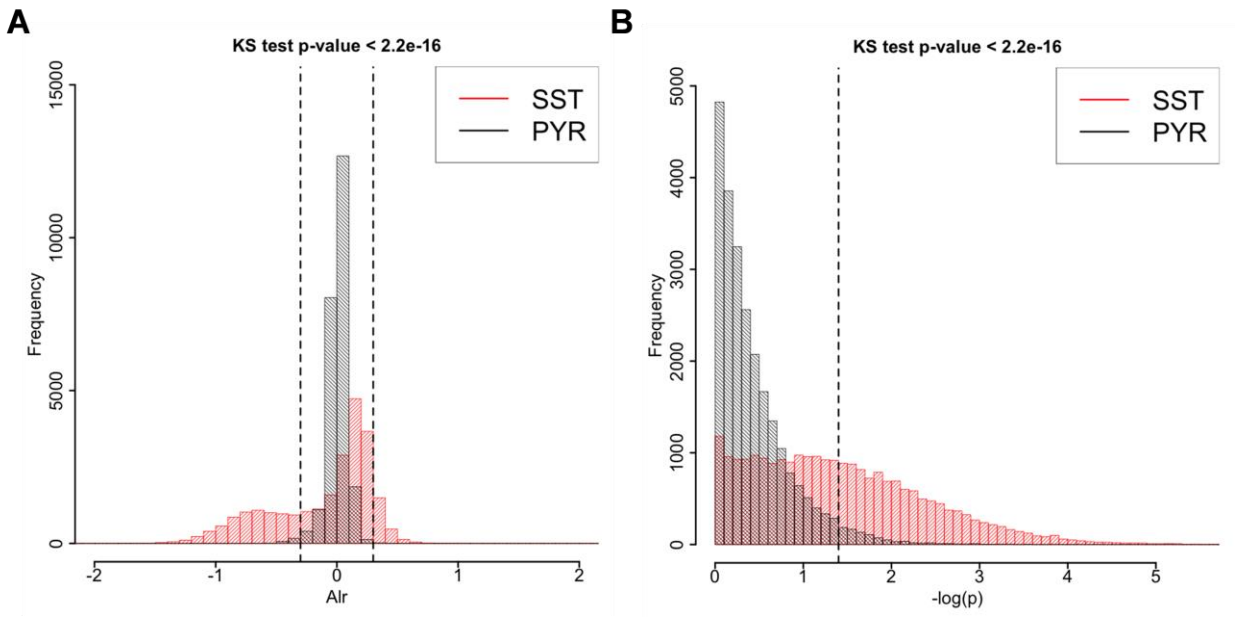

Figure 19. Stress effects on the whole transcriptome profiles in SST-containing interneurons and pyramidal neurons.

Distributions of stress effects for (**A**) effect size (Average $\log_2$ ratio; Alr; changes > 20%; horizontal dashed lines) and (**B**) significance (*p*-value; $p < 0.05$; horizontal dashed lines) of all expressed probesets in SST interneurons (red lines) and pyramidal neurons (PYR; black lines) were presented as density plots. These probability distributions between SST neurons and pyramidal neurons were significantly different (Kolmogorov-Smirnov test, $p < 0.001$).

5.4.2 Unpredictable chronic mild stress down-regulated cellular markers of SST neurons

Sst and *Gad67* were among the genes affected by UCMS, which were further confirmed by independent qPCR assays (**Figures 19A-D).** Four altered genes were chosen and confirmed by qPCR based on their roles in affected pathways of interest (**Figures 19E**).

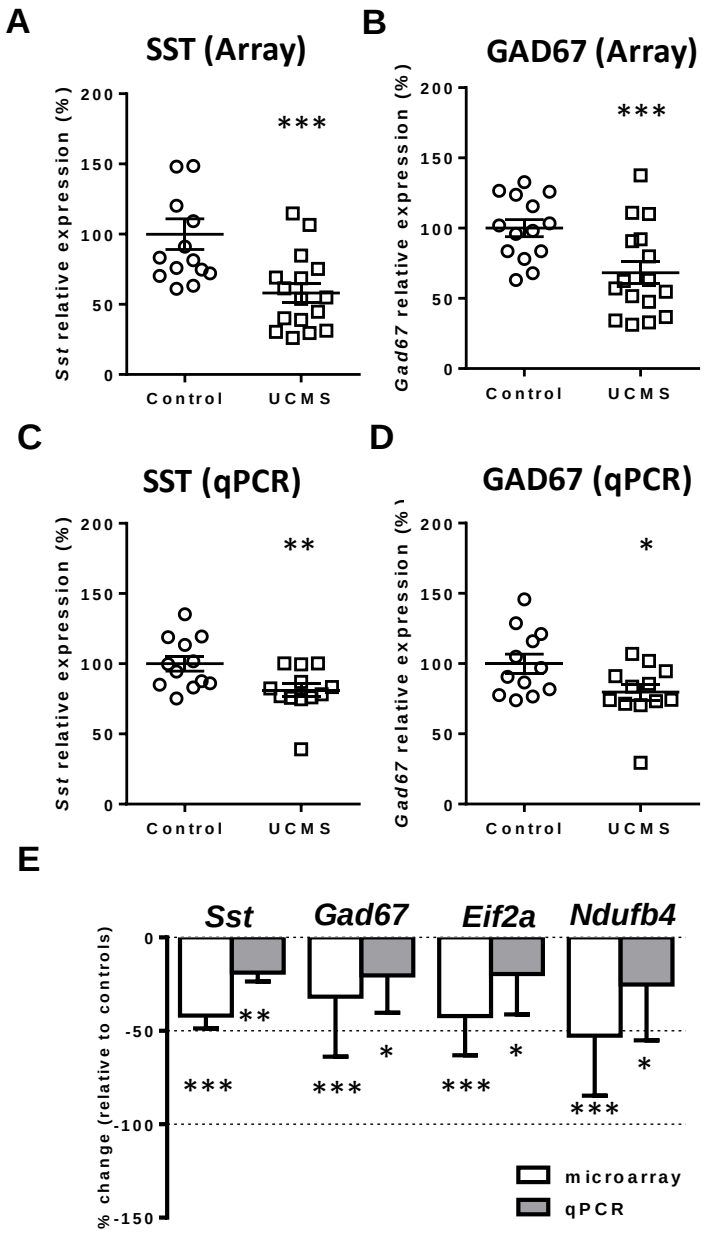

Figure 20. Validation of microarray data.

(A) Down-regulation of SST probes in SST cells exposed to UCMS. (B) Down-regulation of GAD67 probes in SST cells exposed to UCMS. (C-D) qPCR confirmed significant down-regulation of these genes. (E) Blank bars represent the percentage of fold change (UCMS-exposed SST neurons compared to non-stressed SST neurons) by microarray experiment; black bars represent the percentage of fold change using qPCR. A ratio of less than 0 indicates down-regulation. The X axis showed a selected panel of genes. * $p < 0.05$, ** $p < 0.01$, . *** $p < 0.005$ Error bars represent the standard error of the mean (Microarray n=14-16/group; qPCR n=12/group).

5.4.3 Stress links SST neuronal deficits to EIF2 signaling

To assess the biological implications of the transcriptome results, we applied IPA Canonical pathway analysis on differentially-expressed genes under moderate stringency (changes ≥ 20%; $p < 0.005$). Results indicated a striking enrichment of affected genes in protein and functions. The EIF2 pathway was the most significantly affected (p = 7.38E-21) with multiple down-regulated genes in Sst neurons of UCMS-treated mice (**Table 5**).

Table 5. Top ranked canonical pathways affected in SST neurons of cingulate cortex from mice exposed to chronic stress.

Genes were tested for differential expression between UCMS and control groups. Statistical significance for differential expression was reached at fold-change > 20% and $p < 0.005$. The resulting signature was submitted to IPA to test for over-representation of canonical pathways. p-value was calculated by right-tailed *Fisher's exact tests* (Fisher 1922). The ratio was calculated by the number of differentially expressed genes, divided by total number of genes that make up in a given pathway.

Ingenuity Canonical Pathways	P-Value (Fisher Exact test)	Ratio	Regulated Molecules (IFCI>1.2, P<0.005)	
			Up	Down
EIF2 Signaling	7.38E-21	4.03E-01	PIK3CG, INS	RPL11,RPL22,MAPK1,PIK3R1,PDPK1,KRAS,EIF3C/EIF3CL,RPS23, EIF2A,RPS7,RPS3A,EIF4G2,RPL7A,EIF3D,MAPK3,RPL19,RPL8, GSK3B,PPP1CA,RPL36A/RPL36A-HNRNPH2,RPL3,RPL27, RPL37,RPL23A,EIF3E,RPLP0,RPL10A,RPL15,FAU,RPS4X,RPL39, RPS15,RPS25,RPSA,EIF3K,RPL24,PPP1CC,RPS18,RPL22L1, PPP1CB,RPS8,RPS13,RPS21,RPL35A,EIF4E,RPL7,RPL6,RPL35, RPL18A,PIK3C3,RPS9,EIF3A,AKT3,RPS5,RPL31,RPL18, MAP2K1,RPL29,RPL13,RPS24,RPL4,EIF3H,RPS2,RPL17,AGO2, RPL21,RPL23,RPL9,RPS12,EIF2S2,RPS16,RPS26,RPL28,UBA52, AGO3,EIF4A1,EIF3I,RPL38,RPS14
Oxidative Phosphorylation	8.57E-14	4.08E-01	COX6B2	NDUFA9,ATP5D,UQCR11,COX8A,NDUFB5,ATP5L,MT-CO2, NDUFB10,NDUFA5,ATP5G1,NDUFS6,NDUFA10,ATP5F1, ATP5G3,NDUFB3,Cycs,ATP5A1,SDHC,NDUFS5,ATP5B, NDUFA6,NDUFB7,UQCRC2,COX5B,NDUFA4,COX7B,SDHB, UQCRH,COX6A1,NDUFA2,Atp5e,NDUFAB1,ATP5J2,NDUFS2, COX4I1,SDHA,NDUFV1,COX7A2,COX6B1,NDUFB4,ATP5O, NDUFV3,NDUFS3,NDUFA11,CYC1,COX5A,NDUFA3,UQCRQ
Mitochondrial Dysfunction	2.24E-12	2.88E-01	COX6B2, LRRK2, CPT1B	MAP2K4,NDUFA9,ATP5D,UQCR11,COX8A,NDUFB5,ATP5L, MT-CO2,NDUFB10,PDHA1,NDUFA5,GPD2,ATP5G1,NDUFS6, NDUFA10,GPX4,ATP5F1,ATP5G3,NDUFB3,ATP5A1,SDHC,GSR, PRDX3,NDUFS5,ATP5B,NDUFA6,UQCRC2,NDUFB7,MAPK10, VDAC1,SNCA,COX5B,NDUFA4,COX7B,SDHB,UQCRH,COX6A1, NDUFA2,Atp5e,NDUFAB1,ATP5J2,NDUFS2,OGDH,COX4I1, SDHA,NDUFV1,NDUFB4,COX6B1,COX7A2,ATP5O,NDUFV3, MAPK8,NDUFS3,APP,NDUFA11,CYC1,COX5A,NDUFA3,UQCRQ
Remodeling of Epithelial Adherens Junctions	2.62E-09	4.43E-01	CDH1	NME1,RALA,RAB5B,TUBB,CLIP1,ARF6,CTNNA2,EXOC2,ARPC3, TUBA1C,CTNNB1,ACTN1,TUBB3,TUBB4B,ACTB,TUBB2A, TUBA4A,RAB7A,DNM3,ACTG1,TUBA1B,DNM1,TUBA1A, ARPC1A,ARPC2,MAPRE2,ACTN4,DNM1L,ARPC4,MAPRE3
GABA Receptor Signaling	1.00E-08	4.29E-01		AP2B1,AP2A1,AP2M1,ABAT,GABRA4,UBQLN1,GABBR1,Ubb, AP1B1,GABRB2,DNM1,GABBR2,NSF,SLC6A11,GAD2,GABRB3, GAD1,GABRB1,SLC6A1,GABARAP,UBC,GABRA1,GABRA2, GABRA3
Huntington's Disease Signaling	3.43E-08	2.62E-01	PIK3CG, GNG12	MAP2K4,MAPK1,PIK3R1,NAPG,PDPK1,Ubb,CDK5R1,GNB1,NSF, CTSD,MAPK3,DLG4,PLCB1,RASA1,GRM1,IFT57,HSPA9,CLTC, CREBBP,DNM3,GNG3,STX1A,RPH3A,ATF2,TAF9B,HDAC5,HSPA8, DYNC1I2,DNAJC5,ATP5B,HTT,POLR2I,SNCA,SDHB,PACSIN1, POLR2B,VTI1B,GNG7,EP300,POLR2A,PIK3C3,IGF1R,AKT3, PRKCE,NCOR1,NAPB,SDHA,GRIN2B,GLS,MAPK8,GNAQ,Hdac9, SNAP25,ZDHHC17,GRM5,POLR2L,DNM1,PRKCI,DCTN1,STX16, GNG5,UBC,DNM1L,PRKCB
Protein Kinase A Signaling	6.84E-08	2.40E-01	PTPN4, GYS2, PDE6B, TNNI2,PDE12,TCF7L1, TGFB2, PDE6G, TNNI3, TCF3, MYL10, LEF1, H2BFM, NTN1, PPP1R3D, GNG12	MYH10,MYL6,PTPN5,GNB1,CAMK2A,PLCB1,DUSP7,NFKBIB, GNG12,KDELR1,PDE2A,YWHAG,PTCH1,CREBBP,YWHAZ, PLCL2,PTP4A1,ATF2,ACP1,ANAPC5,PTPRA,CAMK2G,RAP1B, TCF4,Calm1,PTK2B,AKAP7,GNG7,EP300,AKAP11,PTPN4, PTPRJ,PRKCE,CTNNB1,PTPRT,PPP3CA,PTPRK,GNAQ,ADD3, ADD1,GNG5,PRKCB,PRKACB,MAPK1,YWHAH,PTEN,ROCK2, Camk2b,PPP1R7,MAPK3,PPP3R1,GSK3B,PPP1CA,YWHAE, PDE10A,YWHAB,GNG3,PTPRM,ANAPC4,H3F3A/H3F3B, MYL12B,RHOA,PTPRS,PPP1R12A,SIRPA,PPP1CC,MYL6B, PPP1CB,PDE1A,BRAF,PPP1R10,,PTPRN,MAP2K1,ADCY2,RYR2, CHP1,GNAI1,PDE4D,Ptprd,PRKCI,AKAP9,PRKAR1A
Regulation of eIF4 and p70S6K Signaling	1.21E-07	2.72E-01	PIK3CG	MAPK1,PIK3R1,RPS18,RPS13,RPS8,PDPK1,KRAS,RPS21,PAIP2, RPS23,EIF3C/EIF3CL,EIF4E,EIF2A,RPS7,RPS3A,EIF4G2,EIF3D, MAPK3,PIK3C3,RPS9,EIF3A,AKT3,RPS5,MAP2K1,RPS24,EIF3H, RPS2,AGO2,EIF3E,RPS12,EIF2S2,PPP2CB,FAU,RPS4X,PPP2R1A, MAPK14,RPS16,RPS26,AGO3,EIF4A1,EIF3I,RPS15,RPS25, PPP2R5E,RPS14,RPSA,EIF3K

Based on the array data, *Sst* expression was highly correlated with *Eif2a* expression (**Figure 20A**), suggesting that EIF2A may be associated with SST deficits. Downregulation of *Eif2a* expression in stress-exposed mouse Sst neurons were validated by qPCR (**Figured 20B**) and high-resolution RNAScope *in situ* hybridization (**Figures 20C-D**).

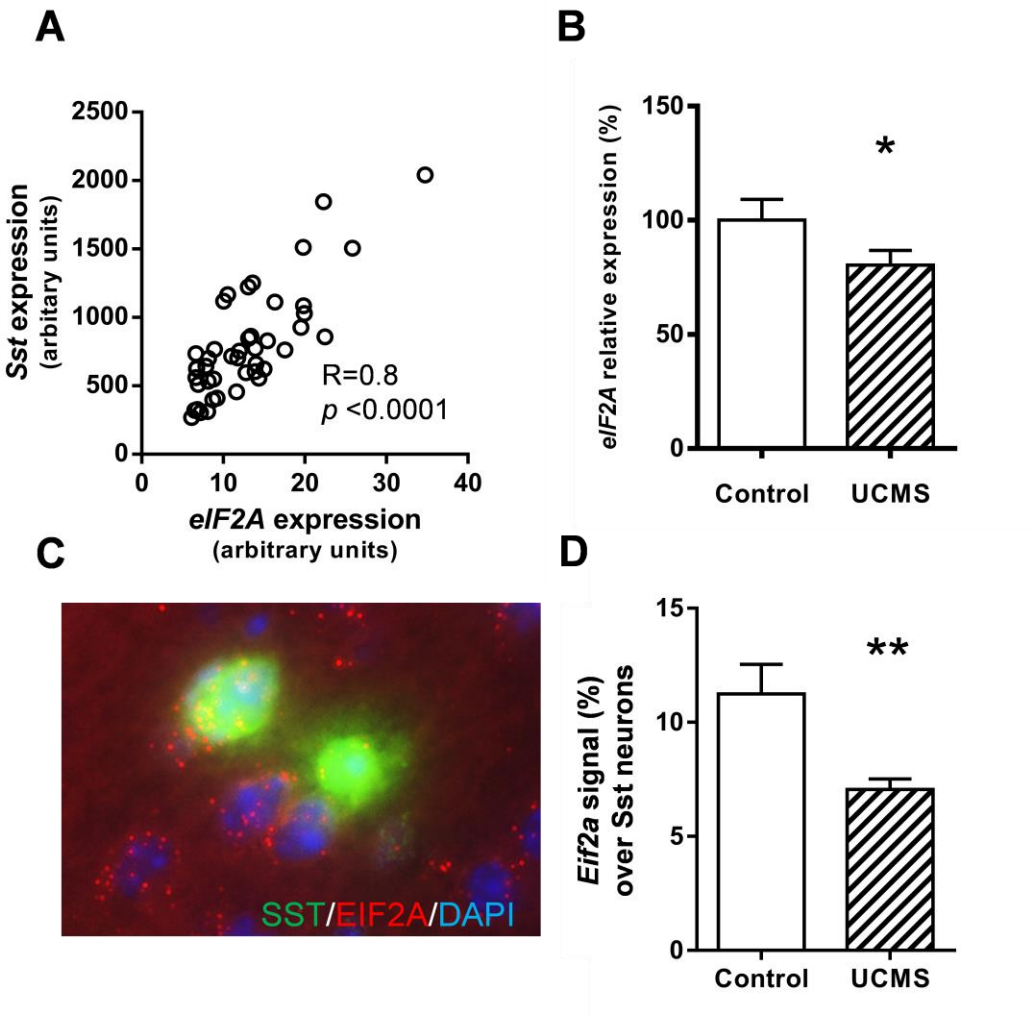

Figure 21. Validation of microarray data of *Eif2a*.

(A) Expression of *Eif2a* was highly correlated with SST expression in mouse SST neurons. (B) qPCR confirms significant down-regulation of *Eif2a* transcripts in UCMS-exposed mouse SST neurons.(C) Representative image of triple-labeling, high-resolution RNAscope *in situ* hybridization. (D) RNAscope *in situ* hybridization validated the downregulation of *Eif2a* in the cortical SST cells. * p <0.05, ** p <0.01. Error bars represent the standard error of the mean (n =12-15/group).

5.4.4 Upstream regulators of molecular signatures in stressed SST neurons

To identify putative causal factors for robust changes in differentially-expressed genes (changes ≥ 20%; $p < 0.005$), we applied the upstream regulators analysis in IPA that predicts upstream regulators based on the literature and compiled in the Ingenuity® Knowledge Base (Kramer *et al.*, 2014). Surprisingly, we found that the top ranked regulators have been previously associated with neurodegenerative diseases (e.g., *MAPT*, *APP*, *PSEN1*, *HTT*) (**Table 6**).

Table 6. Predicted Top 10 upstream regulators of transcripts affected in stressed SST neurons

Upstream regulator	*p* -value
Microtubule-associated protein tau (MAPT)	1.13E-41
Amyloid beta (A4) precursor protein(APP)	2.49E-37
Presenilin 1(PSEN1)	1.56E-30
Huntingtin (HTT)	6.38E-25
N-myc proto-oncogene protein (MYCN)	2.95E-20
CD 437 (apoptosis inducer)	2.98E-20
Histone deacetylase 4 (HDAC4)	6.11E-20
5-fluorouracil (antitumor agent)	4.57E-17
sirolimus (Rapamycin; antitumor agent)	3.99E-16
Fragile X mental retardation 1 (FMR1)	9.41E-16

Note: A Fisher's Exact Test p-value is calculated to assess the significance of enrichment of the gene expression data (change > 20% and $p < 0.005$) for the genes downstream of an upstream regulator.

5.4.5 EIF2 kinase inhibition blocks the development of stress-induced anxiety/depressive-like behaviors

If the process of EIF2 signaling is central to all neurological disorders, then it would be expected that an intervention that modulates this process would also affect shared symptoms, such as mood dysregulation. Compounds that inhibit EIF2A kinase or phosphatase have been developed and validated for use in mice, including for brain-related neurodegenerative models (Moreno *et al.*, 2013; Kim *et al.*, 2014). Given previous findings, we predicted that stress-induced anxiety/depressive-like behaviors would be affected by salubrinal (an inducer of EIF2A phosphorylation via inhibiting EIF2A phosphatase; i.e. pathway blocked; mimic disease effects) (Boyce *et al.*, 2005) or GSK2606414 (an inhibitor of EIF2A phosphorylation via inhibiting EIF2 kinase PERK; i.e. pathway activated; mimic therapeutic effects) (Axten *et al.*, 2012). Results showed that, as predicted, anxiety/depressive-like behaviors in the NSF (**Figure 21A**) and overall emotionality (**Figure 21B**) increased after UCMS treatment. Mice treated with GSK2606414 showed a significant reduction of UCMS-induced anxiety/depressive-like behaviors in the NSF (**Figure 21A**) and emotionality z-scores (**Figure 21B**) that were undistinguishable from control non-stressed mice. However, salubrinal did not significantly exacerbate UCMS-induced anxiety/depressive-like behaviors, suggesting either no effect of salubrinal at a dose of 1.5 mg/kg or a "ceiling effect" of stress on behavioral emotionality. Locomotion (**Figure 21C**), feeding behavior in the NSF (**Figure 21D**), anxiety-like and locomotor behaviors in EPM (**Figures 21E, F, I),** and OF (**Figures 21G, H, J**) were not affected by drug treatments. Together, the results suggest that activation of the EIF2 pathway through GSK2606414 may relieve stress-related mood disturbances.

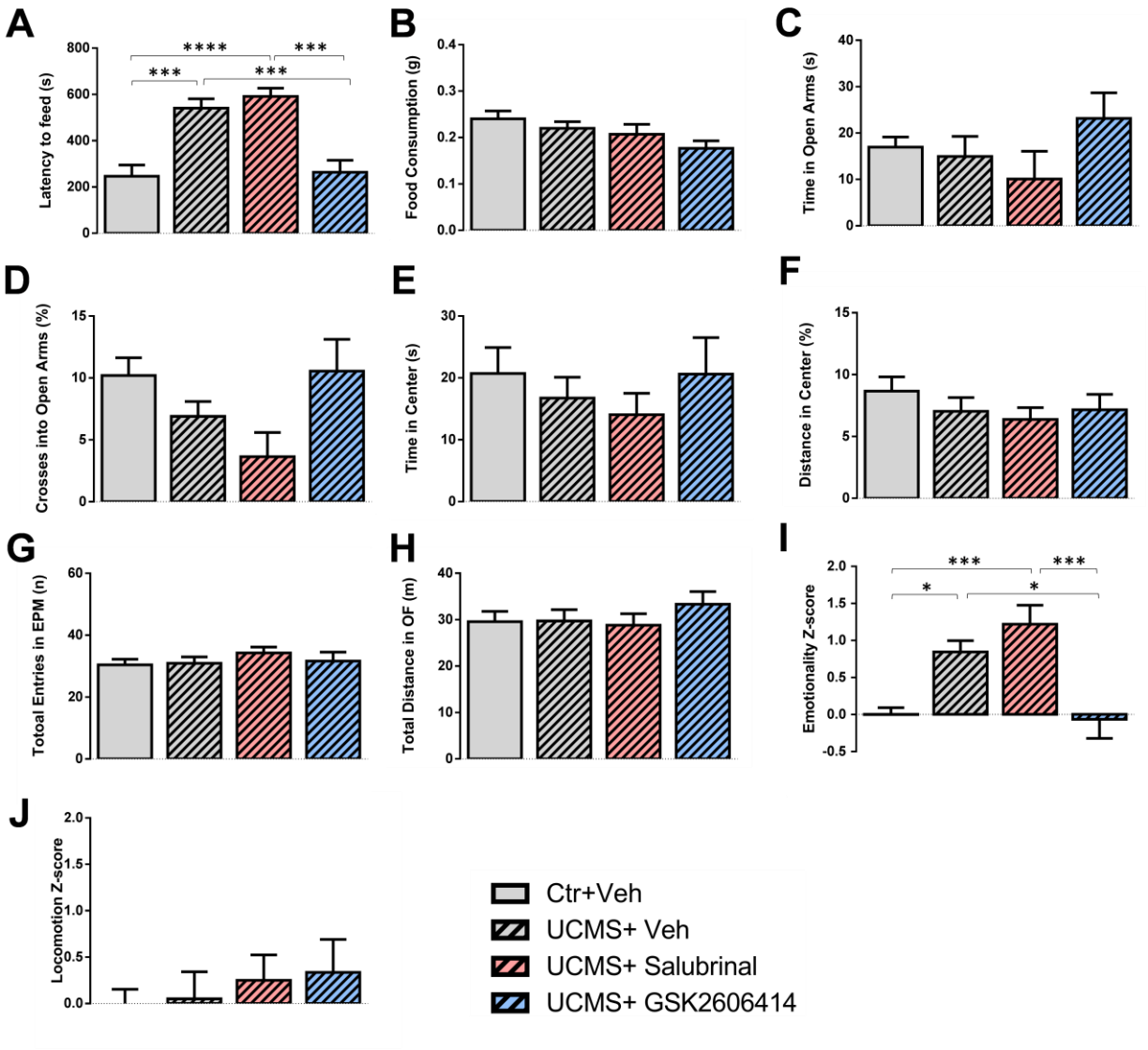

Figure 22. Assessment of anxiety/depressive-like behaviors, locomotor activity, and feeding behavior in mice treated with GSK2606414 or Salubrinal.

Assessment of anxiety/depressive-like behaviors, locomotor activity, and feeding behavior in mice treated with GSK2606414 or Salubrinal. Behavioral phenotypes, including scores in the novelty suppressed feeding test (NSF; A, B), elevated plus maze (EPM; C, D), open field (OF; E, F), locomotion in EPM (G) and OF (H), overall emotionality (I) and locomotion (J), were examined in mice treated with GSK2606414 or Salubrinal. * p <0.05, ** p <0.01, *** p < 0.005, **** p < 0.001. Error bars represent the standard error of the mean. (n = 8-12/group).

5.5 CONCLUSION AND DISCUSSION

Here we used SST-GFP mice to study the effects of chronic stress on the transcriptome profiling of excitatory pyramidal neurons and GABAergic SST interneurons. After exposure to UCMS, we found a selective vulnerability of transcriptome patterns in mouse SST neurons from the cingulate cortex, compared to nearby pyramidal neurons (**Figure 18**). The mRNA expression levels of *Sst* and *Gad67* were significantly decreased in stressed SST neurons. Furthermore, we found a significant effect of chronic stress on the pathways involved in protein translation initiation. Among the deregulated transcript, we observed a striking down-regulated expression of genes in the EIF2/EIF4/mTOR pathways and mitochondrial genes (**Table 5**), suggesting comprised protein translation and mitochondrial function in stressed SST neurons. Reductions in protein translation signaling may act early at ER to protect against oxidative stress and mitochondrial dysfunction. Interestingly, there was a positive correlation between *Eif2a* and *SST* expression. Furthermore, activation of EIF2 signaling with an EIF2 kinase inhibitor mitigated mouse anxiety/depressive-like behaviors induced by UCMS. Thus, these findings suggest that chronic stress suppresses protein translation via EIF2-related pathways and reduce SST-related genes, which may lead to mood dysregulation.

Defects in translational control at any level (signaling pathways, general or specific translation factors) can contribute to disease development. Evidence in human postmortem studies indicated that UPR markers in the brain are temporally and spatially linked to the accumulation and occurrence of misfolded pathological proteins (Roussel *et al.*, 2013; Hetz & Mollereau, 2014). Based on the IPA upstream regulators analysis of affected transcripts in stressed SST neurons (**Table 5**), we found that the top ranked regulators have been previously associated with neurodegenerative diseases (e.g., *MAPT*, *APP*, *PSEN1*, *HTT*) (**Table 6**). These

disease-linked proteins are prone to aggregation and contribute to neuronal dysfunction and death in neurodegeneration, includin Aβ, tau, presenilins, and huntingtin. In addition to supporting a link between stress and neurodegenerative processes, these findings are consistent with the notion that SST deficits are frequently observed in neurodegenerative diseases. Moreover, these results are in line with a previous study demonstrating that SST ablation alters the metabolism of amyloid β peptide (Aβ; primary pathogenic protein of Alzheimer's disease) and specifically increases Aβ42 that has high amyloidogenicity and neurotoxicity (Saito *et al.*, 2005).

Translation control is a key regulatory principle in regulating cell physiology and responses. EIF2 plays a crucial role in binding the initiator methionly-tRNA Met to the 40S ribosomal subunit to form a 43S preinitiation complex. The endoplasmic reticulum (ER) responds to environmental stress through activation of an evolutionarily conserved, protective mechanism termed the unfolded protein response (UPR). UPR activation directly phosphorylates and inhibits eukaryotic translation initiation factor 2α (EIF2A), which confers a general inhibition of protein translation and is thought to protect cells against the ER stress-induced apoptosis cascade (Harding *et al.*, 2000). Decreased EIF2 pathway activation has been reported in aging process, Alzheimer's (AD), Parkinson's disease (PD), animal models of AD, prion disease, and amyotrophic lateral sclerosis (Kimball *et al.*, 1992; Nagata *et al.*, 2007; Ma *et al.*, 2013; Kim *et al.*, 2014). Subjects with AD and a murine AD model showed high eIF2A phosphorylation (eIF2A-P) levels, and the majority of neurons with eIF2A-P were co-localized with strong immunoreactivity for phosphorylated tau (Chang *et al.*, 2002; Hoozemans *et al.*, 2009). Hence, there is considerable interest in understanding the functional role of EIF2 signaling in neurological disorders.

A specific EIF2A kinase inhibitor (GSK2606414) has been shown to alleviate the development of prion infection in mice and protected neurons from prion-related neurodegeneration (Moreno *et al.*, 2013). GSK2606414 is a highly selective inhibitor of Protein kinase R (PKR)-like ER kinase (PERK) in the UPR pathway (Axten *et al.*, 2012). Once activated, PERK phosphorylates EIF2A at serine 51 to inhibit translation initiation and reduce overall protein synthesis. Its half-life measured in rat is approximately 2.5 hours (Axten *et al.*, 2013). Compared to the other optimized PERK inhibitor (GSK2656157) selected for preclinical development, GSK2606414 is more lipophilic and brain-penetrant and appears to be the best available compound for oral administration (Axten *et al.*, 2013). However, GSK2606414 broadly inhibited cytochrome P450s in human liver, potentially leading to further damage to the liver (Axten *et al.*, 2012). Interestingly, an inducer of EIF2A phosphorylation (salubrinal) can reduce the accumulation of α-synuclein in PD-model mice and delay progressive manifestations of weakening and paralysis in ALS-model (Saxena *et al.*, 2009; Colla *et al.*, 2012). However, salubrinal can also exacerbate neurotoxicity and reduce survival rates in prion-diseased mice, and enhance ER stress-mediated stress granules in ALS-model mice (Walker *et al.*, 2013). These findings reflect a complex scenario of sustaining cellular proteostasis and a promising therapeutic target on neurodegeneration depending on the disease context and processes. As the last experiment in this dissertation, we directly probed whether EIF2 signaling has a functional role in stress-associated behavioral emotionality by treating UCMS-exposed mice with GSK2606414 or salubrinal.

The maintenance of a healthy cellular proteome is essential to suppress neurodegeneration. We speculated that the suppressed EIF2 signaling in stressed SST neurons may be an early adaptive mechanism to reduce the burden of destabilized proteins associated

with stress, but at the cost of reduced ability to alter translational activity under chronic stress conditions. Hence, chronically suppressed proteostasis may increase SST deficits and make SST-releasing neurons more vulnerable to stressors and diseases. Accordingly, one plausible explanation for normalized emotionality in stressed mice after activation of EIF2 pathway via GSK2606414 treatment (**Figure 21**) would be that boosting protein translation allows stressed Sst neurons to exert a routine protective response, which then up-regulates stress-responsive genes (e.g., SST-GABA signaling) necessary for neuroplasticity and mood regulation. Salubrinal did not significantly exacerbate UCMS-induced anxiety/depressive-like behaviors, suggesting either no effect of salubrinal at a 1.5 mg/kg dose or a ceiling effect of stress on behavioral emotionality.

The interactions between translational regulation and neurodegeneration in mood regulation have only been examined in a limited context (Calkhoven *et al.*, 2002; Moylan *et al.*, 2013). Different EIF2 signaling branches of UPR might control specific cellular events dependent the context of neurological disorders. Future studies aimed at cell-specific alterations of EIF2 signaling will provide a more comprehensive coverage of complex neural circuits and behaviors. Moreover, it is important, as a future study, to validate EIF2A's role in SST neuron function or loss *in vivo*. For this, four approaches could be fruitful: (1) performing a longitudinal immunohistochemistry study to look at EIF2A expression in SST neurons under baseline unstressed condition, after acute stress, after chronic stress, during recovery from chronic stress, and at end-stage (i.e. after second hit of chronic stress exposure); (2) performing a similar immunohistochemistry study in postmortem brains of depressed subjects; (3) generating transgenic mice carrying SST neuron-specific null mutation of EIF2A gene by using the Cre-lox system and/or viral vectors. These double-engineered mice could then be used to assess the

impact of the EIF2A deletion within SST neurons on the onset of disease manifestations or during disease processes caused by UCMS; (4) investigating layer-specific alterations of cortical SST neurons; (5) EIF2A was only one of the top genes inferred by the IPA based on the previous studies; in order to understand the complete translational machinery that make SST neuronal dysfunction or loss, the pathological significance of the other related genes needs to be investigated as well.

The most recognized function of microarray analysis is high-throughput genomic profiling; however, this method has several disadvantages in comparison to RNA-Seq assays and ribosome profiling. As discussed in recent reviews (Wang *et al.*, 2009; Metzker, 2010; Ingolia, 2014), microarrays have high background signals, limited dynamic range of detection, high cost of amplification step, and limited transcript detection that relies on prior knowledge of genome sequence. Additional deep sequencing to directly determine the cDNA sequence or the amount of proteins in stressed SST neurons is needed to provide further insights into the molecular mechanisms of selective vulnerability of SST neurons.

Beyond mood disorders, a variety of mental health conditions, including Alzheimer's disease, Parkinson's disease and Huntington's diseases, are linked to changes in SST expression and ER stress. Thus, our finding of suppressed EIF2 signaling in stressed SST neurons may be a general mechanism underlying neurological disorders, or at least often occurred in neurons under physiological and cellular stress.

6.0 GENERAL DISCUSSION

Previous human postmortem studies raised the possibility that SST and SST-containing interneurons in the local cortical circuits of individuals with depression and other neurological disorders are altered, and thus could represent a shared common pathological feature. Therefore, in order to better understand the pathophysiology of SST interneurons and how SST deficits contribute to mood disturbances, this thesis explored behavioral alterations by SST ablation, as well as explored possible upstream mechanisms of selective SST neuronal vulnerability to chronic stress. We identified a causal role of SST in HPA hyperactivity, down-regulated BDNF-GABA signaling, and anxiety/depressive-like behaviors in mice. However, HPA hyperactivity is not sufficient to explain anxiety/depressive-like behaviors associated with SST deficits. We also identified a selective vulnerability of SST neurons to chronic stress. Among deregulated pathways, translational machinery was suppressed in SST neurons of stressed mice. Activation of EIF2 signaling with an EIF2 kinase inhibitor mitigated anxiety/depressive-like behaviors induced by UCMS. Thus, mood symptoms in neurological disorders might occur when chronic environmental/psycho-social stressors affect the translational machinery in the cortical SST neurons and then compromise SST-related inhibitory neurotransmission. Our GSK2606414 finding further suggests that EIF2 signaling may also have anxiolytic/antidepressant effects. Although still preliminary, the use of proteostasis therapeutics could be a unique opportunity to

gain further insight on the physiology of selective neuronal vulnerability and its involvement in mood dysregulation.

Depression and anxiety have a high co-morbidity and co-occurrence rate (Gorman, 1996; Pollack, 2005), behavioral assessment from a battery of tests provides a dimensional view of neurobiology underlying mood regulation. Accordingly, we applied emotionality z-score to integrate behavioral results in the four commonly used tests, including elevated plus maze, open field, novelty- suppressed feeding (NSF), and sucrose preference test. Interestingly, we consistently observed robust phenotypes in the NSF across different experiments in this dissertation. Compared to other behavioral tests, NSF has a distinct sensitivity to detect chronic efficacy of antidepressants but not acute or sub-chronic treatments in rodents, which agrees with the clinical observations in human (Dulawa & Hen, 2005). The origins of the robust phenotypes in the NSF and differences in behavioral responses across tests are not known, but it could reflect that NSF test is sensitive to chronic SST deficits induced by genetic manipulation or UCMS.

Every cell in the central nervous system receives cellular stress, but some types of cells show selective dysfunction or die during early disease or aging processes. Determinants of neuronal vulnerability might include cell content and location in the neural circuitry, metabolism of disease-specific proteins, and other stress-related mechanisms. In the following sections, I propose a working model of mood dysregulation that is based on results from this dissertation and findings from previous literature. I will also discuss some limitations of the studies in the thesis and propose future directions.

6.1 PROPOSED DISEASE MODEL IN MOOD DYSREGULATION

The goal here is to integrate our and others results that can explain how SST is related to the etiology of mood disorders. Specifically, this dissertation tried to answer the following questions: does low SST play a causal factor in mood disturbances? How does chronic stress affect SST neurons and how does it link to stress-related mood symptoms? The following model of the disease process incorporates our observations (**Figure 22**). A set of genetic predispositions and environmental stressors reduces BDNF/GABA-related SST signaling. Several downstream mechanisms trigger protein suppression via suppressed EIF2 signaling in selectively vulnerable neurons, such as SST-containing interneurons. The following alterations of GABA signaling in the local cortical circuits and hyperactive HPA axis activity may impair structure and function of cingulate cortex, which gives rise to inefficient information processing underlying behavioral phenotypes of mood dysregulation.

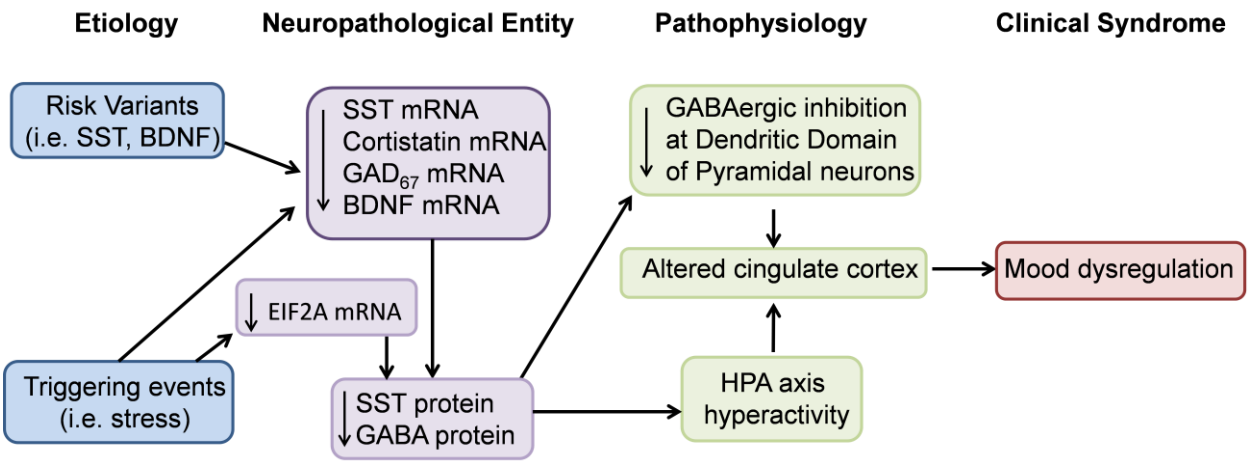

Figure 23. Proposed disease model illustrating potential cascade of events related to mood dysregulation.

6.2 LIMITATIONS AND FUTURE DIRECTIONS

6.2.1 Confirmation of effects of SST deficits in specific brain regions on emotionality

The goal of the studies outlined in this dissertation was to determine whether down-regulation of SST could be a causative factor in mood dysregulation. We examined anxiety/depressive-like behaviors, neuroendocrine phenotype, and the molecular profile of Sst^{KO} and Sst^{HZ} mice. We found that Sst^{KO} mice recapitulated behavioral, molecular, and neuroendocrine changes similar to those seem in MDD. Hence, the results suggest that SST plays a causal role in mood dysregulation. However, it is difficult to conclusively make this statement in global Sst^{KO} mice without controlling for other confounding factors (region specificity, functional compensation, feeding behaviors, etc.) since diseases rarely include full loss of gene function. SST deficits are found throughout the brain in human postmortem studies making it difficult to pinpoint regional effects. Therefore, future experiments that utilize mouse models with region-specific reduction of SST expression are needed to test our hypothesis that SST plays a causal role in mood regulation Future experiments could utilize mice with genetic manipulation in which SST is selectively knocked down *in vivo* utilizing viral-mediated RNA interference. An alternative approach is to cross mutant animals with "floxed" loci of SST gene to a strain expressing Cre recombinase under control of a cell- or tissue-specific promoter. Reducing SST neuronal function acutely and chronically in the frontal cortex yields opposite effects on behavioral emotionality, suggesting complex network adaptations associated with mood regulation that depend on the timeframe and potentially on the set of targeted regions as well (Soumier & Sibille, 2014). We predict that loss of SST in the corticolimbic regions would increase anxiety/depressive-like behaviors.

6.2.2 Confirmation of alterations in protein translation in stressed SST interneurons

We have argued that the massively suppressed expression of EIF2/EIF4/mTOR signaling in stressed SST neurons indicate global protein suppression. The studies within this thesis only examined mRNA expression of these signaling pathways. The functional implications of reductions in mRNA expression can only be true if there is a concurrent reduction in the cognate protein. The concurrent reduction in protein and mRNA needs to be confirmed in future experiments, including total protein synthesis and EIF2A protein levels in SST neurons. In addition, it is important to confirm alterations in protein translation in subpopulations of SST neurons using other stress models. Other stress-sensitive regions, including amygdala and hippocampus, are also attractive targets to test whether there are general effects of stress on EIF2 signaling in SST neurons. Another future research direction is disease progression. If six weeks of UCMS significantly reduced SST expression and suppressed Eif2 signaling, whether and how these effects persist and accumulate with stress load should be studied in depth; further, how long-term changes in protein translation affect inhibitory function of SST neurons in the local neural circuitry remains to be determined.

6.2.3 Identification of unique markers for SST interneurons across species

How do the mouse findings relate to SST cell pathology in human subjects with major depression? Many peptides are difficult to visualize in the cell body under postmortem conditions (Doucet & Morrison, 2011). We did not report an experiment utilizing SST protein antibody in order to characterize transcriptome profiles of SST interneurons in depressed human subjects because of the following potential confound. Some of these interneurons may not

express detectable levels of SST protein. This suggests that any labeling study that is performed with SST antibody in depressed subjects would be biased since the marker (SST protein) is not detectable in some neurons. Therefore, potential alternative markers for SST interneurons that are not altered by stress or in major depression are needed to adequately isolate SST neurons.

6.2.4 Proof of principle experiment: Selective suppression in EIF2 signaling in SST interneurons affects long-term modification of neural circuits and mood regulation

In Chapter 6, we predicted that alterations in EIF2's translational control in SST neurons leads to mood dysregulation. In addition, we found that activation of protein translation via oral treatment of an EIF2 kinase inhibitor reversed stress-induced emotionality in mice. Based on these findings, we hypothesize that suppressed EIF2 signaling in SST neurons will lead to deregulated cellular protein synthesis, which could further contribute to GABAergic inhibition of the dendritic portion of pyramidal neurons. This hypothesis can be tested in mice with knock-down of *Eif2A* in SST neurons (specifically in the cingulate cortex), utilizing viral-mediated RNA interference. There should be observable dysfunctions at synaptic and circuit levels, such as altered firing rates of SST interneurons and pyramidal neurons, as well as reduced presynaptic release probability in GABAergic terminals. By altering the baseline levels of protein translation through EIF2A, dysregulation of SST neuronal protein synthesis may interfere with synaptic modification in response to stress. It will be of interest to determine whether these mice are more vulnerable to develop anxiety/depressive-like behaviors after exposure to chronic stress. If our hypothesis proves to be correct, approaches to restoring normal levels of protein expression may provide a therapeutic strategy for treating mood dysregulation. Using a similar viral-mediated approach, emotionality of mice with over-expression of *Eif2A* in SST neurons can be tested after

exposure to chronic stress. We anticipate that these mice would exhibit less stress-induced phenotypes to further support our hypothesis that EIF2-regulated translation is involved in mood regulation.

The studies in this thesis only examined the functional role of EIF2 signaling in mood regulation using pharmacological manipulations. In Chapter 5, we also identified EIF4 and mTOR signaling as top canonical pathways affected in stressed SST neurons. In addition to EIF2 signaling, the EIF4 and mTOR pathways also play critical roles in protein homeostasis (Gingras *et al.*, 1999; Wang & Proud, 2006), and inhibiting protein synthesis during UPR. EIF4 is involved in directing ribosomes to the cap structure of mRNAs (Calkhoven *et al.*, 2002). mTOR targets EIF4 and S6 protein kinases to mediate cell growth and protein homeostasis in response to metabolic and stress signals (Polak & Hall, 2009; Laplante & Sabatini, 2012), and is implicated in ketamine antidepressant effects (Li *et al.*, 2010). Therefore, we speculate that EIF4 and mTOR signaling pathways in SST neurons also have functional implications in mood regulation.

6.3 CONCLUSIONS ON THE CONTRIBUTION OF SST AND EIF2 SIGNALING

Previous studies from our lab indicate that SST is down-regulated in several regions of MDD subjects. Here, our results indicate that Sst^{KO} mice have: 1) high baseline/trait emotionality, 2) high anxiety/depressive-like syndrome after exposure to chronic stress, 3) robust downregulation of GABA- and BDNF- related transcript, and 4) high basal levels of plasma corticosterone. Using a mouse stress model of depression (UCMS), we found that SST-containing interneurons were selectively vulnerable to chronic stress. EIF2-related transcripts were robust down-

regulated in stressed SST neurons. Re-activation of EIF2 pathway by an EIF2A kinase inhibitor can reduce stress-induced anxiety/depressive-like behaviors in mice. In conclusion, dysfunction of SST and SST neurons could translate to suboptimal inhibitory control of cortical local circuits, priming the system for deregulated physiological responses to stress and inducing multiple endophenotypes associated with mood dysregulation.

APPENDIX A

A HUMAN-MOUSE CONSERVED SEX BIAS IN AMYGDALA GENE EXPRESSION RELATED TO CIRCADIAN CLOCK AND ENERGY METABOLISM

Molecular Brain. 2011 4:18.

Li-Chun Lin, David A. Lewis and Etienne Sibille*

Translational Neuroscience Program, Department of Psychiatry, and Center for Neuroscience

3811 O'Hara Street, University of Pittsburgh, Pittsburgh, PA 15213, USA.

*Correspondence: sibilleel@upmc.edu (ES)

Tel (412) 624-0804. Fax (412) 624-9910

linq@upmc.edu (LCL), lewisda@upmc.edu (DAL)

Abstract

Background: Major depression affects twice as many women as men, but the underlying molecular mechanisms responsible for the heightened female vulnerability are not known. The amygdala, composed of heterogeneous subnuclei, participates in multiple functional circuits regulating emotional responses to stress. We hypothesized that sex differences in molecular structure may contribute to differential mood regulation and disease vulnerability.

Findings: Using gene arrays followed by quantitative PCR validation, we compared the transcriptome profiles between sexes in human and mouse amygdala. We now report sexually dimorphic features of transcriptomes in the basolateral nucleus of the amygdala, and these features are highly conserved across species. A functional analysis of differential gene expression showed that mitochondrial-related gene groups were identified as the top biological pathways associated with sexual dimorphism in both species.

Conclusions: These results suggest that the basolateral amygdala is a sexually dimorphic structure, featuring a regulatory cascade of mitochondrial function and circadian rhythm, potentially linked through sirtuins and hormone nuclear receptors. Hence, baseline differences in amygdalar circadian regulation of cellular metabolism may contribute to sex-related differences in mood regulation and vulnerability to major depression.

Introduction

Males and females differ in behavior and brain structure, as well as in prevalence of neuropsychiatric disorders. The greater prevalence of major depression and rapid cycling bipolar disorder in women (Kendler, 1998; Tondo & Baldessarini, 1998) highlights the importance of studying potential mechanisms for sex differences. Sex chromosome- and hormone-linked genes may directly affect sexually dimorphic neurobiology (Jazin & Cahill). For example, sex hormones regulate the size of the medial amygdala and bed nucleus of the stria terminalis during development (Hines *et al.*, 1992). The lateral (LA) and basal (basolateral; throughout the article we refer to human BA and mouse BLA) nuclei of the amygdala have been identified as critical sites for learned fear and emotion regulation in healthy subjects and in patients with mood disorders (Sheline *et al.*, 2001; Sibille *et al.*, 2009a), but little is known about their sexual dimorphism. The isolation of subnuclei from the amygdala complex improves microarray sensitivity to detect differences in gene expression by reducing sample heterogeneity, and could facilitate the subsequent identification of genetic sex differences. To characterize sex differences in the intrinsic molecular properties of the amygdala, we examined the presence of sexually dimorphic patterns of gene expression in the basolateral nuclei of the amygdala using postmortem samples from control human subjects and mice.

Methods

Human Brain Samples

Postmortem amygdala samples from 12 healthy male controls and 12 healthy female controls (age = 39-64 years) were obtained from the University of Pittsburgh Brain Donation Program

(Table 1), as previously described (Sibille *et al.*, 2009a). Male and female groups were matched in pairs as closely as possible on the basis of RNA integrity, pH, post-mortem interval, age, and sex, and the groups did not differ on any of these parameters ($p>0.05$; Table 1). All subjects died suddenly without prolonged agonal periods. See (Sibille *et al.*, 2009a) for additional details. In contrast to the light acetylcholinesterase (AChE)-stained LA across species, human BA and mouse BLA contained the heavy stained AChE-positive neuropil in the amygdala (Svendsen & Bird, 1985; Kitt *et al.*, 1994), implying that human BA and LA anatomically correspond to the mouse BLA and LA according to the well-defined AChE boundaries. Hence, based on the distribution of AChE activity and thionin staining, human lateral (LA) and basal (BA) amygdala nuclei were defined and separately harvested from 20-μm cryostat sections using a clean RNase-free pipette tip. All procedures were approved by the University of Pittsburgh's Committee for the Oversight of Research Involving the Dead and Institutional Review Board for Biomedical Research.

Mouse Brain Samples

Brains from adult C57BL/6J mice (n = 5 per sex; pooled by 2 from 10 mice/group, 3 months of age) were harvested, fresh frozen and cryo-sectioned at 20 μm on UV-treated laser-capture microscopy slides (Leica Microsystems, Wetzlar, Germany). Sections on the slides were dried and stored at −80°C until used. Lateral (LA) to basolateral (BLA) amygdala nuclei were visualized with rapid thionin staining and dissected with the Leica LMD 6500 laser microdissection system. All mice were maintained on a 12-hour light-dark cycle (lights on 06:00 and lights off on 18:00) with ad libitum food and water. All procedures were approved by the

University of Pittsburgh Institutional Animal Care and Use Committee (protocol # 0911014A-2, Animal Assurance # A3187-01).

RNA extraction for Microarray Samples

Total RNA was extracted using the RNeasy Plus Micro Kit (QIAGEN, Valencia, CA) and processed for microarray analysis according to manufacturer's protocol. RNA samples were amplified with Illumina TotalPrep RNA Amplification Kit (for human tissue; Illumina, San Diego, CA) and Nugen WT-Ovation Pico RNA Amplification System (for mouse tissue; NuGen, San Carlos, CA). The fragmented labeled cRNA samples were processed and hybridized to microarrays (Human HT-12v3 and MouseWG-6v2.0 BeadChips).

Array Data Analysis

For statistical analysis, the $\log_2$-transformed signal intensities of probe-sets that passed the initial expression filters (<30% missing values, detection p-value >0.1), were extracted and renormalized to the same mean and variance across arrays in order to control for any effects of batch. Discovery threshold for male/female differences were applied in both species (two-tailed *t*-test *p*-value <0.05; >20% effect size). Functional analyses were performed on the identified gene list using the Ingenuity Pathways Knowledge Base [9] and compared across species.

Real-time Quantitative PCR (qPCR) Data Analysis

Separate RNA samples were reverse-transcribed using QScript cDNA super mix (QuantaBioscience, Gaithersburg, MD) using a combination of oligo (dT) and random primers. Each PCR reaction was performed in triplicate and compared to three internal controls (GAPDH,

beta-actin and cyclophilin). All designed primer sequences were designed with Primer3Plus (Additional File 1, table S1). Results were calculated as the geometric mean of relative intensities compared to the three internal controls. Validation of the array results was considered at $p<0.05$, using one-tailed unpaired *t*-test.

Results

Using exploratory criteria we generated large and informative parallel human/mouse transcriptome datasets from male and female BA (BLA in mice) and LA nuclei of the amygdala. As an internal control to assess the sensitivity of the array approach, all detected Y-chromosome genes (male-specific) displayed significantly male-biased expression, and expression of numerous X-linked genes showed a female bias (Figure 1). In humans, 1335 sex-biased autosomal genes were identified in BA (Additional File 2, table S2), and fewer (n =165) in LA (Additional File 3, table S3). In mice, ~1% of autosomal genes displayed sex-biased expression (BLA, n =515, Additional File 4, table S4; LA, n =556, Additional File 5, table S5).

To reduce false discovery and focus on the most relevant changes, we characterized the functional and cross-species relatedness of autosomal sex-biased gene sets using the Ingenuity Pathways Analysis (IPA) database. Mitochondrial-related functions were consistently identified among the top four most-represented pathways in human BA ($p<1.57E^{-06}$), mouse BA ($p<8.37E^{-03}$) and mouse LA ($p<6.72E^{-02}$). Assembly of RNA Polymerase III Complex was the only identified canonical pathway in human LA and was at trend level (p <0.1).

Within the mitochondrial-related functions, genes encoding enzymes of the mitochondrial electron transport chain (ETC) consistently displayed high male-biased expression (Figure 2A). Also, two genes coding for mitochondria-localized sirtuins (SIRT3, SIRT5), which serve as

metabolic regulators of circadian rhythms by utilizing NAD^+ (Asher *et al.*, 2008), also showed similar high male-biased expression in human BA and mouse BLA. Of related interest was the identification of sex-biased circadian rhythm signaling in human BA (IPA, $p<5.39E^{-04}$) and mouse LA ($p<3.54E^{-02}$), which included conserved high female-biased expression of selected circadian clock genes (e.g., Period 2 and trend-level for CLOCK; Figure 2A). Intriguingly, as nuclear receptors link the circadian clock to metabolism (Yang *et al.*, 2006), retinoic acid orphan receptor β (RORB) and thyroid hormone receptor α (THRA) displayed high female-biased expression in human BA (RORB: average log ratio [alr] = 0.29, p <0.026; THRA: alr =0.31, p <0.013).

The accuracy and reproducibility of the approach was assessed by qPCR on independent samples. 12 genes out of 18 tested were individually confirmed ($p<0.05$; same direction; Figure 2B). Overall, the qPCR validation results were highly correlated with array data using Pearson tests for significance ($r = 0.86$, $p < 2.5E^{-06}$; Figure 2D).

We next evaluated the anatomical extent of the observed sex-biased gene profiles in other brain areas using existing human array data in cortical regions (Galfalvy *et al.*, 2003). Numerous ETC and SIRT genes in dorsolateral prefrontal cortex (Brodman area 9 [BA9]; Figure 2C), and fewer in the ventrolateral prefrontal cortex (Brodman area 47 [BA47]; Figure 2C) and anterior cingulate cortex (ACC; Figure 2C), consistently displayed high male-biased expression, suggesting variable levels of regional conservation and amygdala enrichment.

Notably, within the limited cohort size and age range, we did not observe statistically significant age-related effects for genes confirmed by qPCR, except for male-biased ATP synthase genes (ATP5A1, $r = -0.78$, $p < 0.005$; ATP6VOD1, $r = -0.58$, $p < 0.05$) in human male amygdala. Since no information was available for menopause or estrogen replacement treatment

for the human female subjects, we interpreted these results as indicative of sexual dimorphism independently of age or estrogen status, although this will need to be tested in larger cohorts.

Discussion

We report sexually dimorphic gene expression profiles in the BA nucleus of the amygdala in human subjects. Changes at the level of single genes extend to homologous BLA nucleus in the mouse amygdala, albeit to a lesser extent. At the functional level, mitochondrial-related gene groups were consistently identified as the top biological pathways associated with male/female differences in both species. Together with prominent differences in other gene groups (Figure 2), our results suggest a sexual dimorphism in the expression level of an evolutionarily conserved pathway - circadian clock and mitochondrial function, potentially linked through sirtuin and nuclear hormone receptors.

In experimental models, circadian genes modulate energy metabolism by setting the periodic oscillations of expression and activity of enzymes to influence physiological and behavioral functions. Substantial evidence has shown that patients with major depression or bipolar disorder often display abnormalities in circadian rhythm, such as disturbances in the sleep/wake cycle and diurnal mood changes. Genetics studies have found associations with CLOCK, PER1-3, and CRY1 , and Sirtuin genes in mood disorders (Soria *et al.*; Roybal *et al.*, 2007; Hampp *et al.*, 2008; Abe *et al.*, 2011). In molecular/genetic studies, mitochondrial dysfunction has been associated with mood disorders (Konradi *et al.*, 2004; Rollins *et al.*, 2009), and mood disorders are common in patients with mitochondrial disorders (Fattal *et al.*, 2007). Thus, our findings suggest that baseline sexual dimorphism in mitochondrial density or functions

may influence energy availability in the amygdala. Notably, while mitochondrial function was systemically identified as a top sex-biased gene family across species, the species-specific orthologous genes were not necessarily and systematically the same, but very close functionally (Figure 2E). Because of identification of mitochondrial-related genes with closely related functions and locations across species, we speculate that the sex-biased mitochondria profile may be under conserved transcription control to display similar sexual dimorphism across species.

Limitations of this study are noted. The results will need to be confirmed at the protein and functional levels in independent and larger cohorts. Similarly, the potential contribution of race-specific amygdala gene expression will need to be assessed in larger cohorts. It is also unclear whether our findings in mid-life adults can be generalized to adolescent and elderly populations. Here we identified age effects in 2 of the 18 genes validated by qPCR, suggesting that aging may not contribute to the evolutionary conserved genetic sex differences in amygdala. In addition, this study sampled 10 intact female mice and 12 female human subjects from 39-64 years old, which should considerably lower the impact of variable estrogen levels on our findings of genetic sex difference, although we cannot exclude residual effects.

In conclusion, we present evidence for significant male/female differences in amygdala gene expression across species. Delineating the contribution of mitochondrial and circadian signaling in mood disorders will require additional work. For instance, sex-biased gene expression of circadian clock, nuclear hormone receptors, mitochondrial sirtuins and electron chain enzymes in an interlocking-feedback loop, may functionally translate into differential amygdala responsiveness (Figure 2E). This loop may lead to sex differences in metabolic capacity to meet energy demand, and might potentially contribute to the greater female vulnerability to mood disorders.

A Sex Chromosome Genes

(number of genes)	Human BA		Human LA		Mouse BA		Mouse LA	
Y-linked genes	0 ↑* /13	13 ↓*/13	0 ↑* /13	13 ↓*/13	0 ↑* /6	6 ↓*/6	0 ↑* /5	5 ↓*/5
X-linked genes	5 ↑* /12	7 ↓*/12	15 ↑* /48	33 ↓*/48	11 ↑* /26	15 ↓*/26	2 ↑* /3	1 ↓*/3

Autosomal Genes

B Array

Alr	Human		Mouse	
Gene Symbol	BA	LA	BA	LA
NADH dehydrogenase				
NDUFA2			-0.31#	
NDUFA8				-0.44*
NDUFA12	-0.43*			
NDUFB2	-0.39*			-0.32**
NDUFB3	-0.48*			
NDUFB6	-0.52*			
NDUFS3			-0.46**	
NDUFS4	-0.53*			
NDUFS7	0.39*			
NDUFAB1	-0.41**			
succinate dehydrogenase				
SDHA	-0.37*			
SDHB			-0.30#	
ubiquinol-cytochrome c reductase				
UQCRFS1	-0.51*	-0.32#	-0.41**	
UQCRC2	-0.41*			
UQCRH	-0.53*			
cytochrome c oxidase				
COX5B			-0.31*	
COX7B	-0.30*			
COX7C	-0.39*			
COX8A	-0.28*			
COX11			-0.35*	
COX17	-0.35*			
ATP synthase				
ATP5A1	-0.46*			
ATP5B	-0.28*			
ATP5E	-0.41#			
ATP5H	-0.27			
ATP5J	-0.43*			-0.29*
ATP5O	-0.40#			-0.34#
ATP1A2	-0.40*			
ATP6V0C	-0.52*			
ATP6V0D1	-0.41**	-0.32*		
ATP6V1H	-0.52#			
Sirtuin				
SIRT3			-0.46*	
SIRT5	-0.22*			
Clock genes				
PER2	0.44*			0.42*
CLOCK		0.27#		0.33*
CRY1	-0.29*			
CSNK1E	0.38*			

C qPCR

Alr	Human		Mouse	
Gene Symbol	BA	LA	BA	LA
NADH dehydrogenase				
NDUFA2			-0.23(NS)	
NDUFA12	-0.28*			
NDUFB2				-0.63**
NDUFB6	-0.38 *			
NDUFS4	-0.47***			
NDUFAB1	-0.45**			
ubiquinol-cytochrome c reductase				
UQCRFS1	-0.36*	-0.21*	-0.21**	
cytochrome c oxidase				
COX7C	-0.56***			
ATP synthase				
ATP5A1	-0.28*			
ATP5J				-0.43#
ATP6V0D1		-0.03(NS)		
Clock genes				
PER2	0.38*			0.92*
CLOCK		0.09(NS)		1.02#
CRY1	-0.23#			

D Array

Alr	Human		
Gene Symbol	BA9	BA47	ACC
NADH dehydrogenase			
NDUFAB1	-0.50**		
succinate dehydrogenase			
SDHALP1			-0.37*
SDHD		-0.5*	
ubiquinol-cytochrome c reductase			
UQCRFS1	-0.51**		
UQCRC2	-0.40*		
ATP synthase			
ATP5A1	-0.37***		
ATP5G3	-0.45*		
ATP5L	-0.37**		
ATP6V0A1	-0.68*		
ATP6V0E1		-0.36*	
ATP6V1A	-0.83**		
ATP6V1B2	-0.43**		
ATP6V1C1	-1.15***		
ATP6V1D	-0.39**		
Sirtuin			
SIRT3	-0.19***		
SIRT4		-0.12*	0.17**
SIRT5			-0.10***

Note: h= human; m= mouse

↑: higher expressed in females

↓: lower expressed in females

Alr= average log ratio (F/M)

* p<0.05; **p<0.01; ***p<0.001

0.05<p<0.1(trend); NS =Not Significant

E Array-QPCR correlation

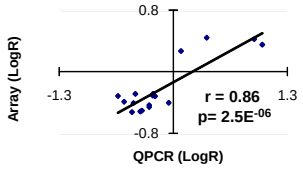

F

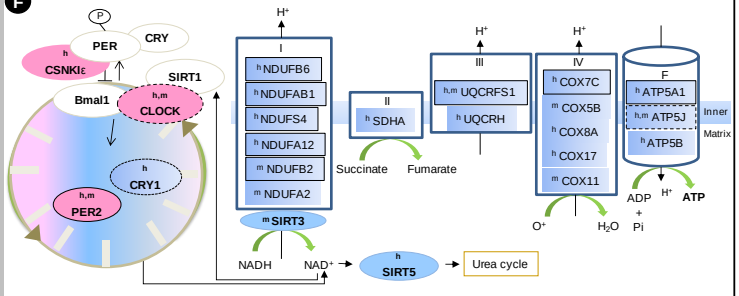

Circadian clock ↔ (Sirtuin) (NHR) ↔ Mitochondrial electron transport chain

APPENDIX B

STATISTICAL RESULTS OF BEHAVIORS IN SST HETEROZYGOUS MOUSE

Table 1. Time in Open Arms of Elevated Plus Maze

Two-way ANOVA	Ordinary
Alpha	0.05

Source of Variation	% of total variation	P value	P value summary	Significant?
Interaction	0.2713	0.6656	ns	No
genotype	0.3743	0.6118	ns	No
treatment	2.963	0.1561	ns	No

ANOVA table	SS	DF	MS	F (DFn, DFd)	P value
Interaction	151.1	1	151.1	F (1, 67) = 0.1884	P = 0.6656
genotype	208.5	1	208.5	F (1, 67) = 0.2600	P = 0.6118
treatment	1650	1	1650	F (1, 67) = 2.058	P = 0.1561
Residual	53737	67	802		

Table 2. % Crosses into Open Arms of Elevated Plus Maze

Two-way ANOVA	Ordinary
Alpha	0.05

Source of Variation	% of total variation	P value	P value summary	Significant?
Interaction	0.6526	0.5087	ns	No
genotype	0.2146	0.7044	ns	No
treatment	0.03108	0.8851	ns	No

ANOVA table	SS	DF	MS	F (DFn, DFd)	P value
Interaction	28.53	1	28.53	F (1, 67) = 0.4414	P = 0.5087
genotype	9.384	1	9.384	F (1, 67) = 0.1452	P = 0.7044
treatment	1.359	1	1.359	F (1, 67) = 0.02103	P = 0.8851
Residual	4331	67	64.64		

Table 3. Total Crosses in Elevated Plus Maze

Two-way ANOVA	Ordinary
Alpha	0.05

Source of Variation	% of total variation	P value	P value summary	Significant?
Interaction	0.4	0.5773	ns	No
genotype	1.671	0.2565	ns	No
treatment	10.87	0.0048	**	Yes

ANOVA table	SS	DF	MS	F (DFn, DFd)	P value
Interaction	19.91	1	19.91	F (1, 67) = 0.3136	P = 0.5773
genotype	83.15	1	83.15	F (1, 67) = 1.310	P = 0.2565
treatment	541	1	541	F (1, 67) = 8.522	P = 0.0048
Residual	4253	67	63.48		

Tukey's multiple comparisons test	Mean Diff.	95% CI of diff.	Significant?	Summary
WT:Control vs. WT:UCMS	-6.714	-13.19 to -0.2361	Yes	*
WT:Control vs. HZ:Control	-3.289	-10.70 to 4.119	No	ns
WT:Control vs. HZ:UCMS	-7.842	-14.81 to -0.8764	Yes	*
WT:UCMS vs. HZ:Control	3.425	-3.983 to 10.83	No	ns
WT:UCMS vs. HZ:UCMS	-1.128	-8.094 to 5.838	No	ns
HZ:Control vs. HZ:UCMS	-4.553	-12.39 to 3.285	No	ns

Test details	Mean 1	Mean 2	Mean Diff.	SE of diff.	N1	N2	q	DF
WT:Control vs. WT:UCMS	28.1	34.81	-6.714	2.459	21	21	3.862	67
WT:Control vs. HZ:Control	28.1	31.38	-3.289	2.812	21	13	1.654	67
WT:Control vs. HZ:UCMS	28.1	35.94	-7.842	2.644	21	16	4.195	67
WT:UCMS vs. HZ:Control	34.81	31.38	3.425	2.812	21	13	1.723	67
WT:UCMS vs. HZ:UCMS	34.81	35.94	-1.128	2.644	21	16	0.6034	67
HZ:Control vs. HZ:UCMS	31.38	35.94	-4.553	2.975	13	16	2.164	67

Table 4. Time in Center of Open Field

Two-way ANOVA	Ordinary
Alpha	0.05

Source of Variation	% of total variation	P value	P value summary	Significant?
Interaction	4.283	0.0716	ns	No
genotype	0.2195	0.6799	ns	No
treatment	7.265	0.02	*	Yes

ANOVA table	SS	DF	MS	F (DFn, DFd)	P value
Interaction	12134	1	12134	F (1, 67) = 3.350	P = 0.0716
genotype	621.8	1	621.8	F (1, 67) = 0.1717	P = 0.6799
treatment	20581	1	20581	F (1, 67) = 5.683	P = 0.0200
Residual	242657	67	3622		

Tukey's multiple comparisons test	Mean Diff.	95% CI of diff.	Significant?	Summary
WT:Control vs. WT:UCMS	61.43	12.50 to 110.4	Yes	**
WT:Control vs. HZ:Control	20.64	-35.32 to 76.60	No	ns
WT:Control vs. HZ:UCMS	28.71	-23.91 to 81.32	No	ns
WT:UCMS vs. HZ:Control	-40.79	-96.74 to 15.17	No	ns
WT:UCMS vs. HZ:UCMS	-32.72	-85.34 to 19.90	No	ns
HZ:Control vs. HZ:UCMS	8.067	-51.14 to 67.27	No	ns

Table 5. % Distance in the Center of Open Field

Two-way ANOVA	Ordinary
Alpha	0.05

Source of Variation	% of total variation	P value	P value summary	Significant?
Interaction	1.603	0.2701	ns	No
genotype	0.1558	0.7299	ns	No
treatment	9.515	0.0086	**	Yes

ANOVA table	SS	DF	MS	F (DFn, DFd)	P value
Interaction	84.38	1	84.38	F (1, 67) = 1.237	P = 0.2701
genotype	8.201	1	8.201	F (1, 67) = 0.1202	P = 0.7299
treatment	500.8	1	500.8	F (1, 67) = 7.340	P = 0.0086
Residual	4572	67	68.23		

Tukey's multiple comparisons test	Mean Diff.	95% CI of diff.	Significant?	Summary
WT:Control vs. WT:UCMS	7.645	0.9289 to 14.36	Yes	*
WT:Control vs. HZ:Control	1.531	-6.149 to 9.212	No	ns
WT:Control vs. HZ:UCMS	4.727	-2.495 to 11.95	No	ns
WT:UCMS vs. HZ:Control	-6.114	-13.79 to 1.566	No	ns
WT:UCMS vs. HZ:UCMS	-2.919	-10.14 to 4.303	No	ns
HZ:Control vs. HZ:UCMS	3.195	-4.931 to 11.32	No	ns

Test details	Mean 1	Mean 2	Mean Diff.	SE of diff.	N1	N2	q
WT:Control vs. WT:UCMS	30.43	22.78	7.645	2.549	21	21	4.241
WT:Control vs. HZ:Control	30.43	28.9	1.531	2.915	21	13	0.7429
WT:Control vs. HZ:UCMS	30.43	25.7	4.727	2.741	21	16	2.439
WT:UCMS vs. HZ:Control	22.78	28.9	-6.114	2.915	21	13	2.966
WT:UCMS vs. HZ:UCMS	22.78	25.7	-2.919	2.741	21	16	1.506
HZ:Control vs. HZ:UCMS	28.9	25.7	3.195	3.084	13	16	1.465

Table 6. Total Distance in Open Field

Two-way ANOVA	Ordinary
Alpha	0.05

Source of Variation	% of total variation	P value	P value summary	Significant?
Interaction	1.627	0.2247	ns	No
genotype	0.04059	0.8471	ns	No
treatment	27.29	< 0.0001	****	Yes

ANOVA table	SS	DF	MS	F (DFn, DFd)	P value
Interaction	44062	1	44062	F (1, 67) = 1.502	P = 0.2247
genotype	1099	1	1099	F (1, 67) = 0.03746	P = 0.8471
treatment	739189	1	739189	F (1, 67) = 25.19	P < 0.0001
Residual	1966000	67	29345		

Tukey's multiple comparisons test	Mean Diff.	95% CI of diff.	Significant?	Summary
WT:Control vs. WT:UCMS	-157.4	-296.7 to -18.12	Yes	*
WT:Control vs. HZ:Control	58.87	-100.4 to 218.2	No	ns
WT:Control vs. HZ:UCMS	-200.2	-350.0 to -50.44	Yes	**
WT:UCMS vs. HZ:Control	216.3	56.99 to 375.6	Yes	**
WT:UCMS vs. HZ:UCMS	-42.81	-192.6 to 107.0	No	ns
HZ:Control vs. HZ:UCMS	-259.1	-427.6 to -90.56	Yes	***

Test details	Mean 1	Mean 2	Mean Diff.	SE of diff.	N1	N2	q	DF
WT:Control vs. WT:UCMS	709.1	866.5	-157.4	52.87	21	21	4.211	67
WT:Control vs. HZ:Control	709.1	650.2	58.87	60.45	21	13	1.377	67
WT:Control vs. HZ:UCMS	709.1	909.3	-200.2	56.85	21	16	4.981	67
WT:UCMS vs. HZ:Control	866.5	650.2	216.3	60.45	21	13	5.059	67
WT:UCMS vs. HZ:UCMS	866.5	909.3	-42.81	56.85	21	16	1.065	67
HZ:Control vs. HZ:UCMS	650.2	909.3	-259.1	63.96	13	16	5.728	67

Table 7. Latency to feed in Novelty Suppressed Feeding Test

Two-way ANOVA	Ordinary
Alpha	0.05

Source of Variation	% of total variation	P value	P value summary	Significant?
Interaction	0.1657	0.7164	ns	No
genotype	0.4196	0.5635	ns	No
treatment	15.68	0.0007	***	Yes

ANOVA table	SS	DF	MS	F (DFn, DFd)	P value
Interaction	2631	1	2631	F (1, 67) = 0.1330	P = 0.7164
genotype	6663	1	6663	F (1, 67) = 0.3370	P = 0.5635
treatment	248955	1	248955	F (1, 67) = 12.59	P = 0.0007
Residual	1325000	67	19773		

Tukey's multiple comparisons test	Mean Diff.	95% CI of diff.	Significant?	Summary
WT:Control vs. WT:UCMS	-108.4	-222.8 to 5.904	No	ns
WT:Control vs. HZ:Control	-7.348	-138.1 to 123.4	No	ns
WT:Control vs. HZ:UCMS	-140.6	-263.6 to -17.68	Yes	*
WT:UCMS vs. HZ:Control	101.1	-29.66 to 231.8	No	ns
WT:UCMS vs. HZ:UCMS	-32.19	-155.1 to 90.75	No	ns
HZ:Control vs. HZ:UCMS	-133.3	-271.6 to 5.060	No	ns

Test details	Mean 1	Mean 2	Mean Diff.	SE of diff.	N1	N2	q
WT:Control vs. WT:UCMS	74.19	182.6	-108.4	43.39	21	21	3.534
WT:Control vs. HZ:Control	74.19	81.54	-7.348	49.62	21	13	0.2094
WT:Control vs. HZ:UCMS	74.19	214.8	-140.6	46.66	21	16	4.262
WT:UCMS vs. HZ:Control	182.6	81.54	101.1	49.62	21	13	2.881
WT:UCMS vs. HZ:UCMS	182.6	214.8	-32.19	46.66	21	16	0.9757
HZ:Control vs. HZ:UCMS	81.54	214.8	-133.3	52.5	13	16	3.59

Table 9. Sucrose consumption in Sucrose Preference Test

Two-way ANOVA	Ordinary
Alpha	0.05

Source of Variation	% of total variation	P value	P value summary	Significant?
Interaction	0.819	0.4248	ns	No
genotype	0.8003	0.4301	ns	No
treatment	15.8	0.0008	***	Yes

ANOVA table	SS	DF	MS	F (DFn, DFd)	P value
Interaction	0.002	1	0.002	F (1, 66) = 0.6451	P = 0.4248
genotype	0.001954	1	0.001954	F (1, 66) = 0.6304	P = 0.4301
treatment	0.03858	1	0.03858	F (1, 66) = 12.44	P = 0.0008
Residual	0.2046	66	0.0031		

Tukey's multiple comparisons test	Mean Diff.	95% CI of diff.	Significant?	Summary
WT:Control vs. WT:UCMS	0.03693	-0.008925 to 0.08278	No	ns
WT:Control vs. HZ:Control	-0.02165	-0.07344 to 0.03014	No	ns
WT:Control vs. HZ:UCMS	0.03705	-0.01165 to 0.08575	No	ns
WT:UCMS vs. HZ:Control	-0.05858	-0.1109 to -0.006292	Yes	*
WT:UCMS vs. HZ:UCMS	0.000125	-0.04910 to 0.04935	No	ns
HZ:Control vs. HZ:UCMS	0.0587	0.003903 to 0.1135	Yes	*

Test details	Mean 1	Mean 2	Mean Diff.	SE of diff.	N1	N2	q
WT:Control vs. WT:UCMS	0.1614	0.1245	0.03693	0.0174	21	20	3.002
WT:Control vs. HZ:Control	0.1614	0.1831	-0.02165	0.01965	21	13	1.558
WT:Control vs. HZ:UCMS	0.1614	0.1244	0.03705	0.01848	21	16	2.836
WT:UCMS vs. HZ:Control	0.1245	0.1831	-0.05858	0.01984	20	13	4.176
WT:UCMS vs. HZ:UCMS	0.1245	0.1244	0.000125	0.01868	20	16	0.009465
HZ:Control vs. HZ:UCMS	0.1831	0.1244	0.0587	0.02079	13	16	3.993

Table 10. Sucrose preference in Sucrose Preference Test

Two-way ANOVA	Ordinary
Alpha	0.05

Source of Variation	% of total variation	P value	P value summary	Significant?
Interaction	1.762	0.2576	ns	No
genotype	2.05	0.2224	ns	No
treatment	5.853	0.0413	*	Yes

ANOVA table	SS	DF	MS	F (DFn, DFd)	P value
Interaction	345.6	1	345.6	F (1, 66) = 1.304	P = 0.2576
genotype	402.1	1	402.1	F (1, 66) = 1.517	P = 0.2224
treatment	1148	1	1148	F (1, 66) = 4.331	P = 0.0413
Residual	17493	66	265		

Tukey's multiple comparisons test	Mean Diff.	95% CI of diff.	Significant?	Summary
WT:Control vs. WT:UCMS	12.77	-0.6330 to 26.18	No	ns
WT:Control vs. HZ:Control	-0.3556	-15.50 to 14.79	No	ns
WT:Control vs. HZ:UCMS	3.367	-10.87 to 17.61	No	ns
WT:UCMS vs. HZ:Control	-13.13	-28.42 to 2.158	No	ns
WT:UCMS vs. HZ:UCMS	-9.407	-23.80 to 4.985	No	ns
HZ:Control vs. HZ:UCMS	3.722	-12.30 to 19.74	No	ns

Test details	Mean 1	Mean 2	Mean Diff.	SE of diff.	N1	N2	q
WT:Control vs. WT:UCMS	90.06	77.29	12.77	5.087	21	20	3.551
WT:Control vs. HZ:Control	90.06	90.42	-0.3556	5.745	21	13	0.08753
WT:Control vs. HZ:UCMS	90.06	86.7	3.367	5.402	21	16	0.8813
WT:UCMS vs. HZ:Control	77.29	90.42	-13.13	5.8	20	13	3.201
WT:UCMS vs. HZ:UCMS	77.29	86.7	-9.407	5.461	20	16	2.436
HZ:Control vs. HZ:UCMS	90.42	86.7	3.722	6.079	13	16	0.8659

Table 11. Emotionality Z-score

Two-way ANOVA	Ordinary
Alpha	0.05

Source of Variation	% of total variation	P value	P value summary	Significant?
Interaction	0.3644	0.5819	ns	No
genotype	0.3836	0.5722	ns	No
treatment	19.35	0.0001	***	Yes

ANOVA table	SS	DF	MS	F (DFn, DFd)	P value
Interaction	0.1459	1	0.1459	F (1, 66) = 0.3062	P = 0.5819
genotype	0.1536	1	0.1536	F (1, 66) = 0.3223	P = 0.5722
treatment	7.744	1	7.744	F (1, 66) = 16.25	P = 0.0001
Residual	31.45	66	0.4765		

Tukey's multiple comparisons test	Mean Diff.	95% CI of diff.	Significant?	Summary
WT:Control vs. WT:UCMS	-0.7704	-1.339 to -0.2020	Yes	**
WT:Control vs. HZ:Control	0.002418	-0.6397 to 0.6445	No	ns
WT:Control vs. HZ:UCMS	-0.5821	-1.186 to 0.02170	No	ns
WT:UCMS vs. HZ:Control	0.7728	0.1247 to 1.421	Yes	*
WT:UCMS vs. HZ:UCMS	0.1884	-0.4219 to 0.7986	No	ns
HZ:Control vs. HZ:UCMS	-0.5845	-1.264 to 0.09488	No	ns

Test details	Mean 1	Mean 2	Mean Diff.	SE of diff.	N1	N2	q
WT:Control vs. WT:UCMS	-0.001429	0.769	-0.77	0.2157	21	20	5.1
WT:Control vs. HZ:Control	-0.001429	-0.0038	0.0024	0.2436	21	13	0
WT:Control vs. HZ:UCMS	-0.001429	0.5806	-0.582	0.2291	21	16	3.6
WT:UCMS vs. HZ:Control	0.769	-0.0038	0.7728	0.2459	20	13	4.4
WT:UCMS vs. HZ:UCMS	0.769	0.5806	0.1884	0.2315	20	16	1.2
HZ:Control vs. HZ:UCMS	-0.003846	0.5806	-0.585	0.2577	13	16	3.2

Table 12. Locomotion Z-score

Two-way ANOVA	Ordinary
Alpha	0.05

Source of Variation	% of total variation	P value	P value summary	Significant?
Interaction	0.01046	0.924	ns	No
genotype	0.7009	0.4361	ns	No
treatment	21.69	< 0.0001	****	Yes

ANOVA table	SS	DF	MS	F (DFn, DFd)	P value
Interaction	0.009187	1	0.009187	F (1, 67) = 0.009161	P = 0.9240
genotype	0.6155	1	0.6155	F (1, 67) = 0.6138	P = 0.4361
treatment	19.05	1	19.05	F (1, 67) = 18.99	P < 0.0001
Residual	67.19	67	1.003		

Tukey's multiple comparisons test	Mean Diff.	95% CI of diff.	Significant?	Summary
WT:Control vs. WT:UCMS	-1.034	-1.848 to -0.2196	Yes	**
WT:Control vs. HZ:Control	-0.1668	-1.098 to 0.7643	No	ns
WT:Control vs. HZ:UCMS	-1.247	-2.123 to -0.3715	Yes	**
WT:UCMS vs. HZ:Control	0.867	-0.06410 to 1.798	No	ns
WT:UCMS vs. HZ:UCMS	-0.2132	-1.089 to 0.6623	No	ns
HZ:Control vs. HZ:UCMS	-1.08	-2.065 to -0.09509	Yes	*

Test details	Mean 1	Mean 2	Mean Diff.	SE of diff.	N1	N2	q
WT:Control vs. WT:UCMS	-0.00143	1.032	-1.034	0.309	21	21	4.731
WT:Control vs. HZ:Control	-0.00143	0.1654	-0.1668	0.3534	21	13	0.6675
WT:Control vs. HZ:UCMS	-0.00143	1.246	-1.247	0.3323	21	16	5.307
WT:UCMS vs. HZ:Control	1.032	0.1654	0.867	0.3534	21	13	3.47
WT:UCMS vs. HZ:UCMS	1.032	1.246	-0.2132	0.3323	21	16	0.9075
HZ:Control vs. HZ:UCMS	0.1654	1.246	-1.08	0.3739	13	16	4.086

7.0 REFERENCES

Aarsland, D., Larsen, J.P., Lim, N.G., Janvin, C., Karlsen, K., Tandberg, E. & Cummings, J.L. (1999) Range of neuropsychiatric disturbances in patients with Parkinson's disease. *J Neurol Neurosurg Psychiatry*, **67**, 492-496.

Abe, N., Uchida, S., Otsuki, K., Hobara, T., Yamagata, H., Higuchi, F., Shibata, T. & Watanabe, Y. (2011) Altered sirtuin deacetylase gene expression in patients with a mood disorder. *J Psychiatr Res*, **45**, 1106-1112.

Agren, H. & Lundqvist, G. (1984) Low levels of somatostatin in human CSF mark depressive episodes. *Psychoneuroendocrinology*, **9**, 233-248.

Albrecht, A., Thiere, M., Bergado-Acosta, J.R., Poranzke, J., Muller, B. & Stork, O. (2013) Circadian modulation of anxiety: a role for somatostatin in the amygdala. *PLoS One*, **8**, e84668.

Alexopoulos, G.S., Gunning-Dixon, F.M., Latoussakis, V., Kanellopoulos, D. & Murphy, C.F. (2008) Anterior cingulate dysfunction in geriatric depression. *Int J Geriatr Psychiatry*, **23**, 347-355.

Allen-Rowlands, C.F., Allen, J.P., Greer, M.A. & Wilson, M. (1980) Circadian rhythmicity of ACTH and corticosterone in the rat. *J Endocrinol Invest*, **3**, 371-377.

Ambrosio, M.R., Campo, M., Zatelli, M.C., Cella, S.G., Trasforini, G., Margutti, A., Rigamonti, A.E., Muller, E.E. & degli Uberti, E.C. (1998) Unexpected activation of pituitary-adrenal axis in healthy young and elderly subjects during somatostatin infusion. *Neuroendocrinology*, **68**, 123-128.

Asher, G., Gatfield, D., Stratmann, M., Reinke, H., Dibner, C., Kreppel, F., Mostoslavsky, R., Alt, F.W. & Schibler, U. (2008) SIRT1 regulates circadian clock gene expression through PER2 deacetylation. *Cell*, **134**, 317-328.

Axten, J.M., Medina, J.R., Feng, Y., Shu, A., Romeril, S.P., Grant, S.W., Li, W.H., Heerding, D.A., Minthorn, E., Mencken, T., Atkins, C., Liu, Q., Rabindran, S., Kumar, R., Hong, X., Goetz, A., Stanley, T., Taylor, J.D., Sigethy, S.D., Tomberlin, G.H., Hassell, A.M., Kahler, K.M., Shewchuk, L.M. & Gampe, R.T. (2012) Discovery of 7-methyl-5-(1-{[3-(trifluoromethyl)phenyl]acetyl}-2,3-dihydro-1H-indol-5-yl)-7H-p yrrolo[2,3-d]pyrimidin-4-amine (GSK2606414), a potent and selective first-in-class inhibitor of protein kinase R (PKR)-like endoplasmic reticulum kinase (PERK). *J Med Chem*, **55**, 7193-7207.

Axten, J.M., Romeril, S.P., Shu, A., Ralph, J., Medina, J.R., Feng, Y., Li, W.H., Grant, S.W., Heerding, D.A., Minthorn, E., Mencken, T., Gaul, N., Goetz, A., Stanley, T., Hassell, A.M., Gampe, R.T., Atkins, C. & Kumar, R. (2013) Discovery of GSK2656157: An Optimized PERK Inhibitor Selected for Preclinical Development. *ACS Med Chem Lett*, **4**, 964-968.

Barrett, D.M., Black, S.M., Todor, H., Schmidt-Ullrich, R.K., Dawson, K.S. & Mikkelsen, R.B. (2005) Inhibition of protein-tyrosine phosphatases by mild oxidative stresses is dependent on S-nitrosylation. *J Biol Chem*, **280**, 14453-14461.

Bauer, W., Briner, U., Doepfner, W., Haller, R., Huguenin, R., Marbach, P., Petcher, T.J. & Pless (1982) SMS 201-995: a very potent and selective octapeptide analogue of somatostatin with prolonged action. *Life Sci*, **31**, 1133-1140.

Baxter, L.R., Jr., Phelps, M.E., Mazziotta, J.C., Schwartz, J.M., Gerner, R.H., Selin, C.E. & Sumida, R.M. (1985) Cerebral metabolic rates for glucose in mood disorders. Studies with positron emission tomography and fluorodeoxyglucose F 18. *Arch Gen Psychiatry*, **42**, 441-447.

Baxter, L.R., Jr., Schwartz, J.M., Phelps, M.E., Mazziotta, J.C., Guze, B.H., Selin, C.E., Gerner, R.H. & Sumida, R.M. (1989) Reduction of prefrontal cortex glucose metabolism common to three types of depression. *Arch Gen Psychiatry*, **46**, 243-250.

Beal, M.F., Mazurek, M.F. & Martin, J.B. (1986) Somatostatin immunoreactivity is reduced in Parkinson's disease dementia with Alzheimer's changes. *Brain Res*, **397**, 386-388.

Beierlein, M., Gibson, J.R. & Connors, B.W. (2003) Two dynamically distinct inhibitory networks in layer 4 of the neocortex. *J Neurophysiol*, **90**, 2987-3000.

Bevan, J.S. (2005) Clinical review: The antitumoral effects of somatostatin analog therapy in acromegaly. *J Clin Endocrinol Metab*, **90**, 1856-1863.

Bhagwagar, Z., Hafizi, S. & Cowen, P.J. (2003) Increase in concentration of waking salivary cortisol in recovered patients with depression. *Am J Psychiatry*, **160**, 1890-1891.

Bissette, G., Widerlov, E., Walleus, H., Karlsson, I., Eklund, K., Forsman, A. & Nemeroff, C.B. (1986) Alterations in cerebrospinal fluid concentrations of somatostatinlike immunoreactivity in neuropsychiatric disorders. *Arch Gen Psychiatry*, **43**, 1148-1151.

Boyce, M., Bryant, K.F., Jousse, C., Long, K., Harding, H.P., Scheuner, D., Kaufman, R.J., Ma, D., Coen, D.M., Ron, D. & Yuan, J. (2005) A selective inhibitor of eIF2alpha dephosphorylation protects cells from ER stress. *Science*, **307**, 935-939.

Bremner, J.D., Vythilingam, M., Vermetten, E., Vaccarino, V. & Charney, D.S. (2004) Deficits in hippocampal and anterior cingulate functioning during verbal declarative memory encoding in midlife major depression. *Am J Psychiatry*, **161**, 637-645.

Brouwer, J.P., Appelhof, B.C., Hoogendijk, W.J., Huyser, J., Endert, E., Zuketto, C., Schene, A.H., Tijssen, J.G., Van Dyck, R., Wiersinga, W.M. & Fliers, E. (2005) Thyroid and adrenal axis in major depression: a controlled study in outpatients. *Eur J Endocrinol*, **152**, 185-191.

Bruunsgaard, H. & Pedersen, B.K. (2003) Age-related inflammatory cytokines and disease. *Immunol Allergy Clin North Am*, **23**, 15-39.

Bungener, C., Jouvent, R. & Derouesne, C. (1996) Affective disturbances in Alzheimer's disease. *J Am Geriatr Soc*, **44**, 1066-1071.

Burnett, B.B., Gardner, A. & Boles, R.G. (2005) Mitochondrial inheritance in depression, dysmotility and migraine? *J Affect Disord*, **88**, 109-116.

Butte, J.C., Kakihana, R. & Noble, E.P. (1976) Circadian rhythm of corticosterone levels in rat brain. *J Endocrinol*, **68**, 235-239.

Calkhoven, C.F., Muller, C. & Leutz, A. (2002) Translational control of gene expression and disease. *Trends Mol Med*, **8**, 577-583.

Cammalleri, M., Cervia, D., Dal Monte, M., Martini, D., Langenegger, D., Fehlmann, D., Feuerbach, D., Pavan, B., Hoyer, D. & Bagnoli, P. (2006) Compensatory changes in the hippocampus of somatostatin knockout mice: upregulation of somatostatin receptor 2 and its function in the control of bursting activity and synaptic transmission. *Eur J Neurosci*, **23**, 2404-2422.

Candy, J.M., Gascoigne, A.D., Biggins, J.A., Smith, A.I., Perry, R.H., Perry, E.K., McDermott, J.R. & Edwardson, J.A. (1985) Somatostatin immunoreactivity in cortical and some subcortical regions in Alzheimer's disease. *J Neurol Sci*, **71**, 315-323.

Caspi, A., Sugden, K., Moffitt, T.E., Taylor, A., Craig, I.W., Harrington, H., McClay, J., Mill, J., Martin, J., Braithwaite, A. & Poulton, R. (2003) Influence of life stress on depression: moderation by a polymorphism in the 5-HTT gene. *Science*, **301**, 386-389.

Cassano, P. & Fava, M. (2004) Tolerability issues during long-term treatment with antidepressants. *Ann Clin Psychiatry*, **16**, 15-25.

Castera, L., Constant, A., Henry, C., Champbenoit, P., Bernard, P.H., De Ledinghen, V., Demotes-Mainard, J. & Couzigou, P. (2006) Impact on adherence and sustained virological response of psychiatric side effects during peginterferon and ribavirin therapy for chronic hepatitis C. *Aliment Pharmacol Ther*, **24**, 1223-1230.

Celik, C., Erdem, M., Cayci, T., Ozdemir, B., Ozgur Akgul, E., Kurt, Y.G., Yaman, H., Isintas, M., Ozgen, F. & Ozsahin, A. (2010) The association between serum levels of neopterin and number of depressive episodes of major depression. *Prog Neuropsychopharmacol Biol Psychiatry*, **34**, 372-375.

Cerqueira, J.J., Catania, C., Sotiropoulos, I., Schubert, M., Kalisch, R., Almeida, O.F., Auer, D.P. & Sousa, N. (2005) Corticosteroid status influences the volume of the rat cingulate cortex - a magnetic resonance imaging study. *J Psychiatr Res*, **39**, 451-460.

Chang, R.C., Wong, A.K., Ng, H.K. & Hugon, J. (2002) Phosphorylation of eukaryotic initiation factor-2alpha (eIF2alpha) is associated with neuronal degeneration in Alzheimer's disease. *Neuroreport*, **13**, 2429-2432.

Chiu, C.Q., Lur, G., Morse, T.M., Carnevale, N.T., Ellis-Davies, G.C. & Higley, M.J. (2013) Compartmentalization of GABAergic inhibition by dendritic spines. *Science*, **340**, 759-762.

Chung, K., Wallace, J., Kim, S.Y., Kalyanasundaram, S., Andalman, A.S., Davidson, T.J., Mirzabekov, J.J., Zalocusky, K.A., Mattis, J., Denisin, A.K., Pak, S., Bernstein, H., Ramakrishnan, C., Grosenick, L., Gradinaru, V. & Deisseroth, K. (2013) Structural and molecular interrogation of intact biological systems. *Nature*, **497**, 332-337.

Colla, E., Jensen, P.H., Pletnikova, O., Troncoso, J.C., Glabe, C. & Lee, M.K. (2012) Accumulation of toxic alpha-synuclein oligomer within endoplasmic reticulum occurs in alpha-synucleinopathy in vivo. *J Neurosci*, **32**, 3301-3305.

Coryell, W., Nopoulos, P., Drevets, W., Wilson, T. & Andreasen, N.C. (2005) Subgenual prefrontal cortex volumes in major depressive disorder and schizophrenia: diagnostic specificity and prognostic implications. *Am J Psychiatry*, **162**, 1706-1712.

Cruikshank, S.J., Urabe, H., Nurmikko, A.V. & Connors, B.W. (2010) Pathway-specific feedforward circuits between thalamus and neocortex revealed by selective optical stimulation of axons. *Neuron*, **65**, 230-245.

Csaba, Z. & Dournaud, P. (2001) Cellular biology of somatostatin receptors. *Neuropeptides*, **35**, 1-23.

Davies, P., Katzman, R. & Terry, R.D. (1980) Reduced somatostatin-like immunoreactivity in cerebral cortex from cases of Alzheimer disease and Alzheimer senile dementa. *Nature*, **288**, 279-280.

Davies, P. & Terry, R.D. (1981) Cortical somatostatin-like immunoreactivity in cases of Alzheimer's disease and senile dementia of the Alzheimer type. *Neurobiol Aging*, **2**, 9-14.

de Kloet, E.R. & Sarabdjitsingh, R.A. (2008) Everything has rhythm: focus on glucocorticoid pulsatility. *Endocrinology*, **149**, 3241-3243.

de Lecea, L. (2008) Cortistatin--functions in the central nervous system. *Mol Cell Endocrinol*, **286**, 88-95.

de Lecea, L., Criado, J.R., Prospero-Garcia, O., Gautvik, K.M., Schweitzer, P., Danielson, P.E., Dunlop, C.L., Siggins, G.R., Henriksen, S.J. & Sutcliffe, J.G. (1996) A cortical neuropeptide with neuronal depressant and sleep-modulating properties. *Nature*, **381**, 242-245.

de Lecea, L., del Rio, J.A., Criado, J.R., Alcantara, S., Morales, M., Danielson, P.E., Henriksen, S.J., Soriano, E. & Sutcliffe, J.G. (1997) Cortistatin is expressed in a distinct subset of cortical interneurons. *J Neurosci*, **17**, 5868-5880.

DeFelipe, J., Lopez-Cruz, P.L., Benavides-Piccione, R., Bielza, C., Larranaga, P., Anderson, S., Burkhalter, A., Cauli, B., Fairen, A., Feldmeyer, D., Fishell, G., Fitzpatrick, D., Freund, T.F., Gonzalez-Burgos, G., Hestrin, S., Hill, S., Hof, P.R., Huang, J., Jones, E.G., Kawaguchi, Y., Kisvarday, Z., Kubota, Y., Lewis, D.A., Marin, O., Markram, H., McBain, C.J., Meyer, H.S., Monyer, H., Nelson, S.B., Rockland, K., Rossier, J., Rubenstein, J.L., Rudy, B., Scanziani, M., Shepherd, G.M., Sherwood, C.C., Staiger, J.F., Tamas, G., Thomson, A., Wang, Y., Yuste, R. & Ascoli, G.A. (2013) New insights into the classification and nomenclature of cortical GABAergic interneurons. *Nat Rev Neurosci*, **14**, 202-216.

Devinsky, O., Morrell, M.J. & Vogt, B.A. (1995) Contributions of anterior cingulate cortex to behaviour. *Brain*, **118 (Pt 1)**, 279-306.

Di Cristo, G., Wu, C., Chattopadhyaya, B., Ango, F., Knott, G., Welker, E., Svoboda, K. & Huang, Z.J. (2004) Subcellular domain-restricted GABAergic innervation in primary visual cortex in the absence of sensory and thalamic inputs. *Nat Neurosci*, **7**, 1184-1186.

Di Filippo, M., Sarchielli, P., Picconi, B. & Calabresi, P. (2008) Neuroinflammation and synaptic plasticity: theoretical basis for a novel, immune-centred, therapeutic approach to neurological disorders. *Trends Pharmacol Sci*, **29**, 402-412.

Diorio, D., Viau, V. & Meaney, M.J. (1993) The role of the medial prefrontal cortex (cingulate gyrus) in the regulation of hypothalamic-pituitary-adrenal responses to stress. *J Neurosci*, **13**, 3839-3847.

Doucet, J.C. & Morrison, A.D. (2011) Bilateral mandibular condylysis from systemic sclerosis: case report of surgical correction with bilateral total temporomandibular joint replacement. *Craniomaxillofac Trauma Reconstr*, **4**, 11-18.

Douillard-Guilloux, G., Guilloux, J.P., Lewis, D.A. & Sibille, E. (2013) Anticipated brain molecular aging in major depression. *Am J Geriatr Psychiatry*, **21**, 450-460.

Dournaud, P., Cervera-Pierot, P., Hirsch, E., Javoy-Agid, F., Kordon, C., Agid, Y. & Epelbaum, J. (1994) Somatostatin messenger RNA-containing neurons in Alzheimer's disease: an in situ hybridization study in hippocampus, parahippocampal cortex and frontal cortex. *Neuroscience*, **61**, 755-764.

Dowlati, Y., Herrmann, N., Swardfager, W., Liu, H., Sham, L., Reim, E.K. & Lanctot, K.L. (2010) A meta-analysis of cytokines in major depression. *Biol Psychiatry*, **67**, 446-457.

Drevets, W.C., Price, J.L., Simpson, J.R., Jr., Todd, R.D., Reich, T., Vannier, M. & Raichle, M.E. (1997) Subgenual prefrontal cortex abnormalities in mood disorders. *Nature*, **386**, 824-827.

Dulawa, S.C. & Hen, R. (2005) Recent advances in animal models of chronic antidepressant effects: the novelty-induced hypophagia test. *Neurosci Biobehav Rev*, **29**, 771-783.

Duman, R.S., Heninger, G.R. & Nestler, E.J. (1997) A molecular and cellular theory of depression. *Arch Gen Psychiatry*, **54**, 597-606.

Duman, R.S., Malberg, J., Nakagawa, S. & D'Sa, C. (2000) Neuronal plasticity and survival in mood disorders. *Biol Psychiatry*, **48**, 732-739.

Dun, N.J., Dun, S.L., Wong, R.K. & Forstermann, U. (1994) Colocalization of nitric oxide synthase and somatostatin immunoreactivity in rat dentate hilar neurons. *Proc Natl Acad Sci U S A*, **91**, 2955-2959.

Dupont, E., Christensen, S.E., Hansen, A.P., de Fine Olivarius, B. & Orskov, H. (1982) Low cerebrospinal fluid somatostatin in Parkinson disease: an irreversible abnormality. *Neurology*, **32**, 312-314.

Engin, E., Stellbrink, J., Treit, D. & Dickson, C.T. (2008) Anxiolytic and antidepressant effects of intracerebroventricularly administered somatostatin: behavioral and neurophysiological evidence. *Neuroscience*, **157**, 666-676.

Engin, E. & Treit, D. (2009) Anxiolytic and antidepressant actions of somatostatin: the role of sst2 and sst3 receptors. *Psychopharmacology (Berl)*, **206**, 281-289.

Epelbaum, J. (1986) Somatostatin in the central nervous system: physiology and pathological modifications. *Prog Neurobiol*, **27**, 63-100.

Epelbaum, J., Javoy-Agid, F., Enjalbert, A., Krantic, S., Kordon, C. & Agid, Y. (1988) Somatostatin concentrations and binding sites in human frontal cortex are differentially affected in Parkinson's disease associated dementia and in progressive supranuclear palsy. *J Neurol Sci*, **87**, 167-174.

Erickson, K.I., Prakash, R.S., Voss, M.W., Chaddock, L., Heo, S., McLaren, M., Pence, B.D., Martin, S.A., Vieira, V.J., Woods, J.A., McAuley, E. & Kramer, A.F. (2010) Brain-derived neurotrophic factor is associated with age-related decline in hippocampal volume. *J Neurosci*, **30**, 5368-5375.

Erraji-Benchekroun, L., Underwood, M.D., Arango, V., Galfalvy, H., Pavlidis, P., Smyrniotopoulos, P., Mann, J.J. & Sibille, E. (2005) Molecular aging in human prefrontal cortex is selective and continuous throughout adult life. *Biol Psychiatry*, **57**, 549-558.

Fattal, O., Link, J., Quinn, K., Cohen, B.H. & Franco, K. (2007) Psychiatric comorbidity in 36 adults with mitochondrial cytopathies. *CNS spectrums*, **12**, 429-438.

Fava, M. & Davidson, K.G. (1996) Definition and epidemiology of treatment-resistant depression. *Psychiatr Clin North Am*, **19**, 179-200.

Fava, M. & Kendler, K.S. (2000) Major depressive disorder. *Neuron*, **28**, 335-341.

Ferrari, A.J., Charlson, F.J., Norman, R.E., Patten, S.B., Freedman, G., Murray, C.J., Vos, T. & Whiteford, H.A. (2013) Burden of depressive disorders by country, sex, age, and year: findings from the global burden of disease study 2010. *PLoS Med*, **10**, e1001547.

Figueredo-Cardenas, G., Morello, M., Sancesario, G., Bernardi, G. & Reiner, A. (1996) Colocalization of somatostatin, neuropeptide Y, neuronal nitric oxide synthase and NADPH-diaphorase in striatal interneurons in rats. *Brain Res*, **735**, 317-324.

Fishell, G. & Rudy, B. (2011) Mechanisms of inhibition within the telencephalon: "where the wild things are". *Annu Rev Neurosci*, **34**, 535-567.

Fitz-Patrick, D. & Patel, Y.C. (1981) Evidence for somatostatin precursors in human stomach, placenta, and amniotic fluid. *J Clin Endocrinol Metab*, **53**, 372-376.

Gabbott, P.L., Warner, T.A., Jays, P.R., Salway, P. & Busby, S.J. (2005) Prefrontal cortex in the rat: projections to subcortical autonomic, motor, and limbic centers. *J Comp Neurol*, **492**, 145-177.

Galfalvy, H.C., Erraji-Benchekroun, L., Smyrniotopoulos, P., Pavlidis, P., Ellis, S.P., Mann, J.J., Sibille, E. & Arango, V. (2003) Sex genes for genomic analysis in human brain: internal controls for comparison of probe level data extraction. *BMC bioinformatics*, **4**, 37.

Gardner, A., Johansson, A., Wibom, R., Nennesmo, I., von Dobeln, U., Hagenfeldt, L. & Hallstrom, T. (2003) Alterations of mitochondrial function and correlations with personality traits in selected major depressive disorder patients. *J Affect Disord*, **76**, 55-68.

Gavilan, M.P., Revilla, E., Pintado, C., Castano, A., Vizuete, M.L., Moreno-Gonzalez, I., Baglietto-Vargas, D., Sanchez-Varo, R., Vitorica, J., Gutierrez, A. & Ruano, D. (2007) Molecular and cellular characterization of the age-related neuroinflammatory processes occurring in normal rat hippocampus: potential relation with the loss of somatostatin GABAergic neurons. *J Neurochem*, **103**, 984-996.

Geller, B., Tillman, R., Bolhofner, K., Zimerman, B., Strauss, N.A. & Kaufmann, P. (2006) Controlled, blindly rated, direct-interview family study of a prepubertal and early-adolescent bipolar I disorder phenotype: morbid risk, age at onset, and comorbidity. *Arch Gen Psychiatry*, **63**, 1130-1138.

Gentet, L.J., Kremer, Y., Taniguchi, H., Huang, Z.J., Staiger, J.F. & Petersen, C.C. (2012) Unique functional properties of somatostatin-expressing GABAergic neurons in mouse barrel cortex. *Nat Neurosci*, **15**, 607-612.

Gingras, A.C., Raught, B. & Sonenberg, N. (1999) eIF4 initiation factors: effectors of mRNA recruitment to ribosomes and regulators of translation. *Annu Rev Biochem*, **68**, 913-963.

Glorioso, C., Oh, S., Douillard, G.G. & Sibille, E. (2011) Brain molecular aging, promotion of neurological disease and modulation by sirtuin 5 longevity gene polymorphism. *Neurobiol Dis*, **41**, 279-290.

Glorioso, C., Sabatini, M., Unger, T., Hashimoto, T., Monteggia, L.M., Lewis, D.A. & Mirnics, K. (2006) Specificity and timing of neocortical transcriptome changes in response to BDNF gene ablation during embryogenesis or adulthood. *Mol Psychiatry*, **11**, 633-648.

Gold, P.W. & Chrousos, G.P. (1999) The endocrinology of melancholic and atypical depression: relation to neurocircuitry and somatic consequences. *Proc Assoc Am Physicians*, **111**, 22-34.

Gold, P.W. & Chrousos, G.P. (2002) Organization of the stress system and its dysregulation in melancholic and atypical depression: high vs low CRH/NE states. *Mol Psychiatry*, **7**, 254-275.

Gonchar, Y. & Burkhalter, A. (1997) Three distinct families of GABAergic neurons in rat visual cortex. *Cereb Cortex*, **7**, 347-358.

Gonchar, Y., Wang, Q. & Burkhalter, A. (2007) Multiple distinct subtypes of GABAergic neurons in mouse visual cortex identified by triple immunostaining. *Front Neuroanat*, **1**, 3.

Gorman, J.M. (1996) Comorbid depression and anxiety spectrum disorders. *Depress Anxiety*, **4**, 160-168.

Goshen, I., Kreisel, T., Ben-Menachem-Zidon, O., Licht, T., Weidenfeld, J., Ben-Hur, T. & Yirmiya, R. (2008) Brain interleukin-1 mediates chronic stress-induced depression in mice via adrenocortical activation and hippocampal neurogenesis suppression. *Mol Psychiatry*, **13**, 717-728.

Griebel, G. & Holsboer, F. (2012) Neuropeptide receptor ligands as drugs for psychiatric diseases: the end of the beginning? *Nat Rev Drug Discov*, **11**, 462-478.

Grosse, G., Djalali, S., Deng, D.R., Holtje, M., Hinz, B., Schwartzkopff, K., Cygon, M., Rothe, T., Stroh, T., Hellweg, R., Ahnert-Hilger, G. & Hortnag, H. (2005) Area-specific effects of brain-derived neurotrophic factor (BDNF) genetic ablation on various neuronal subtypes of the mouse brain. *Brain Res Dev Brain Res*, **156**, 111-126.

Guerreiro, R., Wojtas, A., Bras, J., Carrasquillo, M., Rogaeva, E., Majounie, E., Cruchaga, C., Sassi, C., Kauwe, J.S., Younkin, S., Hazrati, L., Collinge, J., Pocock, J., Lashley, T., Williams, J., Lambert, J.C., Amouyel, P., Goate, A., Rademakers, R., Morgan, K., Powell, J., St George-Hyslop, P., Singleton, A. & Hardy, J. (2013) TREM2 variants in Alzheimer's disease. *N Engl J Med*, **368**, 117-127.

Guilloux, J.P., Douillard-Guilloux, G., Kota, R., Wang, X., Gardier, A.M., Martinowich, K., Tseng, G.C., Lewis, D.A. & Sibille, E. (2012) Molecular evidence for BDNF- and GABA-related dysfunctions in the amygdala of female subjects with major depression. *Mol Psychiatry*, **17**, 1130-1142.

Guilloux, J.P., Seney, M., Edgar, N. & Sibille, E. (2011) Integrated behavioral z-scoring increases the sensitivity and reliability of behavioral phenotyping in mice: relevance to emotionality and sex. *J Neurosci Methods*, **197**, 21-31.

Guillozet-Bongaarts, A.L., Hyde, T.M., Dalley, R.A., Hawrylycz, M.J., Henry, A., Hof, P.R., Hohmann, J., Jones, A.R., Kuan, C.L., Royall, J., Shen, E., Swanson, B., Zeng, H. & Kleinman, J.E. (2013) Altered gene expression in the dorsolateral prefrontal cortex of individuals with schizophrenia. *Mol Psychiatry*.

Haffer, K.N. (2012) Effects of novel vaccines on weight loss in diet-induced-obese (DIO) mice. *J Anim Sci Biotechnol*, **3**, 21.

Hammen, C. (2005) Stress and depression. *Annu Rev Clin Psychol*, **1**, 293-319.

Hampp, G., Ripperger, J.A., Houben, T., Schmutz, I., Blex, C., Perreau-Lenz, S., Brunk, I., Spanagel, R., Ahnert-Hilger, G., Meijer, J.H. & Albrecht, U. (2008) Regulation of monoamine oxidase A by circadian-clock components implies clock influence on mood. *Curr Biol*, **18**, 678-683.

Harding, H.P., Novoa, I., Zhang, Y., Zeng, H., Wek, R., Schapira, M. & Ron, D. (2000) Regulated translation initiation controls stress-induced gene expression in mammalian cells. *Mol Cell*, **6**, 1099-1108.

Hashimoto, K., Shimizu, E. & Iyo, M. (2004) Critical role of brain-derived neurotrophic factor in mood disorders. *Brain Res Brain Res Rev*, **45**, 104-114.

Hauger, R.L., Risbrough, V., Oakley, R.H., Olivares-Reyes, J.A. & Dautzenberg, F.M. (2009) Role of CRF receptor signaling in stress vulnerability, anxiety, and depression. *Ann N Y Acad Sci*, **1179**, 120-143.

Helyes, Z., Szabo, A., Nemeth, J., Jakab, B., Pinter, E., Banvolgyi, A., Kereskai, L., Keri, G. & Szolcsanyi, J. (2004) Antiinflammatory and analgesic effects of somatostatin released from capsaicin-sensitive sensory nerve terminals in a Freund's adjuvant-induced chronic arthritis model in the rat. *Arthritis Rheum*, **50**, 1677-1685.

Hendry, S.H., Jones, E.G. & Emson, P.C. (1984) Morphology, distribution, and synaptic relations of somatostatin- and neuropeptide Y-immunoreactive neurons in rat and monkey neocortex. *J Neurosci*, **4**, 2497-2517.

Hetz, C. & Mollereau, B. (2014) Disturbance of endoplasmic reticulum proteostasis in neurodegenerative diseases. *Nat Rev Neurosci*, **15**, 233-249.

Heuser, I.J., Schweiger, U., Gotthardt, U., Schmider, J., Lammers, C.H., Dettling, M., Yassouridis, A. & Holsboer, F. (1996) Pituitary-adrenal-system regulation and psychopathology during amitriptyline treatment in elderly depressed patients and normal comparison subjects. *Am J Psychiatry*, **153**, 93-99.

Hines, M., Allen, L.S. & Gorski, R.A. (1992) Sex differences in subregions of the medial nucleus of the amygdala and the bed nucleus of the stria terminalis of the rat. *Brain research*, **579**, 321-326.

Hodes, G.E., Brookshire, B.R., Hill-Smith, T.E., Teegarden, S.L., Berton, O. & Lucki, I. (2012) Strain differences in the effects of chronic corticosterone exposure in the hippocampus. *Neuroscience*, **222**, 269-280.

Hoffman, R.E. & Cavus, I. (2002) Slow transcranial magnetic stimulation, long-term depotentiation, and brain hyperexcitability disorders. *Am J Psychiatry*, **159**, 1093-1102.

Hollingworth, P. & Harold, D. & Sims, R. & Gerrish, A. & Lambert, J.C. & Carrasquillo, M.M. & Abraham, R. & Hamshere, M.L. & Pahwa, J.S. & Moskvina, V. & Dowzell, K. & Jones, N. & Stretton, A. & Thomas, C. & Richards, A. & Ivanov, D. & Widdowson, C. & Chapman, J. & Lovestone, S. & Powell, J. & Proitsi, P. & Lupton, M.K. & Brayne, C. & Rubinsztein, D.C. & Gill, M. & Lawlor, B. & Lynch, A. & Brown, K.S. & Passmore, P.A. & Craig, D. & McGuinness, B. & Todd, S. & Holmes, C. & Mann, D. & Smith, A.D. & Beaumont, H. & Warden, D. & Wilcock, G. & Love, S. & Kehoe, P.G. & Hooper, N.M. & Vardy, E.R. & Hardy, J. & Mead, S. & Fox, N.C. & Rossor, M. & Collinge, J. & Maier, W. & Jessen, F. & Ruther, E. & Schurmann, B. & Heun, R. & Kolsch, H. & van den Bussche, H. & Heuser, I. & Kornhuber, J. & Wiltfang, J. & Dichgans, M. & Frolich, L. & Hampel, H. & Gallacher, J. & Hull, M. & Rujescu, D. & Giegling, I. & Goate, A.M. & Kauwe, J.S. & Cruchaga, C. & Nowotny, P. & Morris, J.C. & Mayo, K. & Sleegers, K. & Bettens, K. & Engelborghs, S. & De Deyn, P.P. & Van Broeckhoven, C. & Livingston, G. & Bass, N.J. & Gurling, H. & McQuillin, A. & Gwilliam, R. & Deloukas, P. & Al-Chalabi, A. & Shaw, C.E. & Tsolaki, M. & Singleton, A.B. & Guerreiro, R. & Muhleisen, T.W. & Nothen, M.M. & Moebus, S. & Jockel, K.H. & Klopp, N. & Wichmann, H.E. & Pankratz, V.S. & Sando, S.B. & Aasly, J.O. &

Barcikowska, M. & Wszolek, Z.K. & Dickson, D.W. & Graff-Radford, N.R. & Petersen, R.C. & van Duijn, C.M. & Breteler, M.M. & Ikram, M.A. & DeStefano, A.L. & Fitzpatrick, A.L. & Lopez, O. & Launer, L.J. & Seshadri, S. & Berr, C. & Campion, D. & Epelbaum, J. & Dartigues, J.F. & Tzourio, C. & Alperovitch, A. & Lathrop, M. & Feulner, T.M. & Friedrich, P. & Riehle, C. & Krawczak, M. & Schreiber, S. & Mayhaus, M. & Nicolhaus, S. & Wagenpfeil, S. & Steinberg, S. & Stefansson, H. & Stefansson, K. & Snaedal, J. & Bjornsson, S. & Jonsson, P.V. & Chouraki, V. & Genier-Boley, B. & Hiltunen, M. & Soininen, H. & Combarros, O. & Zelenika, D. & Delepine, M. & Bullido, M.J. & Pasquier, F. & Mateo, I. & Frank-Garcia, A. & Porcellini, E. & Hanon, O. & Coto, E. & Alvarez, V. & Bosco, P. & Siciliano, G. & Mancuso, M. & Panza, F. & Solfrizzi, V. & Nacmias, B. & Sorbi, S. & Bossu, P. & Piccardi, P. & Arosio, B. & Annoni, G. & Seripa, D. & Pilotto, A. & Scarpini, E. & Galimberti, D. & Brice, A. & Hannequin, D. & Licastro, F. & Jones, L. & Holmans, P.A. & Jonsson, T. & Riemenschneider, M. & Morgan, K. & Younkin, S.G. & Owen, M.J. & O'Donovan, M. & Amouyel, P. & Williams, J. (2011) Common variants at ABCA7, MS4A6A/MS4A4E, EPHA1, CD33 and CD2AP are associated with Alzheimer's disease. *Nat Genet*, **43**, 429-435.

Holsboer, F. (2000) The corticosteroid receptor hypothesis of depression. *Neuropsychopharmacology*, **23**, 477-501.

Hoozemans, J.J., van Haastert, E.S., Nijholt, D.A., Rozemuller, A.J., Eikelenboom, P. & Scheper, W. (2009) The unfolded protein response is activated in pretangle neurons in Alzheimer's disease hippocampus. *Am J Pathol*, **174**, 1241-1251.

Howren, M.B., Lamkin, D.M. & Suls, J. (2009) Associations of depression with C-reactive protein, IL-1, and IL-6: a meta-analysis. *Psychosom Med*, **71**, 171-186.

Hoyer, D., Nunn, C., Hannon, J., Schoeffter, P., Feuerbach, D., Schuepbach, E., Langenegger, D., Bouhelal, R., Hurth, K., Neumann, P., Troxler, T. & Pfaeffli, P. (2004) SRA880, in vitro characterization of the first non-peptide somatostatin sst(1) receptor antagonist. *Neurosci Lett*, **361**, 132-135.

Ingolia, N.T. (2014) Ribosome profiling: new views of translation, from single codons to genome scale. *Nat Rev Genet*, **15**, 205-213.

Ising, M., Horstmann, S., Kloiber, S., Lucae, S., Binder, E.B., Kern, N., Kunzel, H.E., Pfennig, A., Uhr, M. & Holsboer, F. (2007) Combined dexamethasone/corticotropin releasing hormone test predicts treatment response in major depression - a potential biomarker? *Biol Psychiatry*, **62**, 47-54.

Jaglin, X.H., Hjerling-Leffler, J., Fishell, G. & Batista-Brito, R. (2012) The origin of neocortical nitric oxide synthase-expressing inhibitory neurons. *Front Neural Circuits*, **6**, 44.

Jazin, E. & Cahill, L. Sex differences in molecular neuroscience: from fruit flies to humans. *Nature reviews*, **11**, 9-17.

Joeyen-Waldorf, J., Edgar, N. & Sibille, E. (2009) The roles of sex and serotonin transporter levels in age- and stress-related emotionality in mice. *Brain Res*, **1286**, 84-93.

Kaestner, F., Hettich, M., Peters, M., Sibrowski, W., Hetzel, G., Ponath, G., Arolt, V., Cassens, U. & Rothermundt, M. (2005) Different activation patterns of proinflammatory cytokines in melancholic and non-melancholic major depression are associated with HPA axis activity. *J Affect Disord*, **87**, 305-311.

Kakigi, T., Maeda, K., Kaneda, H. & Chihara, K. (1992) Repeated administration of antidepressant drugs reduces regional somatostatin concentrations in rat brain. *J Affect Disord*, **25**, 215-220.

Kapicioglu, S., Gokce, E., Kapicioglu, Z. & Ovali, E. (1997) Treatment of migraine attacks with a long-acting somatostatin analogue (octreotide, SMS 201-995). *Cephalalgia*, **17**, 27-30.

Kathol, R.G. (1985) Etiologic implications of corticosteroid changes in affective disorder. *Psychiatr Med*, **3**, 135-162.

Kawaguchi, Y. & Kubota, Y. (1997) GABAergic cell subtypes and their synaptic connections in rat frontal cortex. *Cereb Cortex*, **7**, 476-486.

Ke, M.T., Fujimoto, S. & Imai, T. (2013) SeeDB: a simple and morphology-preserving optical clearing agent for neuronal circuit reconstruction. *Nat Neurosci*.

Keller, M.C., Neale, M.C. & Kendler, K.S. (2007) Association of different adverse life events with distinct patterns of depressive symptoms. *Am J Psychiatry*, **164**, 1521-1529; quiz 1622.

Kendler, K.S. (1998) Gender differences in the genetic epidemiology of major depression. *J Gend Specif Med*, **1**, 28-31.

Kendler, K.S. & Karkowski-Shuman, L. (1997) Stressful life events and genetic liability to major depression: genetic control of exposure to the environment? *Psychol Med*, **27**, 539-547.

Kendler, K.S., Karkowski, L.M. & Prescott, C.A. (1999) Causal relationship between stressful life events and the onset of major depression. *Am J Psychiatry*, **156**, 837-841.

Kessler, R.C., Berglund, P., Demler, O., Jin, R., Koretz, D., Merikangas, K.R., Rush, A.J., Walters, E.E. & Wang, P.S. (2003) The epidemiology of major depressive disorder: results from the National Comorbidity Survey Replication (NCS-R). *Jama*, **289**, 3095-3105.

Kessler, R.C., Berglund, P., Demler, O., Jin, R., Merikangas, K.R. & Walters, E.E. (2005a) Lifetime prevalence and age-of-onset distributions of DSM-IV disorders in the National Comorbidity Survey Replication. *Arch Gen Psychiatry*, **62**, 593-602.

Kessler, R.C., Chiu, W.T., Demler, O., Merikangas, K.R. & Walters, E.E. (2005b) Prevalence, severity, and comorbidity of 12-month DSM-IV disorders in the National Comorbidity Survey Replication. *Arch Gen Psychiatry*, **62**, 617-627.

Kim, H.J., Raphael, A.R., LaDow, E.S., McGurk, L., Weber, R.A., Trojanowski, J.Q., Lee, V.M., Finkbeiner, S., Gitler, A.D. & Bonini, N.M. (2014) Therapeutic modulation of eIF2alpha phosphorylation rescues TDP-43 toxicity in amyotrophic lateral sclerosis disease models. *Nat Genet*, **46**, 152-160.

Kimball, S.R., Vary, T.C. & Jefferson, L.S. (1992) Age-dependent decrease in the amount of eukaryotic initiation factor 2 in various rat tissues. *Biochem J*, **286 (Pt 1)**, 263-268.

Kitt, C.A., Hohmann, C., Coyle, J.T. & Price, D.L. (1994) Cholinergic innervation of mouse forebrain structures. *The Journal of comparative neurology*, **341**, 117-129.

Kling, M.A., Rubinow, D.R., Doran, A.R., Roy, A., Davis, C.L., Calabrese, J.R., Nieman, L.K., Post, R.M., Chrousos, G.P. & Gold, P.W. (1993) Cerebrospinal fluid immunoreactive somatostatin concentrations in patients with Cushing's disease and major depression: relationship to indices of corticotropin-releasing hormone and cortisol secretion. *Neuroendocrinology*, **57**, 79-88.

Kluxen, F.W., Bruns, C. & Lubbert, H. (1992) Expression cloning of a rat brain somatostatin receptor cDNA. *Proc Natl Acad Sci U S A*, **89**, 4618-4622.

Koch, B.D., Blalock, J.B. & Schonbrunn, A. (1988) Characterization of the cyclic AMP-independent actions of somatostatin in GH cells. I. An increase in potassium conductance is responsible for both the hyperpolarization and the decrease in intracellular free calcium produced by somatostatin. *J Biol Chem*, **263**, 216-225.

Koch, B.D. & Schonbrunn, A. (1984) The somatostatin receptor is directly coupled to adenylate cyclase in GH4C1 pituitary cell membranes. *Endocrinology*, **114**, 1784-1790.

Konradi, C., Eaton, M., MacDonald, M.L., Walsh, J., Benes, F.M. & Heckers, S. (2004) Molecular evidence for mitochondrial dysfunction in bipolar disorder. *Archives of general psychiatry*, **61**, 300-308.

Konradi, C., Yang, C.K., Zimmerman, E.I., Lohmann, K.M., Gresch, P., Pantazopoulos, H., Berretta, S. & Heckers, S. (2011a) Hippocampal interneurons are abnormal in schizophrenia. *Schizophr Res*, **131**, 165-173.

Konradi, C., Zimmerman, E.I., Yang, C.K., Lohmann, K.M., Gresch, P., Pantazopoulos, H., Berretta, S. & Heckers, S. (2011b) Hippocampal interneurons in bipolar disorder. *Arch Gen Psychiatry*, **68**, 340-350.

Koo, J.W. & Duman, R.S. (2008) IL-1beta is an essential mediator of the antineurogenic and anhedonic effects of stress. *Proc Natl Acad Sci U S A*, **105**, 751-756.

Kornstein, S.G., Schatzberg, A.F., Thase, M.E., Yonkers, K.A., McCullough, J.P., Keitner, G.I., Gelenberg, A.J., Ryan, C.E., Hess, A.L., Harrison, W., Davis, S.M. & Keller, M.B. (2000) Gender differences in chronic major and double depression. *J Affect Disord*, **60**, 1-11.

Kramer, A., Green, J., Pollard, J., Jr. & Tugendreich, S. (2014) Causal analysis approaches in Ingenuity Pathway Analysis. *Bioinformatics*, **30**, 523-530.

Kubota, Y., Shigematsu, N., Karube, F., Sekigawa, A., Kato, S., Yamaguchi, N., Hirai, Y., Morishima, M. & Kawaguchi, Y. (2011) Selective coexpression of multiple chemical markers defines discrete populations of neocortical GABAergic neurons. *Cereb Cortex*, **21**, 1803-1817.

Kurnatowska, I. & Pawlikowski, M. (2000) Effect of somatostatin analog-octreotide on the adjuvant arthritis in rat. *Neuro Endocrinol Lett*, **21**, 121-126.

Laplante, M. & Sabatini, D.M. (2012) mTOR signaling in growth control and disease. *Cell*, **149**, 274-293.

Lauritsen, M.B., Nyegaard, M., Betancur, C., Colineaux, C., Josiassen, T.L., Kruse, T.A., Leboyer, M. & Ewald, H. (2003) Analysis of transmission of novel polymorphisms in the somatostatin receptor 5 (SSTR5) gene in patients with autism. *Am J Med Genet B Neuropsychiatr Genet*, **121B**, 100-104.

Le Magueresse, C. & Monyer, H. (2013) GABAergic interneurons shape the functional maturation of the cortex. *Neuron*, **77**, 388-405.

Leach, L.S., Christensen, H., Mackinnon, A.J., Windsor, T.D. & Butterworth, P. (2008) Gender differences in depression and anxiety across the adult lifespan: the role of psychosocial mediators. *Soc Psychiatry Psychiatr Epidemiol*, **43**, 983-998.

Lee, S., Hjerling-Leffler, J., Zagha, E., Fishell, G. & Rudy, B. (2010) The largest group of superficial neocortical GABAergic interneurons expresses ionotropic serotonin receptors. *J Neurosci*, **30**, 16796-16808.

Lesch, K.P., Widerlov, E., Ekman, R., Laux, G., Rupprecht, R., Schulte, H.M. & Beckmann, H. (1989) The influence of human corticotropin-releasing hormone on somatostatin secretion in depressed patients and controls. *J Neural Transm*, **75**, 111-118.

Li, N., Lee, B., Liu, R.J., Banasr, M., Dwyer, J.M., Iwata, M., Li, X.Y., Aghajanian, G. & Duman, R.S. (2010) mTOR-dependent synapse formation underlies the rapid antidepressant effects of NMDA antagonists. *Science*, **329**, 959-964.

Lin, L.C., Lewis, D.A. & Sibille, E. (2011) A human-mouse conserved sex bias in amygdala gene expression related to circadian clock and energy metabolism. *Mol Brain*, **4**, 18.

Lin, L.C. & Sibille, E. (2013) Reduced brain somatostatin in mood disorders: a common pathophysiological substrate and drug target? *Front Pharmacol*, **4**, 110.

Lin, M.T. & Beal, M.F. (2006) Mitochondrial dysfunction and oxidative stress in neurodegenerative diseases. *Nature*, **443**, 787-795.

Livet, J., Weissman, T.A., Kang, H., Draft, R.W., Lu, J., Bennis, R.A., Sanes, J.R. & Lichtman, J.W. (2007) Transgenic strategies for combinatorial expression of fluorescent proteins in the nervous system. *Nature*, **450**, 56-62.

Lopez-Leon, S., Janssens, A.C., Gonzalez-Zuloeta Ladd, A.M., Del-Favero, J., Claes, S.J., Oostra, B.A. & van Duijn, C.M. (2008) Meta-analyses of genetic studies on major depressive disorder. *Mol Psychiatry*, **13**, 772-785.

Lotrich, F.E., Rabinovitz, M., Gironda, P. & Pollock, B.G. (2007) Depression following pegylated interferon-alpha: characteristics and vulnerability. *J Psychosom Res*, **63**, 131-135.

Lozano, A.M., Mayberg, H.S., Giacobbe, P., Hamani, C., Craddock, R.C. & Kennedy, S.H. (2008) Subcallosal cingulate gyrus deep brain stimulation for treatment-resistant depression. *Biol Psychiatry*, **64**, 461-467.

Luby, J.L., Heffelfinger, A., Mrakotsky, C., Brown, K., Hessler, M. & Spitznagel, E. (2003) Alterations in stress cortisol reactivity in depressed preschoolers relative to psychiatric and no-disorder comparison groups. *Arch Gen Psychiatry*, **60**, 1248-1255.

Luque, R.M., Gahete, M.D., Hochgeschwender, U. & Kineman, R.D. (2006) Evidence that endogenous SST inhibits ACTH and ghrelin expression by independent pathways. *Am J Physiol Endocrinol Metab*, **291**, E395-403.

Luscher, B., Shen, Q. & Sahir, N. (2011) The GABAergic deficit hypothesis of major depressive disorder. *Mol Psychiatry*, **16**, 383-406.

Ma, T., Trinh, M.A., Wexler, A.J., Bourbon, C., Gatti, E., Pierre, P., Cavener, D.R. & Klann, E. (2013) Suppression of eIF2alpha kinases alleviates Alzheimer's disease-related plasticity and memory deficits. *Nat Neurosci*, **16**, 1299-1305.

Maciag, D., Hughes, J., O'Dwyer, G., Pride, Y., Stockmeier, C.A., Sanacora, G. & Rajkowska, G. (2010) Reduced density of calbindin immunoreactive GABAergic neurons in the occipital cortex in major depression: relevance to neuroimaging studies. *Biol Psychiatry*, **67**, 465-470.

Maes, M. (2011) Depression is an inflammatory disease, but cell-mediated immune activation is the key component of depression. *Prog Neuropsychopharmacol Biol Psychiatry*, **35**, 664-675.

Maes, M., Mihaylova, I., Kubera, M. & Ringel, K. (2012) Activation of cell-mediated immunity in depression: association with inflammation, melancholia, clinical staging and the fatigue and somatic symptom cluster of depression. *Prog Neuropsychopharmacol Biol Psychiatry*, **36**, 169-175.

Malisch, J.L., Saltzman, W., Gomes, F.R., Rezende, E.L., Jeske, D.R. & Garland, T., Jr. (2007) Baseline and stress-induced plasma corticosterone concentrations of mice selectively bred for high voluntary wheel running. *Physiol Biochem Zool*, **80**, 146-156.

Mancuso, C., Scapagini, G., Curro, D., Giuffrida Stella, A.M., De Marco, C., Butterfield, D.A. & Calabrese, V. (2007) Mitochondrial dysfunction, free radical generation and cellular stress response in neurodegenerative disorders. *Front Biosci*, **12**, 1107-1123.

Markram, H., Toledo-Rodriguez, M., Wang, Y., Gupta, A., Silberberg, G. & Wu, C. (2004) Interneurons of the neocortical inhibitory system. *Nat Rev Neurosci*, **5**, 793-807.

Martel, G., Dutar, P., Epelbaum, J. & Viollet, C. (2012) Somatostatinergic systems: an update on brain functions in normal and pathological aging. *Front Endocrinol (Lausanne)*, **3**, 154.

Martinowich, K., Schloesser, R.J., Jimenez, D.V., Weinberger, D.R. & Lu, B. (2011) Activity-dependent brain-derived neurotrophic factor expression regulates cortistatin-interneurons and sleep behavior. *Mol Brain*, **4**, 11.

Masand, P.S. & Gupta, S. (2002) Long-term side effects of newer-generation antidepressants: SSRIS, venlafaxine, nefazodone, bupropion, and mirtazapine. *Ann Clin Psychiatry*, **14**, 175-182.

Matthews, S.C., Strigo, I.A., Simmons, A.N., Yang, T.T. & Paulus, M.P. (2008) Decreased functional coupling of the amygdala and supragenual cingulate is related to increased depression in unmedicated individuals with current major depressive disorder. *J Affect Disord*, **111**, 13-20.

Mayberg, H.S., Lozano, A.M., Voon, V., McNeely, H.E., Seminowicz, D., Hamani, C., Schwalb, J.M. & Kennedy, S.H. (2005) Deep brain stimulation for treatment-resistant depression. *Neuron*, **45**, 651-660.

McGuffin, P., Rijsdijk, F., Andrew, M., Sham, P., Katz, R. & Cardno, A. (2003) The heritability of bipolar affective disorder and the genetic relationship to unipolar depression. *Arch Gen Psychiatry*, **60**, 497-502.

Melchitzky, D.S. & Lewis, D.A. (2008) Dendritic-targeting GABA neurons in monkey prefrontal cortex: comparison of somatostatin- and calretinin-immunoreactive axon terminals. *Synapse*, **62**, 456-465.

Metzker, M.L. (2010) Sequencing technologies - the next generation. *Nat Rev Genet*, **11**, 31-46.

Miller, A.H., Maletic, V. & Raison, C.L. (2009) Inflammation and its discontents: the role of cytokines in the pathophysiology of major depression. *Biol Psychiatry*, **65**, 732-741.

Molchan, S.E., Hill, J.L., Martinez, R.A., Lawlor, B.A., Mellow, A.M., Rubinow, D.R., Bissette, G., Nemeroff, C.B. & Sunderland, T. (1993) CSF somatostatin in Alzheimer's disease and major depression: relationship to hypothalamic-pituitary-adrenal axis and clinical measures. *Psychoneuroendocrinology*, **18**, 509-519.

Molchan, S.E., Lawlor, B.A., Hill, J.L., Martinez, R.A., Davis, C.L., Mellow, A.M., Rubinow, D.R. & Sunderland, T. (1991) CSF monoamine metabolites and somatostatin in Alzheimer's disease and major depression. *Biol Psychiatry*, **29**, 1110-1118.

Molitch, M.E. (2008) Lanreotide Autogel in the management of acromegaly. *Drugs*, **68**, 724.

Mollenholt, P., Rawal, N., Gordh, T., Jr. & Olsson, Y. (1994) Intrathecal and epidural somatostatin for patients with cancer. Analgesic effects and postmortem neuropathologic investigations of spinal cord and nerve roots. *Anesthesiology*, **81**, 534-542.

Moller, L.N., Stidsen, C.E., Hartmann, B. & Holst, J.J. (2003) Somatostatin receptors. *Biochim Biophys Acta*, **1616**, 1-84.

Montminy, M.R., Sevarino, K.A., Wagner, J.A., Mandel, G. & Goodman, R.H. (1986) Identification of a cyclic-AMP-responsive element within the rat somatostatin gene. *Proc Natl Acad Sci U S A*, **83**, 6682-6686.

Moreno, J.A., Halliday, M., Molloy, C., Radford, H., Verity, N., Axten, J.M., Ortori, C.A., Willis, A.E., Fischer, P.M., Barrett, D.A. & Mallucci, G.R. (2013) Oral treatment

targeting the unfolded protein response prevents neurodegeneration and clinical disease in prion-infected mice. *Sci Transl Med*, **5**, 206ra138.

Moreno, J.A., Radford, H., Peretti, D., Steinert, J.R., Verity, N., Martin, M.G., Halliday, M., Morgan, J., Dinsdale, D., Ortori, C.A., Barrett, D.A., Tsaytler, P., Bertolotti, A., Willis, A.E., Bushell, M. & Mallucci, G.R. (2012) Sustained translational repression by eIF2alpha-P mediates prion neurodegeneration. *Nature*, **485**, 507-511.

Morris, H.M., Hashimoto, T. & Lewis, D.A. (2008) Alterations in somatostatin mRNA expression in the dorsolateral prefrontal cortex of subjects with schizophrenia or schizoaffective disorder. *Cereb Cortex*, **18**, 1575-1587.

Moylan, S., Maes, M., Wray, N.R. & Berk, M. (2013) The neuroprogressive nature of major depressive disorder: pathways to disease evolution and resistance, and therapeutic implications. *Mol Psychiatry*, **18**, 595-606.

Murayama, M., Perez-Garci, E., Nevian, T., Bock, T., Senn, W. & Larkum, M.E. (2009) Dendritic encoding of sensory stimuli controlled by deep cortical interneurons. *Nature*, **457**, 1137-1141.

Murphy, B.E. (1991) Steroids and depression. *J Steroid Biochem Mol Biol*, **38**, 537-559.

Myers, B., McKlveen, J.M. & Herman, J.P. (2014) Glucocorticoid actions on synapses, circuits, and behavior: Implications for the energetics of stress. *Front Neuroendocrinol*, **35**, 180-196.

Nagata, T., Ilieva, H., Murakami, T., Shiote, M., Narai, H., Ohta, Y., Hayashi, T., Shoji, M. & Abe, K. (2007) Increased ER stress during motor neuron degeneration in a transgenic mouse model of amyotrophic lateral sclerosis. *Neurol Res*, **29**, 767-771.

Nanda, S.A., Qi, C., Roseboom, P.H. & Kalin, N.H. (2008) Predator stress induces behavioral inhibition and amygdala somatostatin receptor 2 gene expression. *Genes Brain Behav*, **7**, 639-648.

Neggers, S.J. & van der Lely, A.J. (2009) Somatostatin analog and pegvisomant combination therapy for acromegaly. *Nat Rev Endocrinol*, **5**, 546-552.

Nilsson, A., Stroth, N., Zhang, X., Qi, H., Falth, M., Skold, K., Hoyer, D., Andren, P.E. & Svenningsson, P. (2012) Neuropeptidomics of mouse hypothalamus after imipramine treatment reveal somatostatin as a potential mediator of antidepressant effects. *Neuropharmacology*, **62**, 347-357.

Nyegaard, M., Borglum, A.D., Bruun, T.G., Collier, D.A., Russ, C., Mors, O., Ewald, H. & Kruse, T.A. (2002) Novel polymorphisms in the somatostatin receptor 5 (SSTR5) gene associated with bipolar affective disorder. *Mol Psychiatry*, **7**, 745-754.

Olias, G., Viollet, C., Kusserow, H., Epelbaum, J. & Meyerhof, W. (2004) Regulation and function of somatostatin receptors. *J Neurochem*, **89**, 1057-1091.

Padmos, R.C., Hillegers, M.H., Knijff, E.M., Vonk, R., Bouvy, A., Staal, F.J., de Ridder, D., Kupka, R.W., Nolen, W.A. & Drexhage, H.A. (2008) A discriminating messenger RNA signature for bipolar disorder formed by an aberrant expression of inflammatory genes in monocytes. *Arch Gen Psychiatry*, **65**, 395-407.

Pallis, E., Vasilaki, A., Fehlmann, D., Kastellakis, A., Hoyer, D., Spyraki, C. & Thermos, K. (2009) Antidepressants influence somatostatin levels and receptor pharmacology in brain. *Neuropsychopharmacology*, **34**, 952-963.

Pallis, E.G., Spyraki, C. & Thermos, K. (2006) Chronic antidepressant treatment modulates the release of somatostatin in the rat nucleus accumbens. *Neurosci Lett*, **395**, 76-81.

Patel, Y.C. (1999) Somatostatin and its receptor family. *Front Neuroendocrinol*, **20**, 157-198.

Paus, T., Keshavan, M. & Giedd, J.N. (2008) Why do many psychiatric disorders emerge during adolescence? *Nat Rev Neurosci*, **9**, 947-957.

Perugi, G., Musetti, L., Simonini, E., Piagentini, F., Cassano, G.B. & Akiskal, H.S. (1990) Gender-mediated clinical features of depressive illness. The importance of temperamental differences. *Br J Psychiatry*, **157**, 835-841.

Petrozzi, L., Ricci, G., Giglioli, N.J., Siciliano, G. & Mancuso, M. (2007) Mitochondria and neurodegeneration. *Biosci Rep*, **27**, 87-104.

Pivonello, R., Ferone, D., Lamberts, S.W. & Colao, A. (2005) Cabergoline plus lanreotide for ectopic Cushing's syndrome. *N Engl J Med*, **352**, 2457-2458.

Polak, P. & Hall, M.N. (2009) mTOR and the control of whole body metabolism. *Curr Opin Cell Biol*, **21**, 209-218.

Pollack, M.H. (2005) Comorbid anxiety and depression. *J Clin Psychiatry*, **66 Suppl 8**, 22-29.

Ponomarev, I., Rau, V., Eger, E.I., Harris, R.A. & Fanselow, M.S. (2010) Amygdala transcriptome and cellular mechanisms underlying stress-enhanced fear learning in a rat model of posttraumatic stress disorder. *Neuropsychopharmacology*, **35**, 1402-1411.

Post, R.M., Rubinow, D.R., Kling, M.A., Berrettini, W. & Gold, P.W. (1988) Neuroactive substances in cerebrospinal fluid. Normal and pathological regulatory mechanisms. *Ann N Y Acad Sci*, **531**, 15-28.

Pothion, S., Bizot, J.C., Trovero, F. & Belzung, C. (2004) Strain differences in sucrose preference and in the consequences of unpredictable chronic mild stress. *Behav Brain Res*, **155**, 135-146.

Prosperini, E., Rizzi, M., Fumagalli, F., Tarizzo, G., Samanin, R. & Bendotti, C. (1997) Acute and chronic treatments with citalopram lower somatostatin levels in rat brain striatum through different mechanisms. *J Neurochem*, **69**, 206-213.

Pruessner, M., Hellhammer, D.H., Pruessner, J.C. & Lupien, S.J. (2003) Self-reported depressive symptoms and stress levels in healthy young men: associations with the cortisol response to awakening. *Psychosom Med*, **65**, 92-99.

Rajkowska, G., O'Dwyer, G., Teleki, Z., Stockmeier, C.A. & Miguel-Hidalgo, J.J. (2007) GABAergic neurons immunoreactive for calcium binding proteins are reduced in the prefrontal cortex in major depression. *Neuropsychopharmacology*, **32**, 471-482.

Ramirez, J.L., Mouchantaf, R., Kumar, U., Otero Corchon, V., Rubinstein, M., Low, M.J. & Patel, Y.C. (2002) Brain somatostatin receptors are up-regulated in somatostatin-deficient mice. *Mol Endocrinol*, **16**, 1951-1963.

Reinikainen, K.J., Koponen, H., Jolkkonen, J. & Riekkinen, P.J. (1990) Decreased somatostatin-like immunoreactivity in the cerebrospinal fluid of chronic schizophrenic patients with cognitive impairment. *Psychiatry Res*, **33**, 307-312.

Rivier, J., Erchegyi, J., Hoeger, C., Miller, C., Low, W., Wenger, S., Waser, B., Schaer, J.C. & Reubi, J.C. (2003) Novel sst(4)-selective somatostatin (SRIF) agonists. 1. Lead identification using a betide scan. *J Med Chem*, **46**, 5579-5586.

Robas, N., Mead, E. & Fidock, M. (2003) MrgX2 is a high potency cortistatin receptor expressed in dorsal root ganglion. *J Biol Chem*, **278**, 44400-44404.

Rocheville, M., Lange, D.C., Kumar, U., Patel, S.C., Patel, R.C. & Patel, Y.C. (2000) Receptors for dopamine and somatostatin: formation of hetero-oligomers with enhanced functional activity. *Science*, **288**, 154-157.

Rollins, B., Martin, M.V., Sequeira, P.A., Moon, E.A., Morgan, L.Z., Watson, S.J., Schatzberg, A., Akil, H., Myers, R.M., Jones, E.G., Wallace, D.C., Bunney, W.E. & Vawter, M.P. (2009) Mitochondrial variants in schizophrenia, bipolar disorder, and major depressive disorder. *PloS one*, **4**, e4913.

Rossor, M.N., Emson, P.C., Mountjoy, C.Q., Roth, M. & Iversen, L.L. (1980) Reduced amounts of immunoreactive somatostatin in the temporal cortex in senile dementia of Alzheimer type. *Neurosci Lett*, **20**, 373-377.

Roussel, B.D., Kruppa, A.J., Miranda, E., Crowther, D.C., Lomas, D.A. & Marciniak, S.J. (2013) Endoplasmic reticulum dysfunction in neurological disease. *Lancet Neurol*, **12**, 105-118.

Roybal, K., Theobold, D., Graham, A., DiNieri, J.A., Russo, S.J., Krishnan, V., Chakravarty, S., Peevey, J., Oehrlein, N., Birnbaum, S., Vitaterna, M.H., Orsulak, P., Takahashi, J.S., Nestler, E.J., Carlezon, W.A., Jr. & McClung, C.A. (2007) Mania-like behavior induced by disruption of CLOCK. *Proceedings of the National Academy of Sciences of the United States of America*, **104**, 6406-6411.

Rubinow, D.R., Gold, P.W., Post, R.M. & Ballenger, J.C. (1985) CSF somatostatin in affective illness and normal volunteers. *Prog Neuropsychopharmacol Biol Psychiatry*, **9**, 393-400.

Rubinow, D.R., Gold, P.W., Post, R.M., Ballenger, J.C., Cowdry, R., Bollinger, J. & Reichlin, S. (1983) CSF somatostatin in affective illness. *Arch Gen Psychiatry*, **40**, 409-412.

Rudy, B., Fishell, G., Lee, S. & Hjerling-Leffler, J. (2011) Three groups of interneurons account for nearly 100% of neocortical GABAergic neurons. *Dev Neurobiol*, **71**, 45-61.

Saito, T., Iwata, N., Tsubuki, S., Takaki, Y., Takano, J., Huang, S.M., Suemoto, T., Higuchi, M. & Saido, T.C. (2005) Somatostatin regulates brain amyloid beta peptide Abeta42 through modulation of proteolytic degradation. *Nat Med*, **11**, 434-439.

Sanacora, G., Gueorguieva, R., Epperson, C.N., Wu, Y.T., Appel, M., Rothman, D.L., Krystal, J.H. & Mason, G.F. (2004) Subtype-specific alterations of gamma-aminobutyric acid and glutamate in patients with major depression. *Arch Gen Psychiatry*, **61**, 705-713.

Saveanu, A., Lavaque, E., Gunz, G., Barlier, A., Kim, S., Taylor, J.E., Culler, M.D., Enjalbert, A. & Jaquet, P. (2002) Demonstration of enhanced potency of a chimeric somatostatin-dopamine molecule, BIM-23A387, in suppressing growth hormone and prolactin secretion from human pituitary somatotroph adenoma cells. *J Clin Endocrinol Metab*, **87**, 5545-5552.

Saxena, S., Cabuy, E. & Caroni, P. (2009) A role for motoneuron subtype-selective ER stress in disease manifestations of FALS mice. *Nat Neurosci*, **12**, 627-636.

Schmid, H.A. & Schoeffter, P. (2004) Functional activity of the multiligand analog SOM230 at human recombinant somatostatin receptor subtypes supports its usefulness in neuroendocrine tumors. *Neuroendocrinology*, **80 Suppl 1**, 47-50.

Schreff, M., Schulz, S., Handel, M., Keilhoff, G., Braun, H., Pereira, G., Klutzny, M., Schmidt, H., Wolf, G. & Hollt, V. (2000) Distribution, targeting, and internalization of the sst4 somatostatin receptor in rat brain. *J Neurosci*, **20**, 3785-3797.

Schulz, S., Handel, M., Schreff, M., Schmidt, H. & Hollt, V. (2000) Localization of five somatostatin receptors in the rat central nervous system using subtype-specific antibodies. *J Physiol Paris*, **94**, 259-264.

Sharif, N., Gendron, L., Wowchuk, J., Sarret, P., Mazella, J., Beaudet, A. & Stroh, T. (2007) Coexpression of somatostatin receptor subtype 5 affects internalization and trafficking of somatostatin receptor subtype 2. *Endocrinology*, **148**, 2095-2105.

Sharma, R.P., Bissette, G., Janicak, P.G., Davis, J.M. & Nemeroff, C.B. (1995) Elevation of CSF somatostatin concentrations in mania. *Am J Psychiatry*, **152**, 1807-1809.

Sheline, Y.I., Barch, D.M., Donnelly, J.M., Ollinger, J.M., Snyder, A.Z. & Mintun, M.A. (2001) Increased amygdala response to masked emotional faces in depressed subjects resolves with antidepressant treatment: an fMRI study. *Biological psychiatry*, **50**, 651-658.

Sheppard, M., Shapiro, B., Pimstone, B., Kronheim, S., Berelowitz, M. & Gregory, M. (1979) Metabolic clearance and plasma half-disappearance time of exogenous somatostatin in man. *J Clin Endocrinol Metab*, **48**, 50-53.

Sibille, E., Morris, H.M., Kota, R.S. & Lewis, D.A. (2011) GABA-related transcripts in the dorsolateral prefrontal cortex in mood disorders. *Int J Neuropsychopharmacol*, **14**, 721-734.

Sibille, E., Pavlides, C., Benke, D. & Toth, M. (2000) Genetic inactivation of the Serotonin(1A) receptor in mice results in downregulation of major GABA(A) receptor alpha subunits, reduction of GABA(A) receptor binding, and benzodiazepine-resistant anxiety. *J Neurosci*, **20**, 2758-2765.

Sibille, E., Wang, Y., Joeyen-Waldorf, J., Gaiteri, C., Surget, A., Oh, S., Belzung, C., Tseng, G.C. & Lewis, D.A. (2009a) A molecular signature of depression in the amygdala. *The American journal of psychiatry*, **166**, 1011-1024.

Sibille, E., Wang, Y., Joeyen-Waldorf, J., Gaiteri, C., Surget, A., Oh, S., Belzung, C., Tseng, G.C. & Lewis, D.A. (2009b) A Molecular Signature of Depression in the Amygdala. *Am J Psychiatry*, **166**, 1011-1024.

Sicuteri, F., Geppetti, P., Marabini, S. & Lembeck, F. (1984) Pain relief by somatostatin in attacks of cluster headache. *Pain*, **18**, 359-365.

Siehler, S., Nunn, C., Hannon, J., Feuerbach, D. & Hoyer, D. (2008) Pharmacological profile of somatostatin and cortistatin receptors. *Mol Cell Endocrinol*, **286**, 26-34.

Sohal, R.S. & Weindruch, R. (1996) Oxidative stress, caloric restriction, and aging. *Science*, **273**, 59-63.

Song, C. & Wang, H. (2011) Cytokines mediated inflammation and decreased neurogenesis in animal models of depression. *Prog Neuropsychopharmacol Biol Psychiatry*, **35**, 760-768.

Sorce, S. & Krause, K.H. (2009) NOX enzymes in the central nervous system: from signaling to disease. *Antioxid Redox Signal*, **11**, 2481-2504.

Soria, V., Martinez-Amoros, E., Escaramis, G., Valero, J., Perez-Egea, R., Garcia, C., Gutierrez-Zotes, A., Puigdemont, D., Bayes, M., Crespo, J.M., Martorell, L., Vilella, E., Labad, A., Vallejo, J., Perez, V., Menchon, J.M., Estivill, X., Gratacos, M. & Urretavizcaya, M. Differential association of circadian genes with mood disorders: CRY1 and NPAS2 are associated with unipolar major depression and CLOCK and VIP with bipolar disorder. *Neuropsychopharmacology*, **35**, 1279-1289.

Soumier, A. & Sibille, E. (2014) Opposing Effects of Acute versus Chronic Blockade of Frontal Cortex Somatostatin-Positive Inhibitory Neurons on Behavioral Emotionality in Mice. *Neuropsychopharmacology*.

Spier, A.D. & de Lecea, L. (2000) Cortistatin: a member of the somatostatin neuropeptide family with distinct physiological functions. *Brain Res Brain Res Rev*, **33**, 228-241.

Stafford, R.S., Ausiello, J.C., Misra, B. & Saglam, D. (2000) National Patterns of Depression Treatment in Primary Care. *Prim Care Companion J Clin Psychiatry*, **2**, 211-216.

Starkman, M.N., Schteingart, D.E. & Schork, M.A. (1981) Depressed mood and other psychiatric manifestations of Cushing's syndrome: relationship to hormone levels. *Psychosom Med*, **43**, 3-18.

Stefanescu, C. & Ciobica, A. (2012) The relevance of oxidative stress status in first episode and recurrent depression. *J Affect Disord*, **143**, 34-38.

Stroh, T., Kreienkamp, H.J. & Beaudet, A. (1999) Immunohistochemical distribution of the somatostatin receptor subtype 5 in the adult rat brain: predominant expression in the basal forebrain. *J Comp Neurol*, **412**, 69-82.

Strowski, M.Z., Kohler, M., Chen, H.Y., Trumbauer, M.E., Li, Z., Szalkowski, D., Gopal-Truter, S., Fisher, J.K., Schaeffer, J.M., Blake, A.D., Zhang, B.B. & Wilkinson, H.A. (2003) Somatostatin receptor subtype 5 regulates insulin secretion and glucose homeostasis. *Mol Endocrinol*, **17**, 93-106.

Surget, A., Wang, Y., Leman, S., Ibarguen-Vargas, Y., Edgar, N., Griebel, G., Belzung, C. & Sibille, E. (2009) Corticolimbic transcriptome changes are state-dependent and region-specific in a rodent model of depression and of antidepressant reversal. *Neuropsychopharmacology*, **34**, 1363-1380.

Svendsen, C.N. & Bird, E.D. (1985) Acetylcholinesterase staining of the human amygdala. *Neuroscience letters*, **54**, 313-318.

Szolcsanyi, J., Helyes, Z., Oroszi, G., Nemeth, J. & Pinter, E. (1998) Release of somatostatin and its role in the mediation of the anti-inflammatory effect induced by antidromic stimulation of sensory fibres of rat sciatic nerve. *Br J Pharmacol*, **123**, 936-942.

Tallent, M.K. & Qiu, C. (2008) Somatostatin: an endogenous antiepileptic. *Mol Cell Endocrinol*, **286**, 96-103.

Tamminga, C.A., Foster, N.L., Fedio, P., Bird, E.D. & Chase, T.N. (1987) Alzheimer's disease: low cerebral somatostatin levels correlate with impaired cognitive function and cortical metabolism. *Neurology*, **37**, 161-165.

Tamminga, C.A., Nemeroff, C.B., Blakely, R.D., Brady, L., Carter, C.S., Davis, K.L., Dingledine, R., Gorman, J.M., Grigoriadis, D.E., Henderson, D.C., RB, B.I., Killen, J., Laughren, T.P., McDonald, W.M., M. Murphy GM, J., Paul, S.M., Rudorfer, M.V., Sausville, E., Schatzberg, A.F., Scolnick, E.M. & Suppes, T. (2002) Developing novel treatments for mood disorders: accelerating discovery. *Biol Psychiatry*, **52**, 589-609.

Tan, Z., Hu, H., Huang, Z.J. & Agmon, A. (2008) Robust but delayed thalamocortical activation of dendritic-targeting inhibitory interneurons. *Proceedings of the National Academy of Sciences of the United States of America*, **105**, 2187-2192.

Taniguchi, H., He, M., Wu, P., Kim, S., Paik, R., Sugino, K., Kvitsiani, D., Fu, Y., Lu, J., Lin, Y., Miyoshi, G., Shima, Y., Fishell, G., Nelson, S.B. & Huang, Z.J. (2011) A resource of Cre driver lines for genetic targeting of GABAergic neurons in cerebral cortex. *Neuron*, **71**, 995-1013.

Tasker, J.G. & Herman, J.P. (2011) Mechanisms of rapid glucocorticoid feedback inhibition of the hypothalamic-pituitary-adrenal axis. *Stress*, **14**, 398-406.

Taura, P., Planella, V., Balust, J., Beltran, J., Anglada, T., Carrero, E. & Burgues, S. (1994) Epidural somatostatin as an analgesic in upper abdominal surgery: a double-blind study. *Pain*, **59**, 135-140.

Thompson, M., Weickert, C.S., Wyatt, E. & Webster, M.J. (2009) Decreased glutamic acid decarboxylase(67) mRNA expression in multiple brain areas of patients with schizophrenia and mood disorders. *J Psychiatr Res*, **43**, 970-977.

Tondo, L. & Baldessarini, R.J. (1998) Rapid cycling in women and men with bipolar manic-depressive disorders. *The American journal of psychiatry*, **155**, 1434-1436.

Tostivint, H., Lihrmann, I. & Vaudry, H. (2008) New insight into the molecular evolution of the somatostatin family. *Mol Cell Endocrinol*, **286**, 5-17.

Tringali, G., Greco, M.C., Lisi, L., Pozzoli, G. & Navarra, P. (2012) Cortistatin modulates the expression and release of corticotrophin releasing hormone in rat brain. Comparison with somatostatin and octreotide. *Peptides*, **34**, 353-359.

Tripp, A., Kota, R.S., Lewis, D.A. & Sibille, E. (2011) Reduced somatostatin in subgenual anterior cingulate cortex in major depression. *Neurobiol Dis*, **42**, 116-124.

Tripp, A., Oh, H., Guilloux, J.P., Martinowich, K., Lewis, D.A. & Sibille, E. (2012) Brain-derived neurotrophic factor signaling and subgenual anterior cingulate cortex dysfunction in major depressive disorder. *Am J Psychiatry*, **169**, 1194-1202.

Trivedi, M.H., Rush, A.J., Wisniewski, S.R., Nierenberg, A.A., Warden, D., Ritz, L., Norquist, G., Howland, R.H., Lebowitz, B., McGrath, P.J., Shores-Wilson, K., Biggs, M.M., Balasubramani, G.K. & Fava, M. (2006) Evaluation of outcomes with citalopram for depression using measurement-based care in STAR*D: implications for clinical practice. *Am J Psychiatry*, **163**, 28-40.

Uylings, H.B., Groenewegen, H.J. & Kolb, B. (2003) Do rats have a prefrontal cortex? *Behav Brain Res*, **146**, 3-17.

Vela, J., Gutierrez, A., Vitorica, J. & Ruano, D. (2003) Rat hippocampal GABAergic molecular markers are differentially affected by ageing. *J Neurochem*, **85**, 368-377.

Vepsalainen, S., Helisalmi, S., Koivisto, A.M., Tapaninen, T., Hiltunen, M. & Soininen, H. (2007) Somatostatin genetic variants modify the risk for Alzheimer's disease among Finnish patients. *J Neurol*, **254**, 1504-1508.

Vertes, R.P. (2004) Differential projections of the infralimbic and prelimbic cortex in the rat. *Synapse*, **51**, 32-58.

Vezzani, A. & Hoyer, D. (1999) Brain somatostatin: a candidate inhibitory role in seizures and epileptogenesis. *Eur J Neurosci*, **11**, 3767-3776.

Viollet, C., Lepousez, G., Loudes, C., Videau, C., Simon, A. & Epelbaum, J. (2008) Somatostatinergic systems in brain: networks and functions. *Mol Cell Endocrinol*, **286**, 75-87.

Viollet, C., Vaillend, C., Videau, C., Bluet-Pajot, M.T., Ungerer, A., L'Heritier, A., Kopp, C., Potier, B., Billard, J., Schaeffer, J., Smith, R.G., Rohrer, S.P., Wilkinson, H., Zheng, H. & Epelbaum, J. (2000) Involvement of sst2 somatostatin receptor in locomotor, exploratory activity and emotional reactivity in mice. *Eur J Neurosci*, **12**, 3761-3770.

Walker, A.K., Soo, K.Y., Sundaramoorthy, V., Parakh, S., Ma, Y., Farg, M.A., Wallace, R.H., Crouch, P.J., Turner, B.J., Horne, M.K. & Atkin, J.D. (2013) ALS-associated TDP-43 induces endoplasmic reticulum stress, which drives cytoplasmic TDP-43 accumulation and stress granule formation. *PLoS One*, **8**, e81170.

Walter, M., Henning, A., Grimm, S., Schulte, R.F., Beck, J., Dydak, U., Schnepf, B., Boeker, H., Boesiger, P. & Northoff, G. (2009) The relationship between aberrant neuronal activation in the pregenual anterior cingulate, altered glutamatergic metabolism, and anhedonia in major depression. *Arch Gen Psychiatry*, **66**, 478-486.

Wang, A.Y., Lohmann, K.M., Yang, C.K., Zimmerman, E.I., Pantazopoulos, H., Herring, N., Berretta, S., Heckers, S. & Konradi, C. (2011) Bipolar disorder type 1 and schizophrenia are accompanied by decreased density of parvalbumin- and somatostatin-positive interneurons in the parahippocampal region. *Acta Neuropathol*, **122**, 615-626.

Wang, S.S., Kamphuis, W., Huitinga, I., Zhou, J.N. & Swaab, D.F. (2008) Gene expression analysis in the human hypothalamus in depression by laser microdissection and real-time PCR: the presence of multiple receptor imbalances. *Mol Psychiatry*, **13**, 786-799, 741.

Wang, X. & Proud, C.G. (2006) The mTOR pathway in the control of protein synthesis. *Physiology (Bethesda)*, **21**, 362-369.

Wang, X.M., Tresham, J.J., Coghlan, J.P. & Scoggins, B.A. (1987) Intracerebroventricular infusion of a cyclic hexapeptide analogue of somatostatin inhibits hemorrhage-induced ACTH release. *Neuroendocrinology*, **45**, 325-327.

Wang, Z., Gerstein, M. & Snyder, M. (2009) RNA-Seq: a revolutionary tool for transcriptomics. *Nat Rev Genet*, **10**, 57-63.

Warren, T.G. & Shields, D. (1984) Expression of preprosomatostatin in heterologous cells: biosynthesis, posttranslational processing, and secretion of mature somatostatin. *Cell*, **39**, 547-555.

Webster, M.J., Knable, M.B., O'Grady, J., Orthmann, J. & Weickert, C.S. (2002) Regional specificity of brain glucocorticoid receptor mRNA alterations in subjects with schizophrenia and mood disorders. *Mol Psychiatry*, **7**, 985-994, 924.

Weckbecker, G., Lewis, I., Albert, R., Schmid, H.A., Hoyer, D. & Bruns, C. (2003) Opportunities in somatostatin research: biological, chemical and therapeutic aspects. *Nat Rev Drug Discov.*, **2**, 999-1017.

Wei, J., Xu, H., Davies, J.L. & Hemmings, G.P. (1992) Increase of plasma IL-6 concentration with age in healthy subjects. *Life Sci*, **51**, 1953-1956.

Weiss, S.R., Nguyen, T., Rubinow, D.R., Helke, C.J., Narang, P.K., Post, R.M. & Jacobowitz, D.M. (1987) Lack of effect of chronic carbamazepine on brain somatostatin in the rat. *J Neural Transm*, **68**, 325-333.

Willner, P., Towell, A., Sampson, D., Sophokleous, S. & Muscat, R. (1987) Reduction of sucrose preference by chronic unpredictable mild stress, and its restoration by a tricyclic antidepressant. *Psychopharmacology (Berl)*, **93**, 358-364.

Wilson, N.R., Runyan, C.A., Wang, F.L. & Sur, M. (2012) Division and subtraction by distinct cortical inhibitory networks in vivo. *Nature*, **488**, 343-348.

Wolkowitz, O.M., Burke, H., Epel, E.S. & Reus, V.I. (2009) Glucocorticoids. Mood, memory, and mechanisms. *Ann N Y Acad Sci*, **1179**, 19-40.

Wong, M.L., Kling, M.A., Munson, P.J., Listwak, S., Licinio, J., Prolo, P., Karp, B., McCutcheon, I.E., Geracioti, T.D., Jr., DeBellis, M.D., Rice, K.C., Goldstein, D.S., Veldhuis, J.D., Chrousos, G.P., Oldfield, E.H., McCann, S.M. & Gold, P.W. (2000) Pronounced and sustained central hypernoradrenergic function in major depression with melancholic features: relation to hypercortisolism and corticotropin-releasing hormone. *Proc Natl Acad Sci U S A*, **97**, 325-330.

Xu, H., Jeong, H.Y., Tremblay, R. & Rudy, B. (2013) Neocortical somatostatin-expressing GABAergic interneurons disinhibit the thalamorecipient layer 4. *Neuron*, **77**, 155-167.

Xu, X., Roby, K.D. & Callaway, E.M. (2010) Immunochemical characterization of inhibitory mouse cortical neurons: three chemically distinct classes of inhibitory cells. *J Comp Neurol*, **518**, 389-404.

Xue, S., Jia, L. & Jia, J. (2009) Association between somatostatin gene polymorphisms and sporadic Alzheimer's disease in Chinese population. *Neurosci Lett*, **465**, 181-183.

Yang, X., Downes, M., Yu, R.T., Bookout, A.L., He, W., Straume, M., Mangelsdorf, D.J. & Evans, R.M. (2006) Nuclear receptor expression links the circadian clock to metabolism. *Cell*, **126**, 801-810.

Yeung, M., Engin, E. & Treit, D. (2011) Anxiolytic-like effects of somatostatin isoforms SST 14 and SST 28 in two animal models (Rattus norvegicus) after intra-amygdalar and intra-septal microinfusions. *Psychopharmacology (Berl)*, **216**, 557-567.

Yeung, M. & Treit, D. (2012) The anxiolytic effects of somatostatin following intra-septal and intra-amygdalar microinfusions are reversed by the selective sst2 antagonist PRL2903. *Pharmacol Biochem Behav*, **101**, 88-92.

Zeyda, T., Diehl, N., Paylor, R., Brennan, M.B. & Hochgeschwender, U. (2001) Impairment in motor learning of somatostatin null mutant mice. *Brain Res*, **906**, 107-114.

Zeyda, T. & Hochgeschwender, U. (2008) Null mutant mouse models of somatostatin and cortistatin, and their receptors. *Mol Cell Endocrinol*, **286**, 18-25.

Zhao, J., Bao, A.M., Qi, X.R., Kamphuis, W., Luchetti, S., Lou, J.S. & Swaab, D.F. (2012) Gene expression of GABA and glutamate pathway markers in the prefrontal cortex of non-suicidal elderly depressed patients. *J Affect Disord*, **138**, 494-502.